The functional significance of manganese superoxide dismutase binding to mitochondrial DNA

Dissertation zur Erlangung des akademischen Grades eines Doktors der Naturwissenschaften (Dr. rer. Nat.)

vorgelegt von
Muller Nathalie

an der

Universität Konstanz

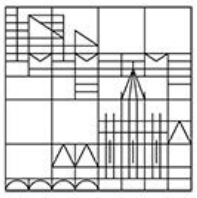

Mathematisch- Naturwissenschaftliche Sektion

Fachbereich Biologie

26 September 2012
1. Referent: Prof. Dr. Alexander Bürkle
2. Referent: Dr. Uwe Schlattner

Parts of this thesis have been published or are in preparation:

Stefan Schildknecht, Regina Pape, Nathalie Muller, Marta Robotta, Andreas Marquardt, Alexander Bürkle, Malte Drescher and Marcel Leist. Neuroprotection by minocycline caused by direct and specific scavenging of peroxynitrite. Journal of Biological Chemistry. 2011 Feb 18

Nathalie Muller et al. An automated Fpg-based FADU assay for the detection of peroxynitrite-induced oxidative lesions. In preparation.

Poster Presentation:

N. Muller, J. Kienhöfer, J. Haar, A. Bürkle and V. Ullrich. Association of Manganese Superoxide Dismutase with mitochondrial DNA in nucleoid structures. The 61rst Mosbacher Kolloquium „The biology of aging: mechanisms and intervention“ organized by the German Society for Biochemistry and Molecular Biology, April 2010

Acknowledgements

First, I would like to thank Prof. Alexander Bürkle for welcoming me into his research group, for letting me work on such a captivating project and for providing the best conditions to carry it out. His interest and input have greatly contributed to the success of this work.

I thank Prof. em. Volker Ullrich for mentoring me throughout the years, for all of the time and implication he has put into my work and his stimulating insight during our many scientific discussions.

I thank Prof. Uwe Schlattner for accepting to be my supervisor, for his availability and for his interest in my work.

I thank Prof. Christof Hauck and Dr Denis Rousseau for participating in the oral examination.

I would like to thank all the members of the Bürkle lab for the excellent working atmosphere throughout the years, you made coming to work in the morning a true pleasure. Aside from the many scientific exchanges, we have also had a lot of fun and you have made my stay in Konstanz an unforgetful experience.
It was a pleasure working alongside all of the past and present Haus 1 coworkers over the years : Julia Köritzer, Elisabeth Müßig, Gosia Debiak, Gabi Lutz, Birgit Gogol and Alex Brenneisen. A special thank you goes to Joachim Kienhöfer for his help during the first few months of my project and for keeping interest after his departure, Janina Haar for the great work during her Master thesis and Arthur Fischbach for the excellent collaboration.
Of course, I have also greatly enjoyed working with the Haus 4 occupants, thanks to Katharina Hüttner for her experimental know-how and her loyal friendship, Rita Martello, Oli Popp and all of the other students, technicians and postdocs. I thank Aswin Mangerich for his time, interest and the fruitful collaboration and Claudia Hoffmann for all of her help and patience.

I would also like to thank AG Dietrich for the great times we've shared in Haus 1 and for making me feel like I was also a part of their group. I thank Prof. Daniel Dietrich for the access to the HPLC and for providing the Xenopus oocytes. A special thank you goes to Oli Okle for the scientific collaboration and for the good laughs we've shared and of course Konstanze Steiner for always being there for me and for being the perfect hostess; you are a true friend.

Thank you Stefan Schildknecht from AG Leist for the numerous collaborations, for the scientific discussions and for being so easy to work with.

I thank Prof. Jörg Hartig for letting me use the Biacore device and David Witte from AG Möller for his technical advice.

I would like to thank the members of the Laboratoire de Bioénergétique Fondamentale et Appliquée in Grenoble for the good times we've shared in the lab. I have greatly enjoyed the time spent in the „bureau des Étudiants" and thank all of the students, particularly Sarah Zorman for her advice and support.

Marc Savasta, thank you for everything : for your time, sensibility, understanding and advice during rough times; your support has meant a lot to me.

A special thank you goes out to my family and all of my wonderful friends who have supported me throughout the years. I particularly thank both my parents, Gertie and Karlheinz Müller, for their support and interest in my studies, for trusting me in my choices and for always providing me with the best conditions to follow my ambitions (and also for having helped me transport my belongings back and forth between Konstanz-Heidelberg-Grenoble !).
Axelle Davidas and Cyrille Martin, I will always remember our productive writing sessions at the MJK, library and other locations.
Cédric Arnould, thank you for always supporting me and knowing when and how to push me in the right direction; your friendship has undoubtedly contributed to the success of this work and for this, I am very grateful .

Summary

Mitochondrial DNA (mtDNA) is organized in nucleoids, structures comprising an association of multiple DNA molecules and proteins with various functions. Its vicinity to the electron transport chain, the main production site of superoxide, makes it highly vulnerable to oxidative damage. Recent findings by our group have revealed the presence of the major superoxide-detoxifying enzyme Manganese Superoxide Dismutase (MnSOD) within the nucleoid structure of tissues from different species and of several cell lines. The binding of MnSOD to DNA was shown to be direct and salt-sensitive, suggesting the implication of ionic forces.

This led to the investigation in the present work of the nature of this binding and the possible involvement of positively charged lysine residues of the enzyme with the negatively charged backbone of the mtDNA. After mutation of three specific lysines of human MnSOD by site-directed mutagenesis, expression in E. coli and purification, binding of MnSOD mutants to oligonucleotides was measured by a Surface Plasmon Resonance based method. Wild-type and mutant MnSODs all exhibited an association with DNA, suggesting that the binding does not rely on these specific lysines or at least not exclusively.

The isolation of nucleoids on sucrose density gradients revealed the lack of an association of MnSOD to mtDNA in the Hela cell line and in the Parkinson model cell line LUHMES. MnSOD was present in nucleoids of *Xenopus laevis* oocytes of stages 1 and 6 while absent in oocytes of stage 3.

An Fpg-based version of the automated Fluorimetric Analysis of DNA Unwinding assay for the detection of 8-oxo-7,8-dihydroguanine (8-oxodG) was developed by our group. The method was validated by the concurrent detection of 8-oxodG levels in the same plasmid DNA samples by HPLC coupled with LC/MS which displayed a high correlation in the values measured. The method allowed the detection of 8-oxodG formation induced by the peroxynitrite donor 3-Morpholinosyndnomine (Sin-1) in a dose-dependent manner which was prevented by addition of MnSOD, as well as uric acid and minocycline.

The damaging effects of peroxynitrite on mitochondrial biomolecules were further investigated by the detection of tyrosine nitration of mitochondrial proteins in peroxynitrite-treated human platelets by Western Blot. Peroxynitrite induced tyrosine nitration of recombinant human MnSOD which led to its inactivation. RAW264.7 macrophage cells treated with Sin-1 exhibited increased 8-nitroguanine levels detected by immunofluorescence and increased mitochondrial 8-oxodG levels measured by HPLC LC/MS.

Zusammenfassung

Die mitochondriale DNA (mtDNA) besteht aus Nukleotiden, dabei handelt es sich um Strukturen, die aus einer Assoziation von multiplen DNA Molekülen und Proteinen unterschiedlicher Funktion zusammengesetzt sind. Ihre Nähe zu der Atmungskette, der Hauptproduktionsstätte von Superoxid, macht sie für oxidative Schäden besonders anfällig.
Nach neuesten Erkenntnissen unserer Arbeitsgruppe ist das Superoxid-detoxifizierende Enzym Mangan Superoxid Dismutase (MnSOD) innerhalb der nukleoiden Struktur von Geweben verschiedener Spezies und Zelllinien nachweisbar. Es konnte gezeigt werden, dass das Zusammenwirken von MnSOD mit der DNA zu einer gesteigerten Empfindlichkeit gegenüber hohen Salzkonzentrationen führt, was auf die Implikation von ionischen Kräften hindeutet.
Aus diesem Grund war es Ziel dieser Arbeit die Ursache dieses Zusammenwirkens , speziell im Hinblick auf eine mögliche Beteiligung von positiv geladenen Lysin-Resten des Enzyms an dem negativ geladenen Rückgrat der DNA zu untersuchen. Nach Mutation von drei bestimmten Lysinresten in der humanen MnSOD durch gezielte Mutagenese, anschließender Expression in E. coli und Purifikation wurde die Interaktion von MnSOD Mutanten mit Oligonukleotiden durch eine Oberflächenplasmonenresonanz-Messung (engl.: surface plasmon resonance, SPR) durchgeführt. Sowohl Wildtyp und als auch Mutanten MnSODs wiesen eine Assoziation mit der DNA auf. Dies legt nahe, dass die Verbindung nicht von diesen spezifischen Lysinen abhängt oder zumindest nicht ausschließlich.
Die Isolation von Nukleoiden mittels eines Saccharose Dichtegradienten zeigen, dass keine Assoziation von MnSOD mit der mtDNA in der Hela Zelllinie und der Parkinson Modell Zelllinie LUHMES vorliegt. MnSOD war in Nukleoiden von *Xenopus laevis* Oozyten im Stadium 1 und 6 vorhanden, jedoch nicht in den Oozyten des Stadium 3.
Für den Nachweis von 8-oxo-7,8-Dihydroguanin (8-oxodG) wurdevon unserer Arbeitsgruppe eine modifizierte Version der automatisierten fluorimetrischen Analyse des DNA Unwinding Assays entwickelt. Diese Methode wurde zusätzlich durch die Messung des 8-oxodG Gehalts in den gleichen Plasmid DNA Proben mittels HPLC kombiniert mit LC/MS validiert. Die durch beide Methoden gemessenen Werte wiesen eine hohe Korrelation auf. Es konnte einekonzentrationsabhängige 8-oxodG Bildung als Folge einer Peroxynitrit generierende 3-Morpholinosyndnomine (Sin-1) Behandlung nachgewiesen werden. Zugabe von MnSOD, Harnsäure und Minozyklin hat die Bildung dieser 8-oxodG Läsionen verhindert.

Des Weiteren wurde die schädigende Auswirkung von Peroxynit auf mitochondriale Biomoleküle untersucht. Dafür wurden humanen Thrombozyten mit Peroxynitrit exponiert , um anschließend Tyrosin Nitrierungen mitochondrialer Proteine mittels Western Blot zu detektieren. Die Nitrierung von MnSOD durch diese Exposition führte zur Inaktivierung des Enzyms. Mit Sin-1 behandelte RAW264.7 Makrophagen wiesen eine erhöhte 8-Nitroguanin Konzentration auf, welches zum einen mittels Immunofluoreszens als auch durch einen erhöhten mitochondriale 8-oxodG Level (HPLCLC/MS) gezeigt werden konnte.

Résumé

L'ADN mitochondrial (ADNmt) est organisé en nucléoides, des structures composées d'une association de plusieurs molécules d'ADN et de protéines aux functions variées. Sa proximité à la chaîne respiratoire, le lieu majeur de production de superoxyde, le rend particulièrement vulnérable aux lésions oxydatives. De récentes recherches menées par notre équipe ont révélé la présence de l'antioxydant Superoxyde Dismutase Manganese (MnSOD) au sein des nucléoides de différents tissus et cellules. La liaison de la MnSOD à l'ADN est directe et peut être rompue par l'addition de NaCl, suggérant l'implication d'intéractions ioniques.

Ceci a conduit à l'étude de la nature de cette liaison et l'éventuelle participation de lysines positivement chargées de l'enzyme avec l'ADN négativement chargé. Après la mutation de trois lysines de la MnSOD humaine par mutagénèse dirigée, leur expression dans E. coli et leur purification, l'interaction des mutants de la MnSOD avec des oligonucléotides a été mesurée par résonance plasmon de surface. Aussi bien la protéine sauvage que les mutants se sont liés à l'ADN, indiquant que la liaison ne dépend pas de ces lysines ou du moins pas de manière exclusive.

L'isolement de nucléoides par gradient de sucrose a révélé une absence d'association de la MnSOD à l'ADNmt dans les cellules Hela et la lignée cellulaire LUHMES (modèle parkinsonien). La MnSOD était présente dans les nucléoides d'ovocytes des stades 1 et 6 chez le Xénope mais absente dans les ovocytes de stade 3.

Une version modifiée de la méthode Fluorimetric analysis of DNA Unwinding a été établie dans notre équipe pour la détection de 8-oxo-7,8-dihydroguanine (8-oxodG) avec l'utilisation de la Formamidopyrimidine glycosylase. La méthode a été validée en mesurant en parallèle les mêmes échantillons d'ADN plasmidique par HPLC couplée à LC/MS, ce qui a révélé à une forte corrélation entre les valeurs mesurées par les deux méthodes. Ces méthodes ont permis de détecter la formation de 8-oxodG induites par le générateur de peroxynitrite, 3-Morpholinosyndnomine (Sin-1) de facon dose dépendante. L'addition préliminaire de MnSOD, acide urique et minocycline a empêché la formation de ces lésions.

Les effets du peroxynitrite sur l'endommagement de biomolécules mitochondriales ont été étudiés par la détection par Western Blot de la nitration des tyrosines de protéines mitochondriales dans des thrombocytes humains traités avec du

peroxynitrite. La nitration de la MnSOD par cet agent a entraîné l'inactivation de l'enzyme. Des valeurs élevées de 8-nitroguanine et de 8-oxodG ont été détectées respectivement par immunofluorescence et HPLC LC/MS dans des macrophages RAW264.7 traités avec du Sin-1.

Table of content

1 Introduction

1.1 The mitochondrial genome

1.1.1 Origin and structure of mitochondrial DNA

The mitochondrion is a ubiquitous membrane-enclosed organelle, often described as the power plant of the eukaryotic cell, as it is the place of energy production in the form of ATP. The serial endosymbiosis theory stipulates that mitochondria originate from a bacterial endosymbiont having progressively fused with a host cell to form a single eukaryotic cell approximately 1,5 billion years ago, when substantial amounts of oxygen entered the atmosphere[1]. This theory, already described in the 19th century, was based on the similarities between bacteria and mitochondria as well as between cyanobacteria and chloroplast with respect to respiration.

Upon the discovery of the existence of a distinct mitochondrial genome in chicken tissue sections by electron microscopy in the 1960's, the theory received considerable legitimacy[2]. With the development of the molecular biology field, various phylogenetic analyses ensued with the confirmation of a common α-probacterial genetic background.

The mitochondrial DNA (mtDNA) is a small DNA molecule located in the mitochondrial matrix. It is often referred to as plasmid-like, owing to its double stranded, covalently closed, circular organization in most organisms. However, it may also be found in a linear conformation in some unicellular organisms[3].

MtDNA size varies tremendously in metazoans, from 14kbp in nematode Caenorhabditis elegans to 85,5 in Saccharomyces cerevisiae[4] and can reach 2,500kbp in plants [5]. Human mtDNA has a size of 16,569kbp, a contour length of about 5μM and exists from 1000 to 10000 copies per somatic cell[6].

MtDNA presents a high density of genetic information because of its small size and its lack of introns. It encodes 13 subunits of complexes I, III, IV and V of respiratory chain, as well as 22 tRNAs and 2 rRNAs required for the translation of the mtDNA encoded mRNAs in the mitochondrial matrix[7,8].

As mtDNA only encodes 13 out of the roughly 1000 proteins composing the mitochondrial proteome, most proteins are imported into the mitochondria. During evolution, a number of mitochondrial precursor genes have been transferred to the nuclear genome, as reports have shown that some species may possess orthologous genes in the mitochondrial genome that

other species have in their nuclear genome. Mitochondrial replication, transcription and translation rely almost exclusively on nuclear encoded proteins, limiting to a certain extent mitochondrial autonomy and demanding constant cross talk between nucleus and mitochondria.

The reasons for maintaining a distinct mtDNA molecule that only encodes 13 polypeptides has been argued in the literature. One reason is that the genetic code in mtDNA sequences slightly differs from the standard universal code which may make gene transfer more difficult. For instance, in mammals, AGA and AGG are translated into the arginine residue in the case of nuclear DNA whereas they become a stop codon in the case of mtDNA. Another reason is that some proteins may be too hydrophobic to be imported and need to be produced directly within the mitochondrion, such as the highly hydrophobic cytochrome c oxidase subunit 1[9]. Lastly, is is also postulated that the maintenance of mitochondrial genes is necessary for metabolic control within the eukaryotic cell[10].

A few organisms, such as the parasite Cryptosporidium parvum, are completely devoid of mtDNA, presumably because all of their genes have been transferred or lost[11].

Viable avian and human cells lacking mtDNA, the so-called p0 cells, have been established and rely exclusively on glycolysis for their energy requirements to compensate for the absence of respiration[12,13].

1.1.2 Transcription and replication of mtDNA

The two mtDNA strands display an assymetric distribution of guanine and cytosine nucleotides; the cytosine rich strand being referred to as the light strand and the guanine rich as the heavy strand (Figure 1.1). This difference in density makes it possible to separate both strands on an alkaline cesium chloride gradient. The mtDNA comprises 37 genes, 9 of which are located on the light strand and 28 on the heavy strand.

Transcription is initiated at one of the heavy strand promoters (H1 and H2) or at the light strand promoter (LSP) and progresses in both directions. Transcription from these promoters produces a polycistronic precursor mRNA, containing all of the genetic information of the specific strand, which is later processed into mRNAs, rRNAs and tRNAs. Each protein encoding gene and rRNA gene is immediately flanked by one or more tRNA genes, highlighting the importance of RNA processing, involving among others RNase P[7].

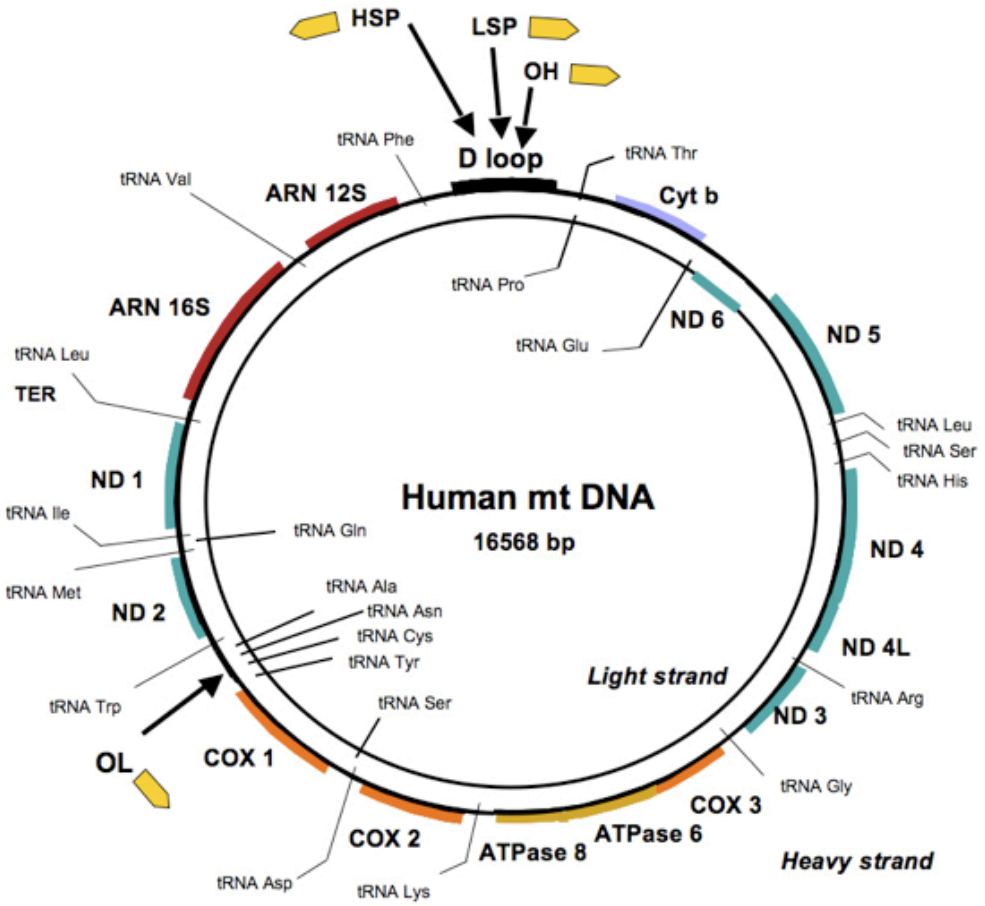

Figure 1.1 : The human mitochondrial genome
The genes encoding the 13 polypeptides and the 2 rRNAs are depicted in different colors and those for the tRNAs are placed with the arrows. The inner circle represents the L-strand with its origin of replication O_H and the outer circle the H-strand with its origin O_L. Transcription of the H-strand is polycistronic and is initiated at the H-strand promoter (HSP) and transcription of the H-strand starts at the LSP. The Displacement Loop (D-loop) is the triple stranded non coding regulatory region. ND1-6: NADH dehydrogenase subunits, COX1-3: Cytochrome c oxidase subunits, ATP6 and ATP8: subunits of ATP synthase, Cyt b: Cytochrome b.
Figure from [14].

There is a high conservation of gene order and genetic content in mtDNA in vertebrate species; however, a considerable variation in organization and sequence has been reported in the regulatory region of the mtDNA, the so-called control region.

The control region is the only non coding sequence of the mtDNA molecule and has a size of 1122bp in humans. It harbors all of the promoters for transcription initiation as well as essential elements for replication, thus ensuring a tight link between transcription and replication[15]. RNA transcripts initiated at the LSP are the primers for mtDNA replication at the heavy strand origin (OH). This region also contains a displacement loop (D-loop) formed by the addition of the replicated segment of the H-strand serving as a third strand binding to

the L-strand by a hydrogen bond. The D-loop sequence is highly variable in vertebrates and has been especially useful in understanding evolutionary history among species[16].

A traditional model was proposed 30 years ago in which replication of mammalian mtDNA occurs by an asynchronous strand displacement mechanism starting in the D-loop region[17]. The H-strand replication is initiated at OH and progresses through approximately two-thirds of the circular molecule. At this point, the replication of the L-strand begins at OL after displacement of the mother H-strand as a single strand by the daughter H-strand. Both daughter molecules are then separated, the RNA primers are removed, the missing fragments are completed and ligated and superhelical turns are added to the molecule to obtain a covalently closed circular mtDNA.

In recent years, an alternative mtDNA synthesis mechanism, the strand-coupled model, has been reported in human cell lines[18]. In this model, replication is initiated at a different origin located within the D-loop region and occurs simultaneously for both strands (Figure 1.2).

As opposed to nuclear DNA synthesis, mtDNA replication is not phase specific and occurs continuously during the cell cycle.

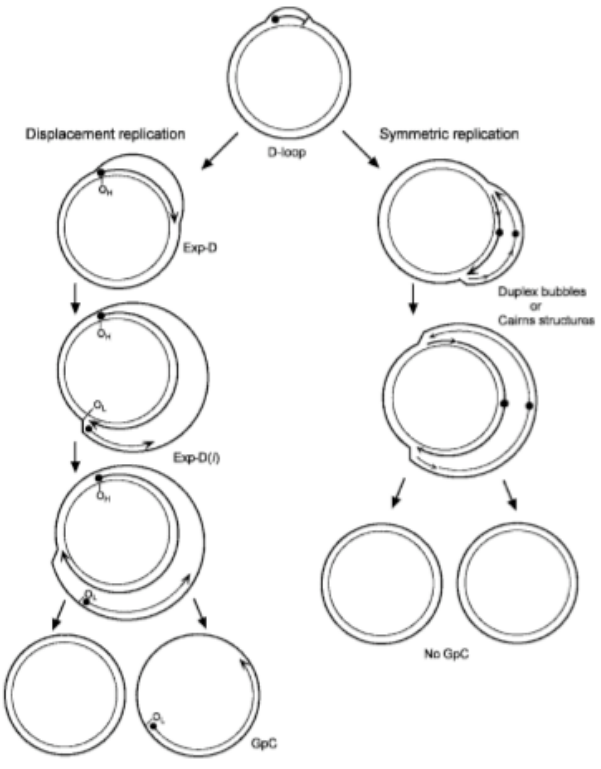

Figure 1.2 : The assymetric and strand-coupled models of mtDNA replication
In both models, DNA replication is initiated at the D-Loop. The displacement-model of replication is starts with single-stranded replication of the H-strand with the expansion and displacement of the D-loop. The intermediates are called expanded D-loops (Exp-D). When the O_L is exposed, synthesis of the new L-strand starts in the opposite direction. This asymmetry results in one daughter molecule with an incompletely synthesized L-strand: the gapped circle (GpC). In the strand-coupled or synchronous model of replication, both strands

are synthesized bidirectionally.
Figure from [19].

MtDNA sequence studies are ideal for investigating the phylogeny of organisms, as mtDNA is highly prone to mutations and is variable between species. MtDNA is highly polymorphic; the nucleotide substitution rate in mammals is 5 to 10 times faster in mtDNA than in single-copy nuclear DNA[20].
At the levels of the tissue, the cell and even the mitochondrion, a mixture of wild type and mutant mtDNA molecules may coexist, a phenomenon known as heteroplasmy DNA.

1.1.3 MtDNA in fusion and fission

Mitochondria were perceived as distinct entities for many years; it has since been shown that they are highly dynamic organelles within a network and frequently migrate and undergo morphological changes, as observed by time lapse imagin [21]. This serves as a well organized system for delivering energy or channeling calcium within the cell [21]. Mitochondrial growth, fusion and fission are essential processes for maintaining mitochondrial shape, distribution and copy number but is also necessary for exchanging material such as metabolic substrates but also mtDNA[22]. The mosaic distribution of mutated DNA that is observed in cells may be explained by the fact that heteroplasmic mutations are segregated during cell division.

1.1.4 MtDNA inheritance and the bottleneck theory

In most multicellular organisms, mtDNA is strictly of maternal origin as mitochondria are exclusively inherited from the mother. Different mechanisms are involved in the selection of maternal mitochondria during fertilization. First of all, an oocyte contains 10^3-fold more mtDNA molecules than the sperm, accounting for an initial prevalence of the maternal material. Moreover, upon entering the oocyte, the sperm cell may lose its tail, in the base of which most mitochondria are located. After fertilization, mitochondria from mammalian sperm are immediately destroyed, most likely after recognition by the oocyte of ubiquitinated prohibitin, a protein of the outer membrane[23].
One would assume that this asexual mode of genetic transmission should be prone to an accumulation of deleterious mutations, according to Muller's ratchet.

However, this is not the case in mtDNA inheritance as a study on Holstein cows showed rapid shifts in mtDNA variants between generations and among the offspring of a same mother with a return to homoplasmy after only two to three generations[24].

A mature mammalian oocyte contains a high mtDNA copy number (around 10^5 copies) and undergoes only a few cell divisions during oogenesis. Nevertheless, they are derived from just a small fraction of the different copies present in the precursor cell, demonstrating a very rapid segregation of mtDNA sequence variants in an attempt to reset the mtDNA mutation rate between generations

To account for this, the bottleneck theory was proposed in oogenesis, but also in early embryogenesis. The molecular mechanisms are unclear and are subject to controversy. Segregation of heteroplasmic mtDNA mutations occurs at a very early stage in oogenesis, with a massive drop in mtDNA copy number[25]. During the maturation of the primary oocyte, the mtDNA content subsequently increases 100-fold (from 10^3 to 10^5 copies), with the selection and replication of only a subset of mtDNA variants, therefore leading to the decrease in sequence heterogeneity.

Initially, this drastic reduction in mtDNA content was reported in Primordial Germ Cells (PGC) of mice during embryonic development and was evaluated at about 200 mtDNA copies [26]. More recent publications contradicted these results, claiming the bottleneck occurs without this decrease in PGCs[27,28].

Whether mtDNA undergoes random genetic drift or conversely, is subject to a positive or negative selection in the germ cell line remains an area of great debate. On one hand, studies of the occurrence of mtDNA mutation inheritance in families with mtDNA-associated diseases display no selection, arguing in favor of the random drift hypothesis[29]. On the other hand, studies on human mtDNA variation have shown a tendency for mutations displaying an adaptive advantage to be selectively retained whereas deleterious mutations would be eliminated[30].

1.2 The mitochondrial nucleoid

1.2.1 The nucleoid structure and composition

It is now well established that the circular mtDNA does not exist as a naked molecule in the mitochondrion but rather as tightly packed DNA-protein macro-complexes called nucleoids, as reported already from early electron microscopy based studies in the 1960's [9].

The average size of nucleoids determined by confocal microscopy is 270 nm in mammalian cells [31]. In post-mitotic cells, they contain between 2-10 copies of mtDNA and several thousands of copies exist in a cell, when taking into account the number of mitochondria per cell. It should be noted however that recent studies using stimulated emission depletion microscopy suggested that mammalian nucleoids contain only a single mtDNA copy (more precisely, an average of 1,4 mtDNA molecules per nucleoid).[31]
It was only upon replacement of the early mtDNA isolation methods using cesium salt gradients that caused the disruption of the nucleoids by a gentler lysis of mitochondria followed by sequential gradient centrifugation, that it was possible to identify many new proteins involved in these complexes.

Over the years, an extensive list of these proteins has been continuously updated. Depending on the stringency of the purification method, some nucleoid proteins may or may not be recovered according to the nature of their binding while others may not actually be intrinsic nucleoid proteins.
A study comparing formaldehyde cross-linked and native nucleoids suggested a layered model in which nucleoid components are distributed into two subsets: the central core and the peripheral proteins. The central core is composed of proteins involved in mtDNA maintenance, replication and transcription, such as mitochondrial transcription factor A (TFAM), mitochondrial single stranded DNA binding protein (mtSSB), DNA polymerase γ, T/-like helicase, TFBM1, TFBM2, Terf1, mitochondrial topoisomerase I, suv-3 like helicase, DEAD box protein 28 and DHX30. Peripheral proteins play a role in translation, protein folding and quality control, such as Hsp60, Hsp70, Hsp40, prohibitins 1 and 2, and the ClpX and Lon proteases[32].

Some nucleoid components are bi (multi) -functional; many identified nucleoid proteins are known for their primary function, but their role within the nucleoid still remains unclear.
The most abundant mtDNA binding protein in higher eukaryotes is TFAM, even though reports diverge as to which extent it covers the mtDNA molecule, TFAM:mtDNA ratios ranging from 50:1 to 1700:1[33,34]. Even though TFAM is capable of binding DNA in a non sequence-specific way, it presents preferred binding sites such as the control region[35]. TFAM is a member of the high mobility group (HMG) family of proteins that contribute to the regulation of gene expression. Initially identified as a mtDNA transcription factor, it has also revealed its role in mtDNA packaging[11] and displays a histone-like function in bending DNA

in order to ensure the formation of nucleoprotein complexes[36]. MtDNA copy number is partly regulated by TFAM as TFAM knockout and overexpressing mice showed respectively low and high mtDNA copy number[37,12].

Other proteins like Polγ and Twinkle also clearly play a role in nucleoid maintenance, their dysfunction being directly involved in mtDNA depletion syndromes in which patients may present nucleoids of abnormal appearance [38]. A decreased Twinkle expression causes a drop in mtDNA copy number [39] just as with TFAM and defects affecting its activity lead to an accumulation of mtDNA deletions, just as is the case in POLγ deficient mice.

Metabolic enzymes located at the inner membrane have also been reported to associate with nucleoids in human cells[40].

Recent data show a direct link between mtDNA and the cytoskeleton : non muscle myosin heavy chain IIA and β-actin strongly bind to mtDNA in rat liver and play a role in mtDNA maintenance [41].

A recently identified AAA+ protein, ATAD3, has been shown to be necessary for the formation or segregation of nucleoids[42]. Its preferential binding and recruitment to the D-loop structure, to which no function had been assigned in over 30 years, suggests an involvement of this D-loop in mtDNA organization as a scaffold for various proteins.

1.2.2 The dynamics of nucleoid composition

It is necessary to note the dynamic feature of the mtDNA nucleoid, which continuously undergoes remodelling and its composition varying under diverse physiological conditions. At a given time, we observe mere "snapshots" of protein – DNA interactions[43].

By the processes of mitochondrial fission and fusion, the nucleoids can be distributed over the whole mitochondrial network which provides the individual nucleoid with a larger pool of proteins required for replication and transcription[32].

It is possible that the distribution of nucleoids may be decisive in the segregation of heteroplasmic mitochondrial genomes in cells bearing a mixture of wild type and mutant mtDNA molecules. To what extent this is the case and the exact mechanisms by which this is achieved remain unclear. Two models have been advanced: the initial "faithful nucleoid" model suggests that nucleoids are relatively inert structures that replicate their own genome without any mtDNA exchange between nucleoids [44] whereas the "dynamic nucleoid" model that proposes a free exchange of mtDNA [45]. In an effort to challenge these models, Gilkerson et al. fused two homoplasmic cell lines carrying non overlapping partial deletions[46]. Both

mtDNAs became transcomplementary within a same cell but did not intermix within a nucleoid, arguing in favor of the "faithful nucleoid" model.

Another major mechanism in nucleoid dynamics that remains poorly understood is the fragmentation and distribution of nucleoids during mitochondrion or cell division. Garrido et al. visualized nucleoids using GFP-tagged Twinkle in living cells by time-lapse fluorescence microscopy and observed their tendency to follow mitochondrial dynamics[47]. In 67% of dividing mitochondria, nucleoids were located near sites of division and displayed division or redistribution to the daughter mitochondria. Conversely, nucleoid division may also occur without mitochondrial division. During fission, nucleoids did not tend to divide and were distributed over the length of the mitochondrion before being redistributed to maintain inheritance.

1.2.3 Nucleoids and mtDNA inheritance

During oogenesis, nucleoids are most likely involved in the mtDNA segregation process[32]. It is postulated that the unevenly packed nucleoid could lead to an uneven distribution of the different mtDNA genotypes, therefore explaining the variation of mtDNA heteroplasmy during embryogenesis.

During Xenopus oogenesis, nucleoid composition undergoes reorganization. TFAM:mtDNA ratios drastically increase between the previtellogenic and mature oocyte stages[48]. It is postulated that TFAM mechanically blocks the access of regulatory proteins to the mtDNA since accumulation of TFAM concurs with a reduced mtDNA transcription and replication rate in mature oocytes.

1.3 Reactive oxygen and nitrogen species in oxidative stress and redox regulation

1.3.1 Reactive oxygen and nitrogen species

Reactive oxygen species (ROS) are highly reactive molecules derived from oxygen, containing one or more unpaired valence shell electrons.

The superoxide anion O_2^- is formed by a one-electron reduction of oxygen and is the precursor of most ROS *(1)*.

(1) $O_2 + e^- \rightarrow O_2^-$

O_2^- is rapidly converted to hydrogen peroxide (H_2O_2), either spontaneously or enzymatically, catalyzed by a superoxide dismutase *(2)*.

(2) $2O_2^- + e^- + 2H^+ \rightarrow H_2O_2$

H_2O_2 can in turn be fully reduced to water *(3)* or partially reduced to the highly reactive hydroxyl radical (OH^-). The latter reaction occurs through the Fenton reaction in the presence of redox active metal ions such as Fe^{2+} and Cu^{2+} *(4)*. The conversion of superoxide and hydrogen peroxide to hydroxyl radicals is known as the Haber-Weiss reaction *(3)* + *(4)* → *(5)*.

(3) $Fe^{2+} + H_2O_2 \rightarrow Fe^{3+} + OH^- + \bullet OH$ *(Fenton reaction)*

(4) $Fe^{3+} + O_2^- \rightarrow Fe^{2+} + O_2$

(5) $O_2^- + H_2O_2 + H^+ \rightarrow O_2 + H2O + {}^{\bullet}OH$ *(Haber-Weiss reaction)*

O_2^- may also react with nitric oxide (NO.) forming the powerful oxidant peroxynitrite ($ONOO^-$) *(6)*.

(6) $NO + O_2^- \rightarrow ONOO^-$

In vivo, O_2^- can be produced non-enzymatically and enzymatically.

The main source of ROS during normal cellular metabolism is the electron transport chain (ETC) where leakage of electrons occurs at several redox centers (Figure 1.3)[49]. These include Complexes I and III, with the production at Complex I being half of that at Complex III[50]. Reports have also mentioned Complex II as a site of superoxide generation to a lesser extent[51]. The capacity to produce ROS using different substrates and the site of production may be tissue-, specie- and age-specific[52]. It also depends on whether mitochondria are actively respiring (state 3) or the electron transport chain is highly reduced (state 4)[53].

The amount of electron leakage in mitochondria is substantial; the most reliable reports estimate O_2^- generation at the ETC at a basal value of 0,1% of consumed oxygen[54].

O_2^- can also be produced by the electron transfer from reduced coenzymes, prosthetic groups and xenobiotics.

Enzymatic production can be executed by cytochrome P450-dependent oxygenases and by NADPH oxidases located on the cell membrane of endothelial cells and even more vigorously in phagocytes-neutrophils and monocytes[55,56]. O_2^- and also H_2O_2 are also generated by the proteolytic conversion of xanthine dehydrogenase to xanthine oxidase[57].

A number of pathological conditions may increase ROS generation rate, such as hypoxia, ischemia, reperfusion and aging.

NO is the precursor to the generation of reactive nitrogen species (RNS), such as nitrogen dioxide (NO_2), nitroxyl (HNO), nitrosonium (NO^+), S-nitrosothiols (RSNO) and most importantly peroxynitrite ($ONOO^-$; PON)[58].

NO results from the breakdown of L-arginine to L-citrulline, a reaction catalyzed by Nitric Oxide Synthases (NOS), a family of NADPH-dependent enzymes. These include neuronal NOS (nNOS), endothelial NOS (eNOS), inducible NOS (iNOS) and a more recently discovered mitochondrial NOS (mtNOS) [59]. MtNOS is associated with the mitochondrial inner membrane and plays a part in regulation of oxygen consumption and membrane potential[60]. Whereas nNOS, eNOS and mtNOS are constitutively expressed, iNOS is only expressed under particular stimuli in cells.

NO production can be considerably increased in different conditions, such as inflammation; for instance, inflammatory stimulation could cause a 9-fold elevation of NO generation in rats[61].

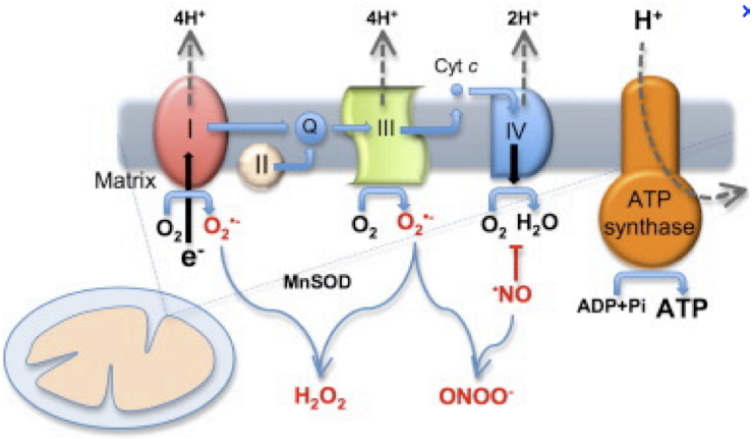

Figure 1.3 : Reactive oxygen and nitrogen species derived from superoxide from the ETC
During normal electron transfer, one-electron donation to O_2 occurs from complexes I and III, hence forming superoxide (O_2^-). O_2^- can be dismutated to H_2O_2 by MnSOD or combined with nitric oxide (NO) to form peroxynitrite anion ($ONOO^-$).
Figure from [62]

1.3.2 Antioxidant systems

Since oxygen levels in the atmosphere began to rise, organisms had to develop protection mechanisms in order to cope with oxygen toxicity (Figure 1.4).

Superoxide dismutases (SOD) are the primary ROS scavenging enzymes of the cell. Three different SOD types exist, encoded by different genes and differing by the metal ion incorporated in the catalytic center. CuZnSOD (SOD1) is a homodimer located primarily in

the cytoplasm and also in the mitochondrial intermembrane space. Extracellular EC-SOD (SOD3) also includes a copper and zinc in its active site but only shares 40-60% amino acid homology with CuZnSOD and is located in the extracellular region. MnSOD exists as a homotetramer and is strictly located in the mitochondrial matrix. A fourth SOD, FeSOD, can be found in some prokaryotes.

This enzyme family catalyzes the conversion of O_2^- to H_2O_2 by dismutation (or disproportionation) in two steps. First the O_2^- anion binds to the central metal ion which is in its oxidized state and in turn, becomes reduced as oxygen is released. The combination of two bound O_2^- anions and two protons leads to the formation and liberation of H_2O_2, allowing the metal ion to return to its oxidized state.

Since SODs release H_2O_2, others antioxidants are required for further detoxification, particularly glutathione peroxidase (GPx) and peroxyredoxins III and V (Prx).

GPx exists in two forms in mitochondria : while GPx1 is located in the matrix, phospholipid-hydroperoxide GPx (PHGPx) is associated with the inner membrane where it reduces lipid peroxides[63]. They reduce H_2O_2 to H_2O by using reduced monomeric glutathione (GSH) as a hydrogen donor, yielding glutathione disulfide (GS-SG) *(7)*.

(7) $2GSH + H_2O_2 \rightarrow GS–SG + 2H_2O$

Oxidized glutathione is then reduced by glutathione reductase (GR) using NAPDH as a substrate, in order to complete the cycle *(8)*.

(8) $GS–SG + NADPH + H^+ \rightarrow 2\,GSH + NADP^+$

Prx use reduced thioredoxin (Trx) as a hydrogen donor in order to decompose H_2O_2 into H_2O_2 *(9)* and thioredoxin reductase reinstates Trx in its reduced state *(10)*.

(9) $Trx\ (red) + H_2O_2 \rightarrow Trx\ (ox) + 2H_2O$

(10) $Trx\ (ox) + NADPH + H^+ \rightarrow Trx\ (red) + NADP^+$

Catalase is also an important antioxidant in the detoxification of mitochondrial derived H_2O_2 in myocardial tissue[64]. The reaction occurs at the iron center of the heme group of the enzyme (Fe-E) in two stages *(11), (12)*.

(11) $H_2O_2 + Fe(III)\text{-}E \rightarrow H_2O + O{=}Fe(IV)\text{-}E(.+)$

(12) $H_2O_2 + O{=}Fe(IV)\text{-}E(.+) \rightarrow H_2O + Fe(III)\text{-}E + O_2$

An often neglected antioxidant is NO itself. Its fast reaction rate as a radical makes it a very efficient free radical scavenger. Reacting with peroxyl radicals at a rate constant above $10^9\ M^{-1}s^{-1}$, NO makes a good inhibitor for lipid peroxidation and could possibly have beneficial effects in pathological cases such as atherosclerotic lesions[9].

Non enzymatic compounds also serve as useful oxidants in the cell, including glutathione or diet-derived antioxidants β-carotene, ascorbate (Vitamin C) and α-tocopherol (vitamin E).

Free amino acids (especially tryptophan, tyrosine, histidine and cysteine), peptides and proteins have a low antioxidant activity but may play a significant role in scavenging ROS when present in high concentrations[65].

Oxidized proteins are in most cases targeted for degradation by the 20s proteosome as well as other proteases[66]. This mechanism may be considered a scavenging system for the cell to decrease levels of ROS and contributes in redox homeostasis maintenance.

Antioxidants are often not sufficient in preventing damage when an organism is exposed to hyperoxic and even normoxic conditions. Upregulation of defences exist in some situations.

Many living organisms, such as bacteria, have developed a response to oxidative stress by increasing levels of ROS scavenging peptides and proteins, like glutathione. Intracellular levels of glutathione are believed to be essential in redox regulation and are presumably dependent on amino acid availability for their synthesis[67].

Regulation of individual antioxidant activity is also possible; for instance, CuZnSOD may exist in a reduced, inactive form and can be activated by O_2^{-} [68].

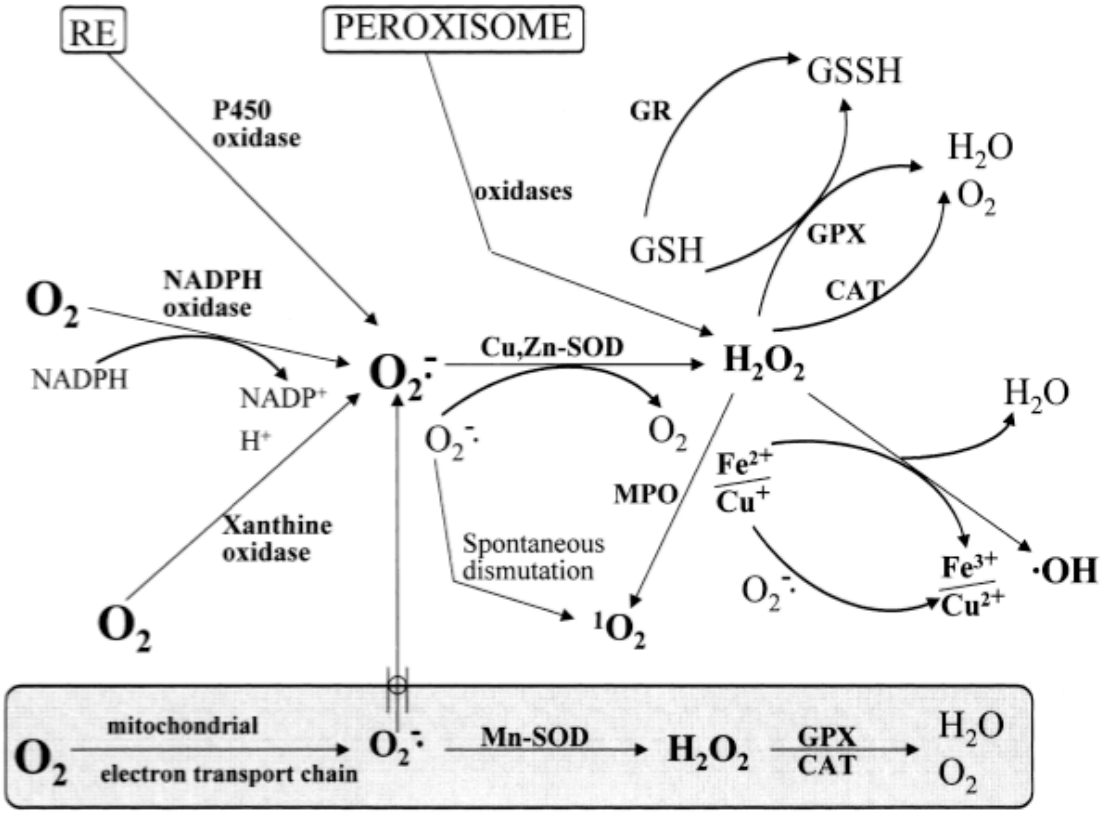

Figure 1.4 : Generation of reactive oxygen species and main defence mechanisms
From [69]

Different sources of O_2^- exist in the cell and can lead to the formation of H_2O_2 and •OH radicals which are scavenged by variety of antioxidant systems.

1.3.3 Oxidative stress and redox regulation

Redox homeostasis is achieved by a balance between ROS production and scavenging by different antioxidant systems.

Oxidative stress is an expression used to describe the deleterious processes caused by an imbalance towards an excess in ROS which may affect the integrity of a multitude of biomolecules and is implicated in aging and in a large panel of disorders and diseases.

O_2^- is charged, relatively unstable and weakly reactive in aqueous solution, and so it does not react at a significant rate with DNA, phospholipids and proteins. Instead, its toxicity is due to its conversion to other ROS, such as H_2O_2, OH• and peroxynitrite.

These are involved in various forms of DNA damage (specified in section 1.4.1), the oxidation of polyunsaturated fatty acids in lipids (lipid peroxidation) and the oxidation of amino acids and proteins. In contrast to the extensive repair mechanisms existing for DNA damage, repair of oxidized proteins is limited to the reduction of the oxidized derivatives and instead, degradation of the damaged proteins often prevails. A balance between free radical production and clearance and the concentration and activity of proteases determines the accumulation of oxidized proteins in the cell. The oxidative modification of proteins may modify their enzymatic and structural integrity and lead to the interruption of key regulatory pathways. Their accumulation is implicated in a wide panel of disorders and diseases.

Much like superoxide, NO does not interact directly with biomolecules in most cases but reacts with other free radicals. NO and O_2^- are present in the cell at low concentrations but when in equal concentrations, they form peroxynitrite, one of the fastest reactions within a cell ($k= 1.6x10^{10} M^{-1} s^{-1}$).

Peroxynitrite acts both as a strong oxidizing and nitrating agent : triggering protein damage such as sulfoxidation of methionine, hydroxylation, nitration of tyrosine and nitrosylation of sulfhydryls or metals and lipid peroxidation. It also induces DNA damage, especially in the form of strand breaks and base modification[70].

For many years, free radicals were regarded as mere toxic by-products of the aerobic environment. Denham Harman, who had discovered the presence of ROS in biological material over 50 years ago, described them as „Pandora's box of evils" responsible for mutagenesis, aging and cancer[71]. Even so, it is now widely accepted that ROS are not only

damaging agents but are also crucial for signal transduction through redox regulation in multiple cell signalling pathways and thus serve a great physiological function (Figure 1.5).

ROS may act as second messengers in signal transduction and have been involved for notably in growth pathways. It has been demonstrated, for instance, that H_2O_2 production induced by some growth factors (EGF, PDGF) is involved in the tyrosine phosphorylation and activation of various proteins[72,73]. Many examples of kinase activation by ROS are available in the literature, including the activation of MAPK and JNK by H_2O_2[74]. This may be mediated by the redox regulation of the cysteine residue of a tyrosine phosphatase [75].

Another well-known model of redox regulation is the activation of NF-κB by a mechanism involving ROS that may trigger degradation of its inhibitor I-κB[76].

Gene transcription can be regulated in bacteria through stimulation of Fnr OxyR and SoxR proteins by O_2^- and H_2O_2 [77]. In mammalian cells also, gene transciption can be redox regulated by modulating the DNA-binding activity of transcription factors.

In mammalian cells, the physiological role of NO has been for many years reduced to two main processes. Macrophages and other immune effector cells produce high levels of NO which play a role in host defense. In neurons and endothelial cells, NO generated by the activated NOS is two to three orders of magnitude lower and serves an important purpose in signal transduction. It is well characterized in its role as a retrograde messenger in neurons and for regulating blood flow and vasodilatation. It is hypothesized that high levels of NO, but also of O_2^- and H_2O_2 produced in immune cells serve a immune function whereas low levels in other cells (chondrocytes, fibroblasts and vascular smooth muscle cells) are involved in signal transduction[78].

NO is suspected to have many more physiological purposes, one of them being the binding to haem groups of cytochrome c oxidase and inhibiting respiration[79]. This provokes a massive production of O_2^- and H_2O_2 that diffuse outside the mitochondria and participate in redox regulated pathways.

Implications of NO in apoptosis have been widely investigated and can serve dual purposes : whereas in some cases NO can induce apoptosis by decreasing the activity of the electron transport chain and releasing cytochrome c into the cytosol, in some cell type, NO can inhibit caspases and therefore protect against cell death[80,81].

Peroxynitrite-induced tyrosine nitration of proteins can lead to their activation, as is the case with angiotensin II-mediated MAPK nitration[82].

ial protein for redox regulation is glutathione, many redox signaling pathways being greatly dependent on intracellular glutathione levels.

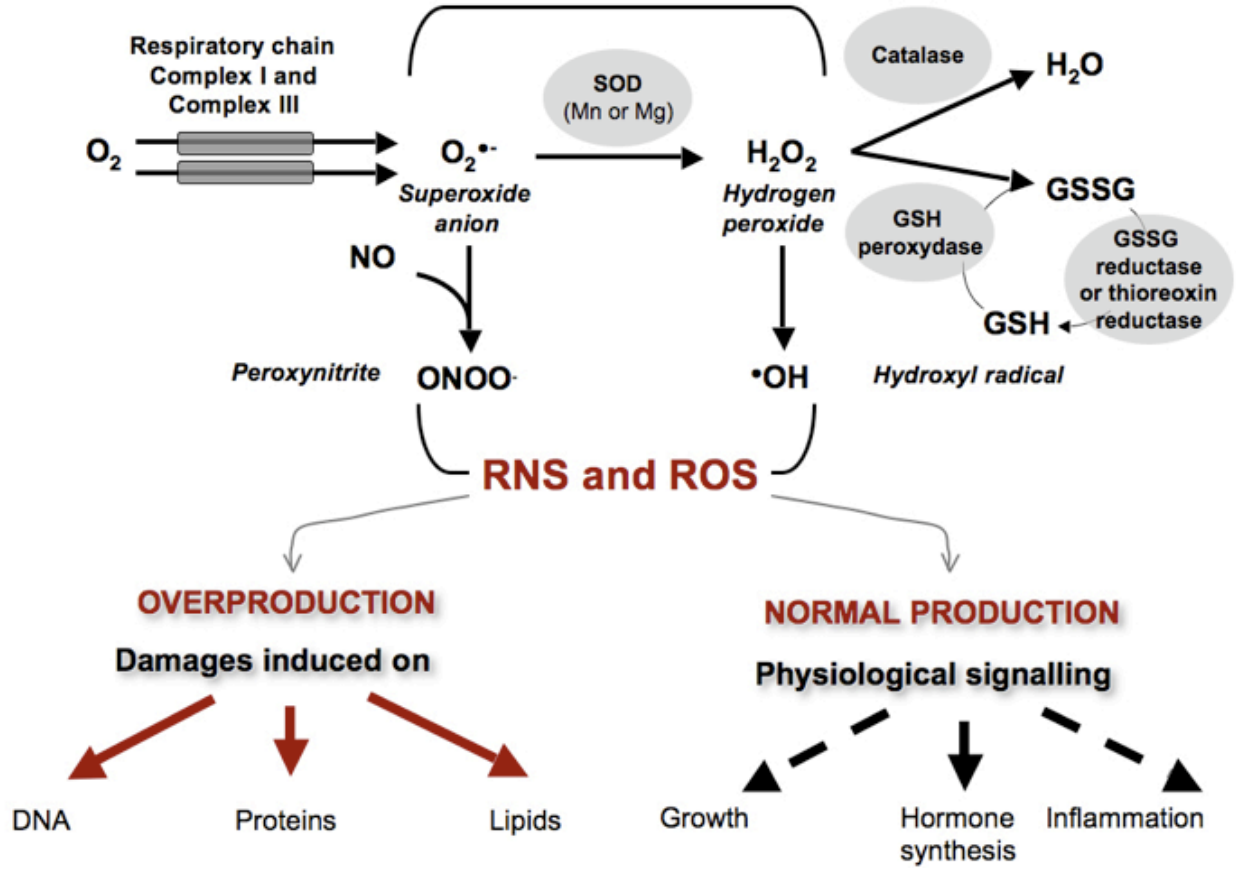

Figure 1.5 : Reactive oxygen and nitrogen species in oxidative stress and redox signalling
The mitochondrion is implicated in the generation of reactive oxygen and nitrogen species. While a normal production of these species is essential in physiological signalling, an overproduction causes damge to a variety of biomolecules.
From [14]

1.4 DNA damage and repair

1.4.1 DNA damage

Since most ROS of the cell originate from electron leakage at the electron transport chain, oxidative damage is particularly relevant in neighboring mtDNA. Due to its lack of histones which confers a protective conformation to nuclear DNA, mtDNA is thought to be particularly vulnerable, partly explaining early reports of a higher incidence in damage than in nuclear DNA[10].

Reactive oxygen and nitrogen species can induce different types of DNA damage, like DNA strand breaks, base oxidation, base alkylation (usually methylation) and base hydrolysis (like deamination, depurination and depyrimidination).

Peroxynitrite particularly causes DNA strand breaks and the formation of 8-oxo-2'-deoxyguanosine (8-oxodG) and 8-nitroguanine (Figure 1.6).

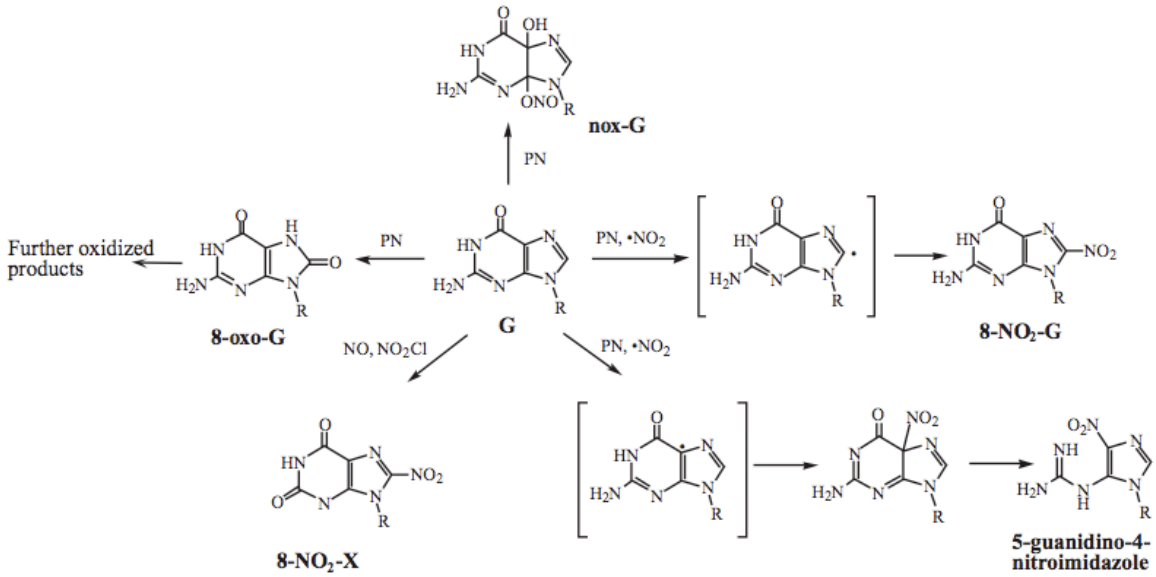

Figure 1.6 : Formation of nitrated derivatives of guanine by peroxynitrite
Figure from [83]

1.4.1.1 8-oxo-2'-deoxyguanosine (8-oxodG)

The oxidation of guanine to 8-oxo-2'-deoxyguanosine (8-oxodG) is one of the most prominent and studied oxidative DNA lesions. It has been first described in the early 1980's that in the presence of oxygen, reducing agents may lead to the addition of an OH group at position 8 of guanine[84].

The abundance of 8-oxodG is partly explained by the fact that guanine has the lowest oxidation potential among DNA bases and is therefore the most easily oxidized nucleic acid base[85]. The even lower oxidation potential of 8-oxodG allows it to undergo further oxidation into such products as spiroiminodihydantoin, guanidinohydantoin and oxazolone[86].

The formation of 8-oxodG can be both cytotoxic and mutagenic [87,88]. Mutations may occur by the misincorporation by replicative or translesion synthesis polymerases, mainly in the form of GC to TA transversions and can therefore compromise genomic stability[89,90,91]. Their assessment has been widely used as a biomarker of oxidative stress in epidemiological as well as in experimental studies and their accumulation has been observed in aging tissues [9293]. Furthermore, mutations in the mitochondrial genome play a role in degenerative diseases of the central nervous and endocrine systems, heart, kidney and skeletal muscle, although the mechanisms are unclear[94,95].

Over the years, basal levels of 8-oxodG have been widely measured but estimates vary considerably among cell lines and tissues but also within a single system. For instance, levels in mtDNA extracted in rat liver can range from 4 to 110 residues per 10^6 guanines[96]. These discrepancies are explained by the large variety of 8-oxodG assessment methods used over the last three decades, which are listed and discussed in the Discussion section.

1.4.1.2 8-nitroguanine (8-NO_2-G)

8-nitroguanine was first described by Yermilov et al. in 1995 as a major product of peroxynitrite reaction with guanine under physiological conditions in *vitro*[97]. Two of the different substances collected from this reaction were yellow, characteristic for nitro- and nitroso- compounds, and after chromatographic and spectral analysis, the major compound was the novel adduct 8-nitroguanine, accounting for 80% of all compounds.

Compared to 8-oxodG, 8-nitroguanine formation in DNA is relatively unstable with an estimated half life of 1 to 4 hours after which they undergo spontaneous depurination[98,99]. These apurinic sites are thought in turn to induce T:A transversions, similarly to 8-oxodG[83].

Studies of 8-nitroguanine formation in biological systems are scarce and little information on its relevance is known.

1.4.2 MtDNA Repair

1.4.2.1 Repair pathways in mitochondria

The persistance of DNA lesions may lead to mutagenesis, cytostasis and cytotoxicity, hence the necessity of DNA repair in mitochondria.

Early studies demonstrated the inability of mitochondria to repair UV-induced pyrimidine dimers as well as some types of alkylating damages[100,101]. This led to the false assumption that they were devoid of DNA repair mechanisms, which may partly explain the still poor understanding of their repair pathways compared to the nucleus.

The discovery of uracil-DNA glycosylase activity in mitochondrial extracts was evidence for the existence of Base Excision Repair (BER) in mitochondria [102]. Since then, this pathway has been shown to be fully efficient in repairing alkylated and oxidized lesions such as O6-methyl-2'-deoxyguanosine[103]. The BER pathway occurs in two steps : first, the specific base lesion is recognized and cleaved and secondly, the generated abasic site is processed, the gap is filled by Polγ and ligated by DNA ligase. Both Long-Patch and Short-Patch BER (LP-BER, SP-BER) have been shown to operate in human cell mitochondria[104].

Very recently, a robust mitochondrial Mismatch Repair pathway (MMR), distinct from nuclear MMR has been added to the list and there has been convincing evidence for the presence of homologous recombination activity in mitochondria[105,106] .

So far, no convincing evidence suggests the existence of Nucleotide Excision Repair (NER) n mammalian mitochondria and it is hypothesized that lesions requiring NER, such as UV-induced pyrimidine dimers may be eliminated by degradation of mtDNA molecules. Nevertheless, the presence of NER should not yet be excluded, as research in mtDNA repair has made a giant leap in the last few years.

1.4.2.2 Repair of 8-oxodG and 8-nitroguanine

8-oxodG lesions are repaired by BER, the first step in which the aberrant base is removed being operated by 8-oxoguanine glycosylase 1 (OGG1) . Alternative splicing of the OGG1 gene gives rise to different isoforms, conserving both the glycosylase and AP-lyase activities but differing in their C-terminus[107]. This determines whether the protein is transported to the nucleus or mitochondria.

8-oxodG levels in liver extracts from OGG1 knockout mice Ogg1-/- were increased 20-fold in mtDNA and only 2-fold in nuclear DNA compared to extracts fom wt mice. OGG1 seems to be more crucial in 8-oxodG repair for mtDNA than nuclear DNA, as the nucleus possesses compensating glycosylases[108].

BER repair efficiency of 8-oxodG is region-dependent in the nucleus: a preferential removal of lesions takes place in transcribed genes compared to non-transcribed genes, possibly through a Transcription Coupled Repair (TCR) mechanism[109]. In contrast, 8-oxodG are repaired uniformly throughout the mtDNA molecule, without differential treatment in heavily transcribed fragments[110].

Interestingly, Thorslund et al. found mitochondrial repair of 8-oxodG to be 1,7-fold faster than the nuclear repair. They postulate a better accessibility of mtDNA to repair enzymes due to its lack of histones, a possible difference in OGG1 splice variant activity and a higher concentration of enzymes in the mitochondrial compartment.

So far, no evidence has arisen stating whether 8-nitroguanine can be enzymatically repaired. While formamidopyrimidine glycosylase (Fpg) recognizes and cleaves 8-oxodG, it has been reported that it is unable to recognize 8-nitroguanine [111]

1.5 The protective role of the nucleoid

The mitochondrion harbors the highly vulnerable mtDNA in close vicinity to the ETC where substantial levels of ROS and RNS are generated but it also contains numerous antioxidant and repair systems. The nucleoid conformation serves numerous purposes, many of which are still unknown. A crucial question is still pending: what is the role of the nucleoid in DNA damage, repair, aging and disease and does it confer a protection to mtDNA ?

1.5.1 Nucleoids in DNA damage, repair and aging

Many reports have attributed the high levels of mtDNA damage to its lack of histones. Histone proteins protect nuclear DNA from oxidative attack, as reports have shown a higher incidence of DNA damage in internucleosomal DNA[10]. If taking into account an estimation of 900 TFAM molecules per mtDNA molecule, it would seem as though mtDNA were entirely covered, suggesting TFAM form histone-like structures which may confer a physical shield for mtDNA protection[112]. The tightly packed conformation of the nucleoid may confer a mechanistic protection to the mtDNA; free mtDNA being indeed more vulnerable to X-ray- or H_2O_2-induced damage[113].
Conversely, although the mtDNA binding proteins may present a mechanical protection, the tight packing may also hinder an efficient repair in the resting state of the nucleoid.

A compilation of interesting studies reveal a possible involvement of TFAM in mtDNA protection or repair but by which mechanism and for what purpose remain unknown:
TFAM binds *in vitro* with a higher affinity to 8-oxodG and cis platin adducts containing DNA fragments than to undamaged DNA[114]. It is hypothesized that this may favor the recruitement of repair proteins to the damaged site or it may prevent signaling of the damaged DNA until it is repaired.
TFAM may also play a role in apoptosis, as tissue-specific knockout of TFAM exhibit a high incidence of apoptosis in mice[115]. In cisplatin-induced apoptosis, p53 has been reported to interact with TFAM, enhancing TFAM binding to cisplatin-modified DNA and inhibiting binding to oxidized DNA[116].
Interestingly, the yeast homologue of TFAM, ABF2, plays an important part in maintaining genome integrity under oxidative stress in yeast strains lacking mitochondrial glycosylase Ntg1p [117]

A remodelling of the nucleoids during aging and as an adjustment to oxidative conditions have been suggested in studies in Saccharomyces Cerevisiae which presented an interesting change in nucleoid composition in aging yeast undergoing caloric restriction; it is postulated that this mechanism leads to a mtDNA conformation more resistant to oxidative damage[16].

1.5.2 An antioxidant system associated with the nucleoids

Studies in E. coli have described that the antioxidant enzyme MnSOD binds to DNA *in vitro* and more interestingly, is a part of the bacterial nucleoid[118].

This evidence along with the oxidative threat on mtDNA in eukaryotes led our group to believe an antioxidant system must be present within the mitochondrial nucleoid. Indeed, Kienhöfer et al. reported for the first time the existence of an antioxidant sytem within the eukaryotic nucleoid structure[119]. The antioxidant proteins MnSOD and GSH-peroxidase were detected in pure sucrose gradient isolated nucleoid fraction in mitochondria from different tissues, including bovine and rat heart as well as human smooth mucle cell lines and Jurkat cells but were absent in ncleoids from bovine endothelial cells. This association has been shown to be salt-sensitive, as the complex was disrupted in the presence of 200mM NaCl, suggesting the involvement of ionic forces in the binding. The proximity of an antioxidant system to the mtDNA most likely confers a more efficient protection against oxidative DNA damage.

2 Aim of the study

The mitochondrion is the redox center of the cell and harbors the electron transport chain, responsible for the production of cellular energy by consumption of oxygen but also for the collateral formation of the superoxide anion by electron leakage. MtDNA is vulnerable to oxidative damage caused by reactive oxygen species. Since it encodes essentially subunits of the ETC complexes, its damage can have drastic consequences on redox homeostasis and has been associated with aging and a variety of diseases. The presence of the major superoxide-scavenging enzyme MnSOD and glutathione peroxidase as an antioxidant system within the nucleoid structure of eukaryotic cells was reported for the first time in our group by Joachim Kienhöfer et al. While an association of MnSOD to the mtDNA was found in bovine and rat heart, human smooth mucle cells and Jurkat cells, it was absent in bovine endothelial cells. A direct binding of MnSOD to DNA was demonstrated and could be disrupted by low concentrations of salt, suggesting the involvement of ionic forces.

1. The first objective of this thesis is to study the nature and significance of this binding.

- The possible involvement of positively charged lysine residues of MnSOD with the negatively charged backbone of mtDNA in an ionic interaction is investigated. Three lysine residues on the C-terminus and N-terminus of the enzyme, which are highly conserved amoung species, are likely candidates and are the object of our investigation.
- The presence or absence of this binding in different cell models as well as in different stages of Xenopus oogenesis is further examined in order to acquire a better understanding of its physiological significance.
- The hypothesis that a bound MnSOD confers a better protection against oxidative damage to mtDNA than the unbound form needs to be validated.

2. For this purpose, we need a reliable method for measuring oxidative damage to DNA. Most available 8-oxodG detection methods are tedious and so, our group has developed a Fpg-based FADU method for the detection of 8-oxodG that still requires optimization and validation by HPLC coupled LC/MS.

3. Our final objective is to demonstrate the relevance of peroxynitrite as a key oxidizing agent of the mitochondrion, with the potential of causing a variety of damage types on different biomolecules.

Ultimately, these experiments are aimed to gain understanding of the functional significance of MnSOD and the role of PON in relation to disease and aging.

3 Material and Methods

3.1 Material

3.1.1 Chemicals

All chemicals were of analytical quality and were purchased from Sigma-Aldrich (Deisenhofen, Germany), Roth (Karlsruhe, Germany), Merck (Darmstadt, Germany), Roche (Mannheim, Germany) or Invitrogen (Karlsruhe, Germany). If not indicated otherwise, double distilled water (ddH2O) was used for buffers and experiments.

3.1.2 Laboratory equipment and consumables

Description	Manufacturer
96-well plates Costar	Corning, Schiphol-Rijk, Netherlands
Agarose gel electrophoresis unit Horizon	Gibco Invitrogen, Karlsruhe, Germany
Agarose gel electrophoresis unit small	Agagel Biometra, Göttingen, Germany
Autoclave 2540-EL	Systec, Wettenberg, Germany
Biacore Series S Sensor Chip SA certified	GE Healthcare, Uppsala, Sweden
Biacore T100 SPR Analysis device	GE Healthcare, Uppsala, Sweden
Centrifuge Biofuge pico	Heraeus, Fellbach, Germany
Centrifuge MiniSpin plus	Eppendorf, Hamburg, Germany
Centrifuge Z233 MK-2	Hermle, Wehingen, Germany
Centrifuge 5810R	Eppendorf, Hamburg, Germany
Chemiluminescence imaging station Fuji Las 1000-Pro	Fujifilm, Düsseldorf, Germany
Clean bench LaminAir H2448	Heraeus, Fellbach, Germany
Cuvettes steriles UVette	Eppendorf, Hamburg, Germany
D-TubeTM Dialyzer Maxi 6-8kDa MWCO	Novagen, Darmstadt, Germany
Electrophoresis power supply E844	Consort, Turnhout, Belgium
Electrophoresis unit Xcell SurelockTM	Invitrogen, Darmstadt, Germany
Electrophoresis unit HoeferTM miniVE	Amersham Biosciences, Freiburg, Germany
Falcon tubes 15ml, 50ml	Corning, Schiphol-Rijk, Netherlands
Filter paper GB002	Schleicher & Schuell, Dassel, Germany
Fluorescence reader Spectra Fluor	Tecan, Crailsheim, Germany
Glassware	Schott, Mainz, Germany
Heat oven VTR 5022	Heraeus, Fellbach, Germany
His-Buster Cobalt SPC08 spin columns	Amocol, Teltow, Germany

HPLC LC-10AT, Waters 2695 Separations Module	Shimadzu, Kyoto, Japan
Impulse tong sealer Polystar 100 GE	Rische+Herfurt, Hamburg, Germany
Incubator for bacterial cultures Minitron	Infors HT, Bottmingen, Switzerland
Laminar Flow workstation	Nunc Intermed, Wiesbaden, Germany
Magnetic stirrer MR 3001	Heidolph, Schwabach, Germany
Mini dialysis units Slide-A-Lyzer 10kDa MWCO	KMF, Lohmar, Germany
Multichannel pipette Transferpette-12	Eppendorf, Hamburg, Germany
NanoDrop 1000	Thermo Scientific, Wilmington, USA
Nitrocellulose protein transfer membrane Hybond-ECL	Amersham Biosciences, Freiburg, Germany
Nucleic acid transfer membrane Hybond-N+	Amersham Biosciences, Freiburg, Germany
Overhead shaker MACSmix	Miltenyi, Bergisch Gladbach, Germany
PCR thermocycler Mastercycler gradient	Eppendorf, Hamburg, Germany
pH meter	Knick, Berlin, Germany
Photometer Ultraspec 2100 pro	Amersham Biosciences, Freiburg, Germany
Pipetboy comfort	IBS Integra Biosciences, Chur, Switzerland
Pipette set	Eppendorf, Hamburg, Germany
Pipettes sterile Costar Stripette	Corning, Schiphol-Rijk, Netherlands
Pipette tips	Sarstedt, Nürnbrecht, Germany
Reaction tubes 1.5ml, 2ml	Sarstedt, Nürnbrecht, Germany
Reaction tubes for PCR (0,2ml)	Biozym Scientific, Oldendorf, Germany
Scale CP2202S	Sartorius, Göttingen, Germany
Scale analytical CP225D	Sartorius, Göttingen, Germany
Scanner Umax Astra 2200	Umax Systems, Willich, Germany
Semi-dry transfer unit Hofer SemiPhor	Amersham Biosciences, Freiburg, Germany
Shaker Polymax 1040	Heidolph, Schwabach, Germany
Slot Blot equipment Minifold II	Schleicher & Schuell, Dassel, Germany
Sterile vacuum filter	Corning, Schiphol-Rijk, Netherlands
Thermomixer Compact	Eppendorf, Hamburg, Germany
UV-light Gel Imager	Intas, Göttingen, Germany
Vortex Genie-2	Roth, Karlsruhe, Germany
Water bath Julabo VC	Julabo, Seelbach, Germany

Table 3.1: Laboratory equipment

3.1.3 Software

Description	Source
AIDA Image Analysis Software 3.10	Raytest, Straubenhardt, Germany
ImageJ 1.43	National Institutes of Health, Wayne Rasband, USA
Microsoft Office 2008	Microsoft Corporation, Redmond, USA
GraphPad Prism 5	GraphPad Software, San Diego, USA
Mendeley	Mendeley Ltd, London, UK

Table 3.2: Software

3.1.4 Oligonucleotides, primers and plasmids

Label	Sequence	Source
JH004	Biotin - CGTAGACACACGAGCATATTTCACCTCCGCTACC	Sigma-Aldrich
JH005	GGTAGCGGAGGTGAAATATGCTCGTGTGTCTACG	
AMa030	TTGCCCTTGGGTAACTTGCTGATATGTG	
AMa032	CTTGAGAAGAATGCTCTGGGCTCTGAAG	
NM01	TGGTCCGATTCCACCCCCTCACGAC	
NM02	GGGCTCAGGCGTTGGTGTTGCAGG	

Table 3.3 : Oligonucleotides and primers

Plasmid	Source
pET-15b : hMnSOD	Master thesis Janina Haar
pAcHLT-A-His6 (UK52); 14 kBp plasmid	Ulrike Kogel, University of Konstanz,

Table 3.4 : Plasmids

3.1.5 Enzymes and proteins

Enzyme / Protein	source
Formamidopyrimidine-DNA glycosylase	New England Biolabs, Frankfurt, Germany
MnSOD E. coli	Sigma-Aldrich, Deisenhofen, Germany
MnSOD human	Ab Frontier, Seoul, Korea
Taq DNA polymerase	Bio&Sell, Feucht, Germany
TFAM	Gift from Prof. Churchill, University of Colorado, Denver, USA
Dnase I	

Nuclease P1 from Penicillum citrinum	Roche Diagnostics, Mannheim, Germany
Phosphodiesterase I	Sigma-Aldrich, Steinheim, Germany US-Biological, USA
Phosphatase, Alkaline from bovine intestinal mucosa	Sigma-Aldrich, Steinheim, Germany
RNase A from bovine pancreas	Sigma-Aldrich, Steinheim, Germany

Table 3.5 : Enzymes

3.1.6 Protein and DNA markers

Description	Source
Prestained SDS-PAGE Standard broad range	Biomol, Hamburg, Germany
Prestained Protein Molecular Weight Marker	MBI-Fermentas, St. Leon-Rot, Germany
GeneRulerTM 1kb DNA Ladder, ready-to-use	MBI-Fermentas, St. Leon-Rot, Germany

Table 3.6: Protein and DNA markers

3.1.7 Antibodies

Primary antibody	Source
Anti-MnSOD: rabbit polyclonal	Assay Designs, Ann Arbor, USA
Anti-TFAM: rabbit polyclonal	Gift from Dr. R. Wiesner, University of Cologne, Germany
Anti-8-nitroguanine : rabbit polyclonal	Gift from Dr Kawanishi, Tokyo, Japan
Anti-nitro-tyrosine : mouse polyclonal	HBT

Table 3.7: Primary antibodies

Secondary antibody	Source
Polyclonal goat anti-rabbit IgG/HRP-conjugated	Thermo Scientific Rockford, USA
Polyclonal goat anti-mouse IgG/HRP-conjugated	Jackson ImmunoResearch, Suffolk, UK
Streptavidin-HRP	Amersham, Buckinghamshire, UK
Alexa Fluor 488: polyclonal goat anti-rabbit IgG	MoBiTec, Göttingen, Germany
Hoechst 33342	Molecular probes, Leiden, Netherlands

Table 3.8: Secondary antibodies

3.1.8 Cell lines

Cell line	Source
Hela S3	Cell line, AG Bürkle, University of Konstanz, Germany
RAW264.7	Cell line, AG Bürkle, University of Konstanz, Germany
LUHMES	Cell line, AG Leist, University of Konstanz, Germany

Table 3.9: Cell lines

3.1.9 Bacteria

Strain	Source
Escherichia coli K12 DH5α	DSMZ, Braunschweig, Germany
Escherichia coli BL21 DE3	Gift from AG Hauck, University of Konstanz (Novagen, Darmstadt, Germany)

Table 3.10: Bacteria

3.1.10 Animals
Dissection of *Xenopus laevis* from AG Dietrich and oocyte bag retrieval were conducted by Oliver Okle.

3.1.11 Media, buffers and solutions

3.1.11.1 Cell culture media

Description	Source	supplements
Dulbecco's Modified Eagle Medium (DMEM) for Hela	Gibco/Invitrogen	4,5 g/l glucose 10% FBS 100 Units/ml penicillin 100 µg/ml of streptomycin
RPMI 1640 for RAW264.7	Biochrom, Berlin, Germany	1% L-glutamine (v/v) 10% FBS (v/v) 100 Units/ml penicillin 100 µg/ml of streptomycin

Table 3.11: Cell culture media

3.1.11.2 Bacterial growth media

Medium	Composition
LB (Luria-Bertani-Broth)	1 % bacto trypton (w/v) 0.5 % bacto yeast extract (w/v) 1% NaCl (w/v) autoclaved supplemented with 0.01 % ampicillin (w/v)

LB agar	LB medium 1.5 % bacto agar (w/v) autoclaved
SOB	2 % bacto trypton (w/v) 0.5 % bacto yeast extract (w/v) 10 mM NaCl 2.5 mM KCl autoclaved
SOC	SOB medium 10 mM MgCl2 10 mM MgSO4 20 mM D(+)-glucose sterile filtrated

Table 3.12: Bacterial growth media

3.1.11.3 General buffers and solutions

SDS-PAGE and Western Blot

Antibody solution	1% fat free milk powder (w/v) in TBS-T
APS for SDS-PAGE	10% APS (w/v)
Blocking solution	5% fat free milk powder (w/v) in TBS-T
Coomassie gel staining solution	0.25% Serva blue R-250 (w/v) 50% trichloroacetic acid (v/v)
Coomassie gel destaining solution	25% methanol (v/v) 7% acetic acid
ECL solution A	ECL solution A 0.1 M Tris-HCl 2.5 mM luminol 0.4 mM p-coumaric acid pH 8.5
ECL solution B	ECL solution B 100 mM Tris-HCl 0.018 % H_2O_2 (v/v) pH 8.5
Laemmli buffer, pH 6.8	300 mM Tris-HCl 200 mM $-mercaptoethanol 8% SDS (w/v) 20% glycerol (w/v) 0.05% bromphenol blue (w/v)

Ponceau S solution	0.1% Ponceau S (w/v) 5% acetic acid (v/v)
SDS-PAGE running buffer (10x)	250 mM Tris-Base 1.9M glycine 1% SDS (w/v)
SDS-PAGE stacking gel buffer (S-buffer) (5x), pH 6.8	625 mM Tris-Base 17 mM SDS
SDS-PAGE separating gel buffer (T-buffer) (5x), pH 8.8	1.86M Tris-Base 15 mM SDS
Semi-Dry buffer	25 mM Tris-Base 160 mM glycine 1.3 mM SDS 20% methanol (v/v)

Table 3.13: Buffers for SDS-PAGE and Western Blot

Protein purification

Lysis buffer, pH 7.0	5 mM imidazole-HCl 50 mM NaH2PO4 25 mM NaCl 10 mM β-mercaptoehanol 1mg/ml lysozyme 1 mM PMSF
Column washing buffer, pH 7.0	5 mM imidazole-HCl 25 mM NaH2PO4 500 mM NaCl
Column elution buffer, pH 7.0	300 mM imidazole-HCl 25 mM NaH2PO4 500 mM NaCl
Dialysis buffer, pH 7.4	50 mM HEPES 500 μM MgCl2

Table 3.14: Buffers for protein purification

Mitochondria and nucleoid complex isolation

Isolation medium I, pH 7.4	250 mM sucrose 10 mM HEPES 1 mM EGTA 0.5% fatty acid free BSA (w/v) 1 mM glutathione (red.)

Isolation medium II, pH 7.4	250 mM sucrose 10 mM HEPES
Mitochondria dilution buffer, pH 7.4	10 mM Tris-HCl 1 mM EDTA
Mitochondria gradient buffer, pH 7.5	10 mM Tris-HCl 1 mM EDTA 0.1% BSA (w/v)
Mitochondria resuspension buffer, pH 7.5	0.8M sucrose 10 mM Tris-HCl 1 mM EDTA 0.1% BSA (w/v)
Nucleoid gradient buffer (GB), pH 7.6	20 mM Tris-HCl 1 mM EDTA 1 mM spermidine 7 mM $-mercaptoethanol 1 x Roche complete protease inhibitor cocktail
Nucleoid isolation buffer (NE2), pH 7.6	250 mM sucrose 20 mM Tris-HCl 2 mM EDTA 7 mM β-mercaptoethanol
Step gradient for nucleoid purification	20% sucrose (w/v) 40% sucrose (w/v) 60% sucrose (w/v) 75% sucrose (w/v) in gradient buffer
Sucrose gradient for mitochondria purification	1 M sucrose 1.5 M sucrose 2 M sucrose in mitochondria gradient buffer

Table 3.14: Buffers for mitochondria and nucleoid complex isolation

FADU-assay

Alkaline unwinding buffer	42.5% lysis buffer (v/v) 200 mv NaOH
Lysis buffer	9 M urea 10 mM NaOH 2.5 mM cyclohexyl-diamin-tetraacetate 0.1% SDS (w/v)

Neutralization buffer	1 M glucose 14 mM $-mercaptoethanol
Suspension buffer, pH 7.4	250 mM meso-inositol 10 mM sodium phosphate 1 mM MgCl2
SYBR Green solution for mitochondrial DNA determination	0.01% SYBR Green (v/v) (from a 10000 x stock)

Table 3.15: Buffers for the FADU-assay

Other buffers and solutions

Agarose gel loading dye (6x)	New England Biolabs, Frankfurt, Germany
Ethidium bromide solution	10 µg/ml ethidium bromide
Phosphate-buffered saline (PBS), pH 7. 4	140 mM NaCl 2.7 mM KCl 8 mM Na_2HPO_4 x $2H_2O$ 1.4 mM KH_2PO_4
PBS-T	1 l PBS (1x) 1% Tween 20 (v/v)
Tris-acetate-EDTA (TAE) buffer (10x), pH 8.5	4400 mM Tris-Base 10 mM Na_2EDTA 200 mM acetic acid
Tris-buffered saline (TBS-T), pH 8.0	10 mM Tris-HCl 100 mM NaCl 0.1% Tween 20
Mitochondrial lysis buffer, pH 7,4 (for mtDNA isolation of RAW264.7 cells)	10mM Tris HCl 150mM NaCl 20mM EDTA 0,5% NP40 100μM BHT 100μM Desferrioxamine
Platelet resuspension buffer, pH 7,4	140mM $NaCl_2$ 2mM Kcl 14mM $NaHCO_3$ 5mM glucose 1mM $MgCl_2$ 5mM Hepes
MBS pH 7,8 (for oocyte defolliculation)	88mM NaCl 1mM Kcl

	1mM $MgSO_4$ 5mM Hepes (pH 7,8) 2,5mM $NaHCO_3$
Master mix (for PCR)	For 10 samples : 45μl H_2O 10μl solution B 10μl $MgCl_2$ 50mM 10μl dNTP 2mM 1μl Taq polymerase
Aqua polymount (for immunofluorescence)	Polysciences, Eppelheim, Germany

Table 3.16: Other Buffers and solutions

3.1.12 Kits and assays

Description	Source
GenEluteTM HP Plasmid Miniprep Kit	Sigma-Aldrich, Deisenhofen, Germany
Giga Prep Kit	Qiagen, Hilden, Germany
Thrombin Cleavage Capture Kit	Novagen, Darmstadt, Germany
SOD Assay Kit	Fluka, Buchs, Switzerland

Table 3.17: Kits and assays

3.2 Methods

3.2.1 E. coli Culture and transformation

During her Master thesis, Janina Haar successfully generated 7 MnSOD variants by site-directed mutagenesis. These proteins displayed different mutations that exchanged 3 specific N-terminal and C-terminal lysines against alanine, glutamine or glutamate residues. The mutants were labeled according to their mutated residue KH-KK (wild-type), KH-AA, KH-QQ, KH-EE, QH-KK, QH-EE, QH-QQ. In this work, the proteins needed to be expressed and purified again for DNA-binding experiments by a SPR-based method.

First, plasmids cloned in chemo-competent E. coli K12 (DH5α) needed to be purified and transformed into chemo-competent E. coli BL21 (DE3) for protein expression. Frozen K12 E. coli bacteria were thawed and plasmids were isolated by GenEluteTM HP Plasmid Miniprep Kit, according to the manufacturer's protocol.

Frozen BL21 E. coli bacteria strains were thawed on ice and 50 μl of bacterial suspension were mixed with 5 μl of purified plasmid. After a 30 min incubation on ice, bacteria were heat-shocked at 42°C for 25 sec in a water bath and immediately placed on ice for 2 min. After addition of 945 μl of pre-warmed SOC medium, bacteria were incubated for 1 h at 37°C. 100 μl of the bacterial solution were plated on an agar Petri dish. After an overnight incubation at 37°C, clones were picked and were further cultivated. .Bacterial cultures were grown in LB medium supplemented with 0.01 % ampicillin (w/v). Sterility was maintained by using autoclaved or ethanol-rinsed material and by working under a bunsen burner.

3.2.2 Protein expression in E. coli

250 ml of LB (+amp) were inoculated with 1 ml of an culture of transformed bacteria and allowed to grow at 37°C at 250 rpm until the OD_{600} value was 0.6. a sample. The subsequent addition of 2,5ml IPTG (0.1 M) to the Erlenmeyer flask induced protein expression. After 6 hours incubation at 37°C at 250 rpm, the bacterial suspension was centrifuged at 6000xg for 10 min and the pellets were shock frozen in liquid nitrogen and stored at -80°C.

3.2.3 Protein purification

The MnSOD variants were fused to an N-terminal His-tag in order to enable protein

purification by Co^{2+}-columns. Bacterial pellets were thawed on ice, resuspended in 10 ml lysis buffer and incubated on ice for 30 min. Bacterial cell lysates were sonicated 5x 45 sec on ice with 1 min intervals for further lysis and centrifuged at 15.000xg for 20 min at 4°C in 2ml tubes. The supernatant was collected and subjected to protein purification using SPC5
His Buster Co^{2+}-affinity gels (Amocol) according to the manufacturer's protocol. All incubation steps were performed on ice, buffers were at 4°C and centrifugation was conducted at 4°C. A total of 5 elution steps were performed as previous experiments had shown that the 2 elutions recommended by the manufacturer were insufficient.
A 30μl samples of each fraction and washing step was collected and frozen at -20°C for SDS-PAGE and Coomassie staining to assess the quality of the purification Eluats were dialyzed overnight against Hepese at 4°C with mild stirring in D-TubeTM Dialyzer tubes with 6-8 kDa molecular weight cut off (MWCO) in order to remove imidazole from the solution.

3.2.4 His-Tag cleavage

The N-terminal amino acid sequence of the MnSOD proteins contains a thrombin cleavage site for removal of the His-tag. The purified and dialyzed proteins were cleaved using the Thrombin Cleavage Capture Kit (Novagen). 1ml of the MnSOD solution was incubated with 10 μl biotinylated thrombin (0.1u/μl) at room temperature for 16 hours. 70μl of 50 % Streptavidin sepharose beads were added to each sample, which were then incubated at room temperature for 45 min with mild rotation. The thrombin captured by the sepahrose beads were removed by subjecting the sample to a spin filter and centrifuging for 5 minat 500xg. The samples were dialyzed for 2 x 12 h against Hepes at 4°C with mild stirring in D-TubeTM Dialyzer tubes (6-8 kDa MWCO) against Biacore binding buffer (50 mM HEPES,
500 μl MgCl2) in order to remove the cleaved oligopeptides. The proper cleavage of the His-tag was verified by SDS-PAGE and coomassie staining.

3.2.5 Real-time SPR analysis of MnSOD-DNA interaction (Biacore)

Surface Plasmon Resonance (SPR) based methods offer a non invasive quantitative measurement of interactions between biomolecules without the necessity of labeling the analytes. Briefly, The technique uses a prism as a light source to transfer photons to a group of electrons on a metal surface (usually gold). This leads to the generation of surface plasmons which are surface electromagnetic waves that are propagated along the metal

surface. The optical biosensor detects changes in the refractive index at the surface of a sensor chip. The angle of the reflected light depends on the mass of material at the surface layer which therefore shifts when biomolecules bind to it.

The SPR biosensor detects and monitors the changes in resonant angle in real time „as a plot of resonance signal (proportional to mass change) versus time“ (Figure 3.1)[120].

In this experimental setup, a biotinylated double-stranded DNA oligonucleotide was immobilized on the surface of a Streptavidin-coated Biacore SA biosensor chip for measurement of DNA-protein interactions with the MnSOD variants.

For this, a random 34 bp sequence derived from the mitochondrial gene for COX1 was chosen. The 5´-biotinylated strand JH004 and the complementary strand JH005 needed to be annealed prior to binding experiments. 40μl JH004 (10μM) and 40μl JH005 (10μM) were mixed with 360μl 50 mM HEPES 50 mM NaCl, heated for 5 min at 95°C and slowly cooled down to room temperature.

Protein samples (MnSOD variants, TFAM and BSA) were injected in a flow cell to determine DNA binding. The values from a reference flow cell without immobilized DNA were subtracted to the values to eliminate the buffer effects on the refraction index. The flow rate was 10 μl/min with a maximal injection time of 2100s and a subsequent regeneration with NaCl and NaOH containing solutions to check the salt-sensitivity of protein-DNA binding and to regenerate the chip surface.

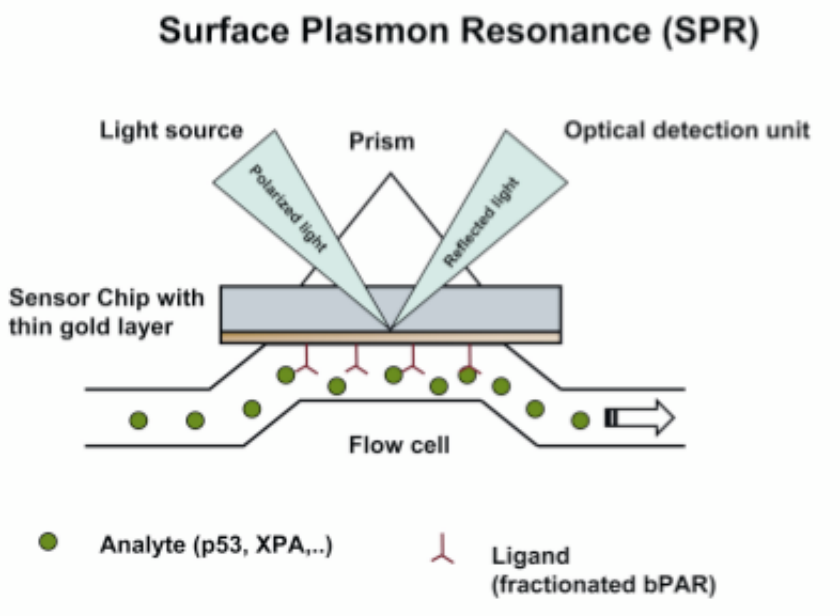

Figure 3.1: Principle of SPR analysis.
From the PhD dissertation of Jörg Fahrer 2007, modified from Cooper et al. [120]

3.2.6 Cell culture

Hela S3 cells were grown in DMEM supplemented with 100 units/ml Penicillin, 100 µg/l Streptomycin, 2 mM L-Glutamin and 10% FBS and RAW264.7 cells were grown in RPMI 1640 medium with pyruvate 100 units/ml Penicillin, 100 µg/l Streptomycin, 2 mM L-Glutamin and 10% FBS. LUHMES cells were cultivated and directly harvested at the Leist laboratory. Optimal growth conditions were provided by changing culture media every 2 days and passaging cells every 4 to 6 days or when cells reached desired confluency. To passage cells, culture media was removed and after 2 washing steps with sterile PBS, cells were detached from the dish or flask by trypsination for 1 to 2 min at 37°C. After centrifugation, cells were resuspended in an appropriate volume of fresh culture media and plated on a new dish or flask.
For immunofluorescence experiments, RAW264.7 cells were grown on cover slips.

3.2.7 Isolation of mitochondria from cultured cells

Mitochondria were isolated from cultured Hela cells, LUHMES cells and RAW264.7 cells, according to the method from the dissertation of Joachim Kienhöfer an adaptation of the protocol of Garrido et al.[47]. Cells were detached from the dishes by scraping or by trypsination in PBS and were collected by centrifugation at 200g. The pellet was resuspended in pre-cooled isolation medium I and disrupted by shear forces in a potter and an electric drill by approximately 100 strokes with the pistil on ice. After the homogenization process, cell disruption was controlled by microscopy. Cell homogenates were then distributed to Falcon tubes, diluted with 1 volume of isolation medium I and centrifuged at 750g for 10 min in the Z233 MK-2 centrifuge at 4°C. The pellet was discarded and the mitochondria-containing supernatant was collected in Eppendorf tubes and further centrifuged at 7,500g for 10 min at 4°C in the Z233 MK-2 centrifuge. The pellet was resuspended in mitochondria resuspension buffer with 0.8 M sucrose and layered on top of a sucrose gradient composed of 1, 1.5 and 2M sucrose in mitochondria gradient buffer, assembled using a syringe with a long needle in a polycarbonate centrifuge tube. The gradient was centrifuged at 80,000g for 2 h with the swinging bucket rotor SW 32 Ti (Optima LE-80K ultra centrifuge). Mitochondria were enriched in the fraction between 1.5 and 2M sucrose and

carefully carefully collected by a pipette. The mitochondria-containg solution was diluted with 2 volumes of mitochondria dilution buffer, pelleted at 16,000g for 15 min (Z233 MK-2 centrifuge) and immediately shock-frozen and stored at - 80°C.

3.2.8 Isolation of mitochondria from Xenopus laevis oocytes

Oocytes were isolated from mature female Xenopus laevis by dissection which was carried out by Oliver Okle. Briefly, the frogs were anesthesized in benzocaine for 25-30 min and after ventral incision, the ovarian lobes were lifted out using forceps. These lobes were cut and oocytes were collected from the oocyte bags and immersed in MBS, $CaCl_2$.
Defolliculation was performed by incubating the open oocyte bags in MBS, 0,1 % $CaCl_2$ collagenase type 1A and shake gently at room temperature until the oocytes are detached from the red-veined follicular coat. After multiple washing steps in MBS1 $CaCl_2$, oocytes were carefully sorted in a culture dish using a Pasteur pipette according to the stage of oogenesis. Figure 3.2 shows the visible aspect of oocytes from different stage 1 to 6. Oocytes from stages 1, 3 and 6 were collected, shock frozen and stored at -80°C.
Frozen oocytes from different frogs were thawed on ice, pooled together and homogenized in isolation medium I using a potter and an electric drill. The following steps were performed as with cultured cells after homogenization (section 3.2.7), with the difference that the two differential centrifugation steps were repeated to remove cell debris completely. After mitochondrial purification with an isopycnic gradient, mitochondria were pelleted, shock frozen and stored at -80°C.

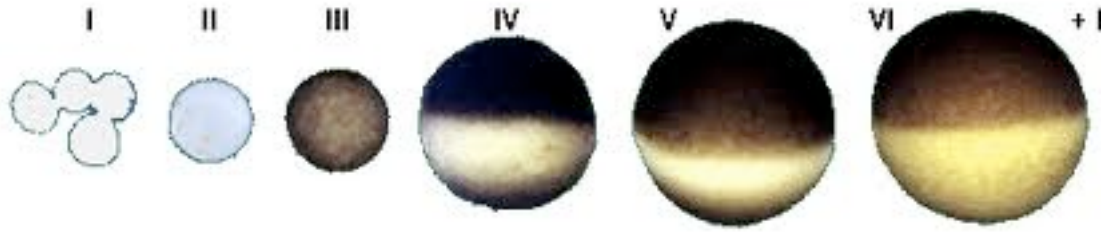

Figure 3.2: Aspect of *Xenopus laevis* oocytes from stages 1 to 6
From *http://www.luc.edu/faculty/wwasser/dev/xenoogen.htm*

3.2.9 Isolation of mitochondria from human platelets

Human peripheral veinous blood was collected from a healthy volunteer using Lithium Heparin and Sodium citrate monovettes. As platelets do not contain nuclei, mitochondrial isolation required a simpler protocol. 50ml blood were centrifuged for at 300g for 15 min at 20°C. The supernatant containing the platelets and proteins was collected and centrifuged at 1,500g for 15 min at 20°C. The pellet was resuspended in 2ml platelet resuspension buffer.

3.2.10 Isolation of mitochondrial nucleoids

Mitochondrial nucleoids were isolated as described in the dissertation of Joachim Kienhöfer, according to a method adapted from Garrido et al.[47]. Isolated mitochondria from cell lines and *Xenopus laevis* oocytes were thawed on ice and resuspended in NE2
buffer. Spermidine was added to a final concentration of 3 mM and mitochondria were lysed by adding 20% NP40 (v/v) to a final concentration of 0.5% (v/v) for 15 min. The lysate was centrifuged at 12,000g for 20 min at 4°C (Z233 MK-2 centrifuge) and separated into supernatant (S) and pellet (P) fractions. The pellet was resuspended in 2ml of NE2 and P and S samples were loaded on top of two sucrose step gradients. The gradient was layered from the bottom to the top (starting with 3,5ml of a 20% sucrose solution, 2,5ml of a 40% solution, 1,8ml of a 60% solution and 0,9ml of a 75% solution) by using a syringe with a long needle in a polycarbonate centrifuge tube (Figure 3.3). The gradients were then centrifuged for 75 min in a swing-bucket rotor SW 32 Ti (Optima LE-80K; 4°C) and were subsequently fractionated into 1ml portions from bottom to top (referred to as P1-P10 and S0-S10). After dialysis against NE2 buffer overnight at 4°C to reduce sucrose concentration, each sample was analysed for protein expression and DNA content by Western Blot analysis and SYBR Green fluorescence. For mtDNA content measurement, 10μl of each P fraction was mixed with 800μl of SYBR Green solution in a 96-well plate. Fluorescence was measured with a Spectra Fluor fluorescence reader at excitation 485nm and emission 535nm.

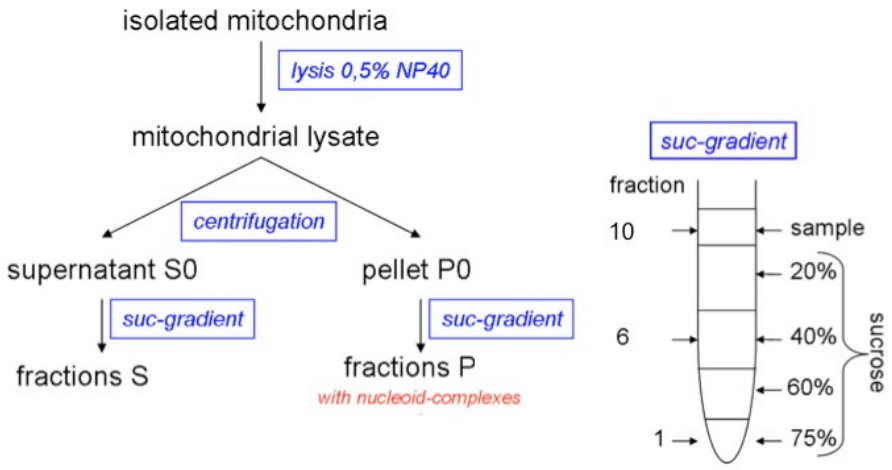

Figure 3.3: Nucleoid isolation procedure and layering of the step gradient
Figure modified from PhD dissertation of Joachim Kienhöfer 2009.

3.2.11 Western Blot analysis

Samples were heated for 5min at 95°C in Laemmli loading buffer and loaded onto 12 % polyacrylamide gels. They were then subjected to the standard SDS polyacrylamide gel electrophoresis (SDS-PAGE) with a running time of ~2 h at 125 V. After gel electrophoresis, proteins were transferred on a nitrocellulose membrane by the semi-dry transfer method for 2 h at 0.8 mA/cm at a maximum of 10V (constant current). The transfer over proteins onto the membrane was verified by Ponceau staining. The membrane was blocked for 1 hour with TBS-T 5% milk to reduce unspecific binding of the antibodies. It was then probed for the protein of interest with a specific primary antibody diluted in TBS-T 1% milk. Primary antibody dilutions were as follows: anti-MnSOD 1:5000, anti-TFAM 1:5000 and anti-N-Tyr 1:1000. The membrane was incubated with the antibody solution for 1 h at room temperature or overnight at 4°C under rotation. It was then washed 3 x 10 min with TBS-T under gentle agitation and probed with goat anti-mouse or goat anti-rabbit secondary for 1 h antibody diluted in TBS-T 1% milk. Secondary antibodies were diluted 1:5000. The membrane was washed th3 x 10 min with TBS-T and 1 ml of ECL solution (500μl of ECL solution A + 500μl of ECL solution B) was distributed evenly over the membrane. Chemiluminiscence was detected with FujiLAS 1000 imaging station with various exposure
times (ranging from 5 sec to 8 min). When using the anti N-Tyr antibody, chemiluminescence was detected in the dark room by applying an X-ray film on the membrane, followed by the

development, washing and fixation of the X-ray film.

3.2.12 Coomassie staining

After electrophoresis, polyacrylamide gels were washed twice for 15 min with H_2O and incubated for 3 hours with 25 ml coomassie brilliant blue staining solution in a closed box at room temperature. The gels were then washed with H_2O 3 x 5 min and incubated with the destaining solution overnight.

3.2.13 Detection of 8-oxodG in plasmid DNA by the Fpg-based FADU method

Preliminary work from Joachim Kienhöfer allowed an optimization of a new Fpg-based method to detect 8-oxodG, using a modified protocol of the automated Fluorimetric Detection of Alkaline Unwinding (FADU) established by Moreno-Villanueva et al. [121]. The original method offered a quantitative detection of DNA single strand breaks in whole cells as a correlation of the partial denaturation/unwinding of double stranded DNA under controlled alkaline conditions. After cell lysis, cells are subjected to an alkaline buffer which unwinds double-stranded DNA under strong alkaline conditions. This unwinding can only be initiated at sites of open DNA, in other words, sites of single strand breaks. This process is stopped by the use of neutralization buffer and the addition of the fluorophor SybrGreen, which solely fluoresces after binding to double stranded DNA, allows the assessment of DNA integrity as a direct correlation with fluorescence intensity. Low fluorescence intensities therefore indicate the presence of a high number of single strand breaks. The T (total) values represent the total amount of double stranded DNA and are obtained by immediately stooping the unwinding by adding neutralization buffer. The P (partial) values represent the partial unwinding increasing with the number of DNA strand breaks. The relative P/T fluorescence ratio is the quantitative measurement of DNA integrity in respect to DNA strand breaks.
In this work, the FADU method was applied to the detection of 8-oxodG directly in plasmid DNA. A preliminary Fpg incubation step has been added to the original protocol in order to adjust it to the specific detection of 8-oxodG lesions. Indeed, the Fpg enzyme specifically recognizes these lesions and removes them from the DNA double-strand, therefore generating a one base gap with a 5´ and 3´ phosphate, via its AP-lyase activity. This gap is similar to a single-strand break and therefore can be detected by the FADU method (Figure 3.4).

As a DNA model system, a 14-kbp plasmid (pAcHLT-A-His6) was amplified in Escherichia coli DH5 cells and extracted using a DNA purification Giga Prep Kit (Qiagen). Each DNA sample was prepared in triplicates of 104μg. Samples were supplemented with uric acid, MnSOD (Ab Frontier), the purified MnSOD variants, minocycline, gentamicin and tetracycline and treated with 100-400μM freshly prepared Sin-1 (Calbiochem) for 40mn at 30°C. They were then distributed into fractions of 4μg and 100μg DNA for FADU and LC-MS analyses respectively.

Each sample was incubated with 8U Fpg and 10X NEB1 Buffer (New England Biolabs) for 30mn at 30°C. Samples were diluted in 280μL Suspension Buffer (250 mM meso-inositol 10 mM sodium phosphate 1 mM MgCl, pH 7,4) and quadruplicates were transferred into a 96-well plate which was positioned into the working space of the robot.

The liquid handling device as well as its positioning were identical as in Moreno-Villanueva et al.[122] The general procedure was conserved with a few minor changes in order to optimize the method for this application. The temperature of the cooling device was maintained at -5°C throughout the entire experiment. 70μL of Lysis Buffer (9 M urea; 10 mM NaOH; 2.5 mM cyclohexyl- diamine-tetraacetate; 0.1% sodium dodecyl sulphate) were dispensed into each well. In contrast to the initial protocol from Moreno-Villanueva et al., there was no incubation time and 70μL of alkaline buffer (0.425 parts lysis solution in 0.2 M NaOH) were added immediately thereafter. Again, the subsequent incubation step was omitted in order to avoid a total unwinding of the plasmid. A volume of 140 µl of neutralization buffer (14 mM β-mercaptoethanol; 1 M glucose) was added at a rate of 200 µl/s. Finally, 156μL of SybrGreen® (MoBiTec, Göttingen, Germany) diluted 1:8,333 in water were dispensed and samples were mixed by pipetting a volume of 400 µl up and down at a rate of 100 µl/s. The read out of the fluorescence was performed in a 96-well-plate fluorescence reader at 492 nm excitation/520 nm emission.

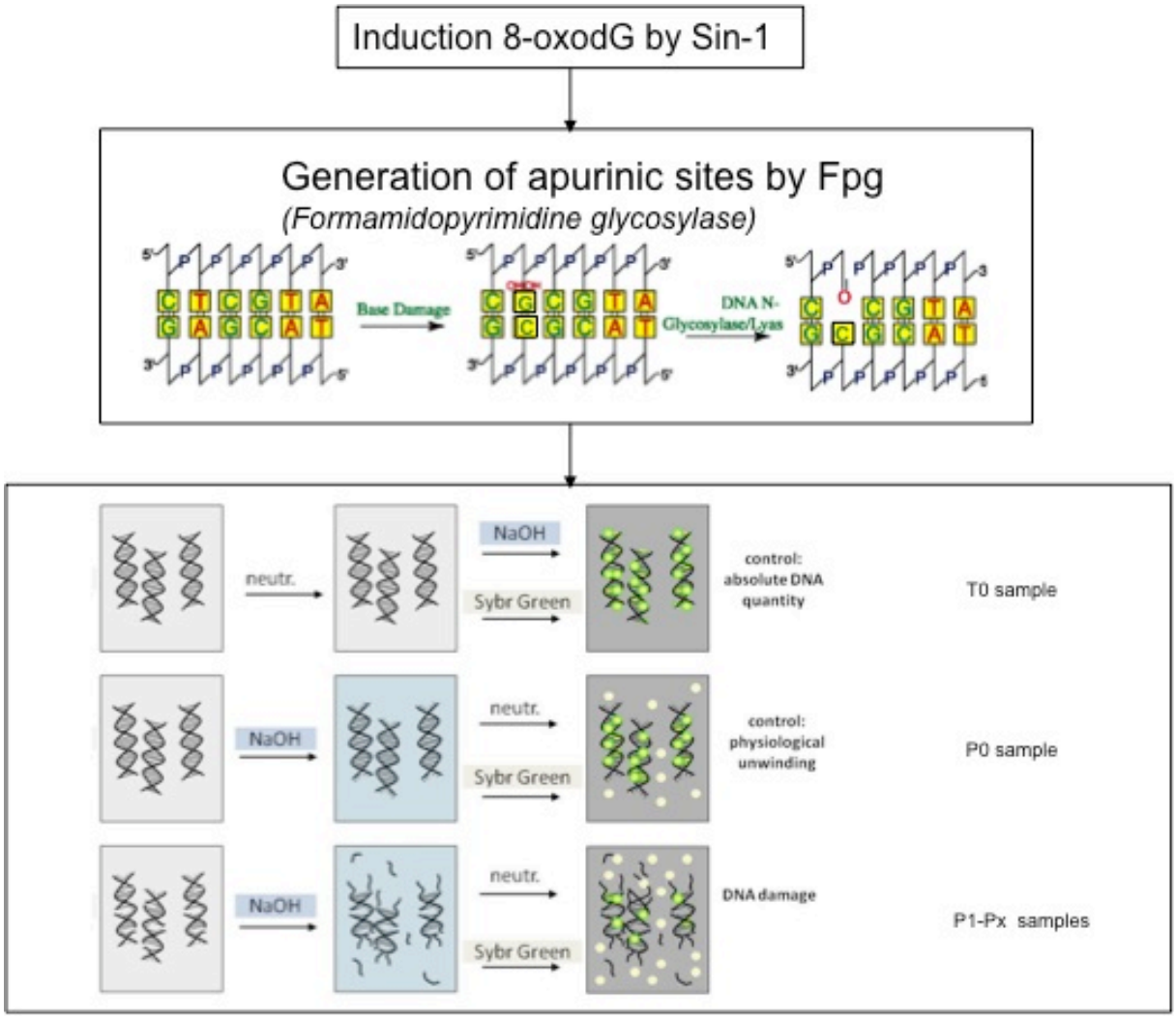

Figure 3.4: Basic principle of the Fpg- based FADU assay for the detection of 8-oxodG
Figure modified from PhD dissertation of Maria Moreno-Villanueva 2007.

3.2.14 Detection of 8-oxodG in plasmid DNA by HPLC coupled with LC/MS

Sample digestion, HPLC prepurification and LC-MS measurements were performed by Arthur Fischbach, in cooperation with Aswin Mangerich (except for results depicted in Figure 4.7).

Samples were treated as described in section 3.2.13.

DNA Digestion

The sample preparation is based on a modified protocol from Taghizadeh, McFaline et al. [123]. Nucleosides were obtained by enzymatic digestion of the DNA in 16mM sodium acetate pH 6.8, 1,8 mM ZnCl2 , 0,36 mg/ml Nuclease P1 (Sigma Aldrich), 73 μg/ml DNase I (Roche) for

3 hours at 37°C. Desferroxamine (0,1 mM) and Butylated Hdroxylene (0,1mM) were included to prevent artifactual oxidative damage. Samples were then incubated in 21,8 mM sodium acetate buffer pH 7.8, 200 KU phosphodiesterase I (US Biological) 34KU Alkaline phosphatase (Sigma-Aldrich) overnight at 37°C. Enzymes were then removed by centrifugation at 16,400 × *g* for 20mn through a 10,000 MW cut-off spin filter.

Reverse phase HPLC prepurification

A LC-10AT HPLC system from Shimadzu was used for 8-oxodG prepurification equipped with a Phenomenex Synergi 4-μm Hydro-RP C18 80A (250 mm x 4.6 mm) column. A solvent gradient of acetonitrile in 8 mM ammonium acetate was set at a flow rate 0.7 ml/min (Table of gradient composition included in Supplemental Figures). The detection was enabled by coupled UV-VIS spectroscopy at 260 nm.The 8-oxodG containing fractions were collected at a retention time of approx. 37-42 min.

LC MS Measurement

The collected 8-oxodG fractions were dried in the speedvac and dissolved in 50 μl MilliQ water. 22.5 μl were injected into the LC/MS-MS (see section 3.2.7). Directly, after measuring the samples, a standard curve was created. All measurements were performed in technical duplicates.

3.2.15 Extraction of mtDNA from RAW264.7 cells

Mitochondria were isolated as described in section 3.2.7 from RAW264.7 cells harvested from 12 150 cm^2 flasks and frozen at 80°C. Mitochondria were thawed on ice and each pellet was resuspended in 1ml mitochondrial lysis buffer and incubated for 30 min at 4°C. Addition of 4μl Rnase 10mg/ml was essential to eliminate contaminating RNA and incubation was carried out for 30 min 37°C under gentle agitation. 1 volume of phenol was added to each sample and followed by an incubation of 5 min at room temperature. After a centrifugation of 1 min at 12,500rpm (Z233 MK-2 centrifuge), 1 volume of chlorofom was added to the top phase. After an incubation of 5 min at room temperature, the samples were centrifuged for 1 min at 12,500rpm and the top phase was collected. The washing step with chloroform was performed a second time. The resulting top phase was mixed with 3 volumes of ethanol 10% sodium acetate 3M and incubated overnight at -20°C. Samples were centrifuged for 1 h at 12500rpm at 4°C and the resulting DNA pellet was air-dried, then resuspended in 120μL

H_2O. DNA concentration was measured using a photometer and purity was verified by calculating the Abs_{260nm}/Abs_{280nm} ratio.

3.2.16 PCR amplification of mtDNA

In order to check for the presence of contaminating nuclear DNA in mtDNA samples isolated from RAW264.7 cells, a PCR experiment was conducted for the amplification of a mitochondrial and a nuclear DNA sequence. Primers for the murine PARP1 sequence (AMa030 and AMa032) and for the murine ND5 sequence (NM01 and NM02) were used for nuclear and mitochondrial DNA amplification respectively.
For each test tube, a reaction volume of 10μl was composed of 1μl DNA sample, 0,7μl forward primer, 0,7μl reverse primer and 7,6μl master mix. The conditons of PCR were 94°C 2 min, 62°C 20 s, 68°C 1 min, (23 cycles of 94°C 20 s, 62°C 20 s, 68°C 1 min) 68°C 10 min. The products of the PCR amplification were verified by agarose gel electrophoresis.

3.2.17 Agarose gel electrophoresis

The amplification products of the PCR from mtDNA samples to which 6X loading buffer was added were run on a 2% agarose gel in TAE buffer at 80V for 2 h alongside a marker. To visualize DNA, the gel was stained with ethidium bromide for 10 min, washed in water and analyzed by UV light at 254nm. Pictures were taken using the INTAS camera and software.

3.2.18 MnSOD treatment with peroxynitrite and Sin-1 and SOD activity assay

Samples containing 1μg of recombinant commercial MnSOD (Ab Frontier) in KPO_4 buffer (pH 7,4) were treated with final concentrations of 10μM to 1mM PON. For every volume of added PON, the same volume of HCl was added simultaneously and immediately vortexed. Treatment with 400μM Sin-1 was followed by an incubation of 40 min at 30°C.
A fraction of each sample (containing 0,2μg MnSOD) was used for triplicate measurement of the activity and the remaining fraction was used for Western Blot analysis of nitro-tyrosine expression (see 3.2.11).
SOD activity was measured with the SOD assay kit (Fluka) according to the manufacturer's instructions.

3.2.19 Immunofluorescence

Raw264.7 cells were grown on cover slips until approximately 75% confluency and treated for 2 to 22 h with 10μg/ml LPS in the growth medium or for 10 min with 1mM Sin-1 in PBS. Cells were fixed in PBS 2% Paraformaldehyde for 30 min at room temperature. After 3 x 2 min washing steps in PBS, cells were permeabilized in PBS 0,1% Triton X100 for 5 min at 4°C, then washed again with TBS 3 x 2 min. Proteinblock DakoCytom. solution was distributed over cover slips which then incubated for 30 min at room temperature. This was followed by an incubation overnight at 4°C with rabbit polyclonal anti-8-nitroguanine antibody diluted 1:200 in antibody diluent. The antibody solution was then washed off by 3 x 2 min washing steps with PBS and the secondary antibody (goat anti-rabbit Alexa 488) diluted 1:400 in antibody diluent was applied for 45 min at 37°C. After 3 x 5 min washing in PBS, samples were incubated in Hoechst diluted 1:25,000 in PBS for 5 min at room temperature. After final washing steps of 3 x 5 min in PBS, the cover slips were mounted with Aqua polymount and stored at 4°C. The glass slides were observed using a Zeiss Axiovert 200M Fluorescence Microscope and images were taken by the on-board camera and analyzed with the AxioVision software.

4 Results

4.1 Manganese Superoxide Dismutase association with mitochondrial DNA

4.1.1 The Nature of Manganese Superoxide Dismutase binding to mitochondrial DNA

MnSOD binding to DNA was shown to be direct and salt-sensitive by a slot blot filter binding assay, suggesting the involvement of an ionic interaction between both biomolecules[124]. Two C-terminal lysine residues are highly conserved among species but exhibit a role neither in enzymatic activity nor in the structure of the enzyme. These are therefore legitimate candidates for a potential role in binding to mtDNA. A third lysine displaying a conformational accessibility at the N-terminus of the protein could also be involved in this process. This led to the investigation of the DNA binding properties of human MnSOD variants of these specific lysines by site-directed mutagenesis. The mutagenesis was successfully conducted by Janina Haar during her Master thesis in our group. The MnSOD variants displayed alanine, glutamine or glutamate residues in exchange of lysines. The mutants were labeled according to their mutated residue KH-KK (wild-type), KH-AA, KH-QQ, KH-EE, QH-KK, QH-EE, QH-QQ. After protein expression, purification and His-tag cleavage, real-time binding measurements were performed by a a surface plasmon resonance (SPR) based method.

In the present work, a few modifications have been made compared to the initial work of Janina Haar as a few minor setbacks had prevented the completion of the experiments. First, protein expression was carried out in medium supplemented with $MnSO_4$ as a source of Mn ions for incorporation into the catalytic domain of the enzyme, which led to a 2,8-fold increase of MnSOD activity (data not shown). Secondly, the amount of purified protein was increased 10-fold, by increasing volumes of bacterial expression and by using Cobalt affinity purification columns with a higher capacity. The final PBS buffer was replaced by a Hepes buffer devoid of salt. All of the different mutated plasmids generated by Janina Haar MnSOD were used for E. coli transformation and subsequent protein expression, which lead to the purification of seven different mutants instead of four. Finally, a few changes have been made in the SPR measurements.

Real time binding measurements were conducted on a SA certified Sensor Chip on which an annealed biotinylated 34 bp oligomer was immobilized by streptavidin-coupling in a Biacore T100 device.

All protein solutions were adjusted to a same concentration of 0,9mg/ml and flow rate was constant at 10μL/min.

The specificity of MnSOD and TFAM binding was confirmed by the lack of interaction of BSA with the surface of the chip (data not shown).

The injection of TFAM into the flow cell of the chip led to an immediate and high increase in response units (RU) of about 950 RU. TFAM binding was very strong, as its dissociation required multiple successive injections of a solution of 2M NaCl and 50mM NaOH (Figure 4.1 panel A).

Commercial recombinant E. coli MnSOD led to a more moderate increase in response units (about 470 RU) and no saturation was observed after a long injection time (Figure 4.1 panel B). The binding was disrupted by addition of 50mM NaCl.

The binding curve of purified human wild type MnSOD exhibited a weak slope and after the maximal injection time allowed by the Biacore T100 device (2100s), no saturation was attained (Figure 4.1 A). This was also the case when testing different protein dilutions and different flow rates (data not shown). In order to assess the binding capacity of a protein through the calculation of the constant of dissociation (Kd), it is essential to procede to kinetic studies at different protein concentrations. Without a saturation, such studies cannot be carried out and it is not possible to compare binding affinity between different proteins.

The only experiment in which saturation was reached with MnSOD was in the case of the MnSOD KH-EE mutant after 1800s (Figure 4.1 panel D). However, after saturation, a spontaneous dissociation appeared in a gradual manner. The MnSOD variant QH-QQ in which all three lysines were mutated also exhibited binding activity, therefore it can be concluded that MnSOD binding to DNA does not depend solely on these three lysines (Figure 4.1 panel E). Without kinetic studies, it is not possible to compare binding affinities between these mutants and the wild type enzyme and so, we cannot draw further conclusions on the involvement of these residues in the binding. The MnSOD mutants QH-KK and KH-QQ also displayed DNA binding without saturation after the maximal injection time of 2100s (Figure 4.1 panels F-J) and different concentrations of KH-QQ were injected in the flow cell (Figure 4.1 panels G-J).

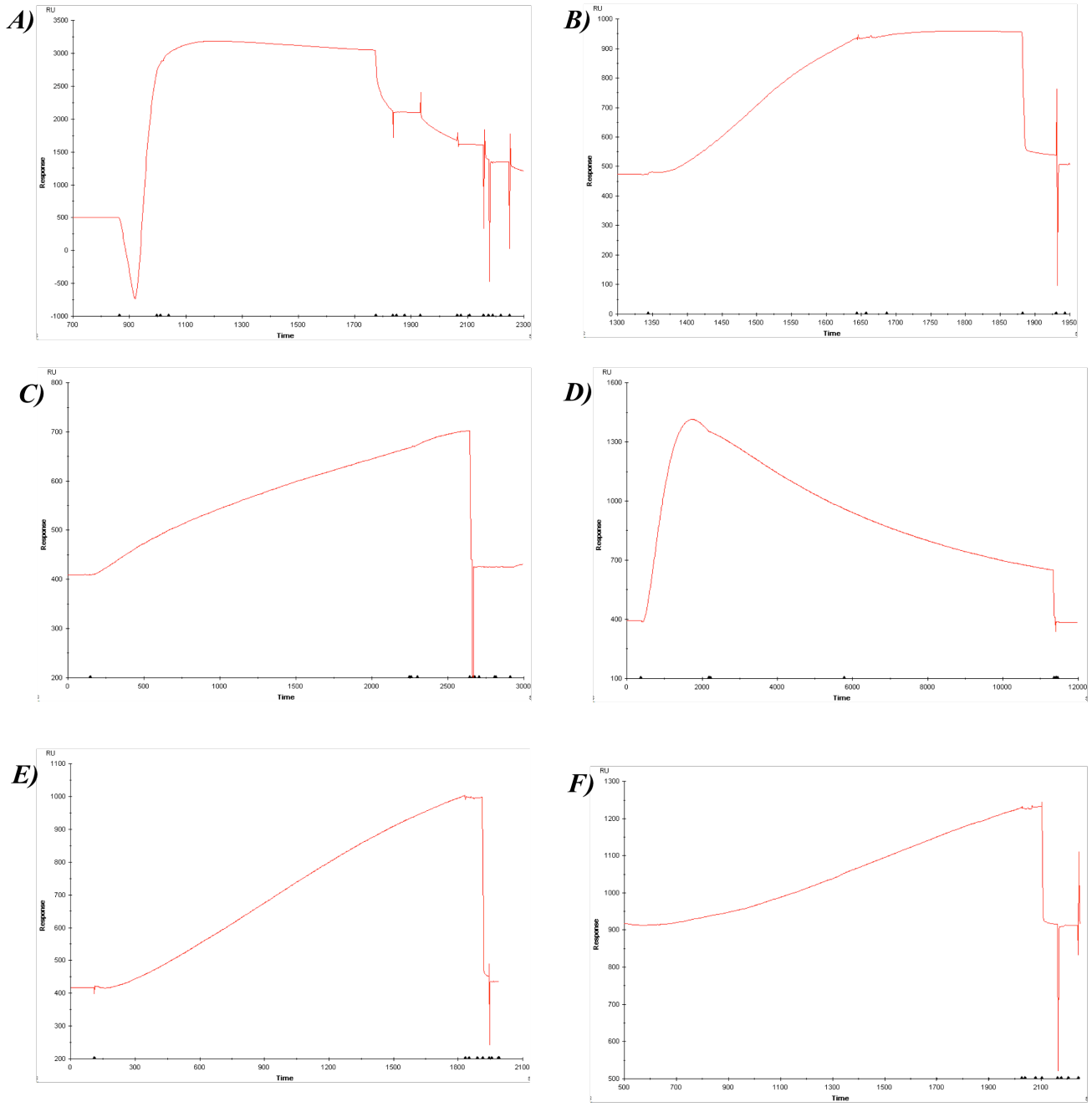
A)
B)
C)
D)
E)
F)
RU
Response
Time

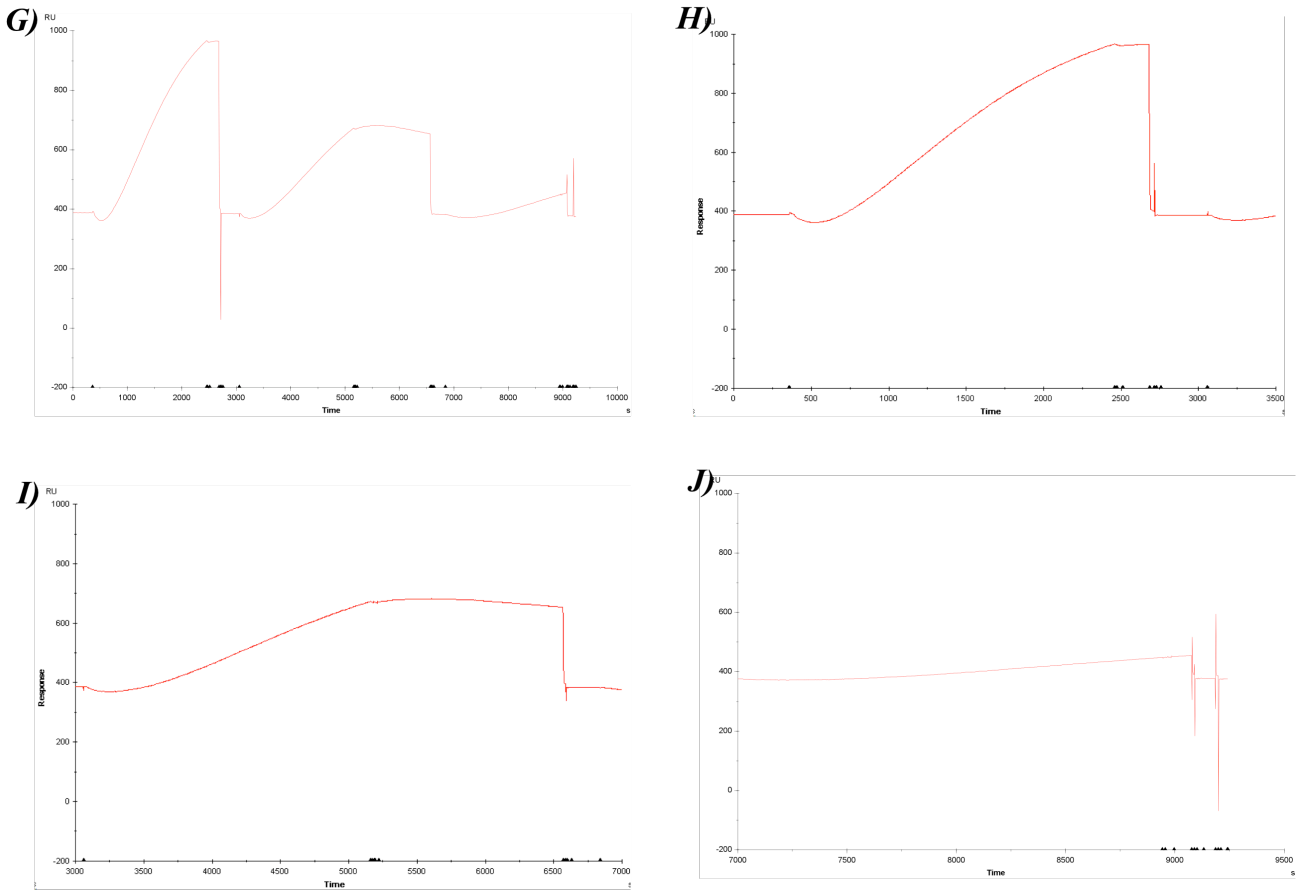

Figure 4.1 : SPR binding analysis of TFAM and different MnSOD variants with DNA 34-mer
Sensorgrams depict binding experiments over a 34-mer DNA of (A) TFAM (B) E.coli MnSOD (C) MnSOD wt (D) MnSOD KH-EE (E) MnSOD QH-QQ (F) MnSOD QH-KK (G-J) MnSOD KH-QQ at different dilutions(1, ½, 1/5). It should be noted that the scale of the axes varies between sensorgrams.

4.1.2 The physiological significance of Manganese Superoxide Dismutase association with mitochondrial DNA

Joachim Kienhöfer has detected the presence of MnSOD in nucleoids in mitochondria of rat and bovine heart, human smooth muscle cells and Jurkat cells whereas no such association was detected in bovine endothelial cells[124]. We therefore further investigated the association of MnSOD to mtDNA in additional cell models in order to acquire information on its possible physiological significance.

The protocol from Garrido et al. modified by Joachim Kienhöfer was applied to the isolation of nucleoids in mitochondria from Hela, LUHMES and Xenopus oocytes of different stages[47] (method described in Material and Methods section). Briefly, mitochondria isolated from

cultured cells or oocytes were lysed and subjected to differential centrifugation leading to the separation of the mitochondrial constituents into supernatant and pellet fractions. These samples were loaded on an isopycnic sucrose gradient and fractionated by ultracentrifugation. Portions of 1ml were gently collected from bottom to top and analyzed for DNA and protein content.

By SYBR Green fluorescence reading, mtDNA was shown to be present only in P fractions and localized mainly in the bottom fractions of the gradient which have the higher sucrose density. Free proteins are found mostly in the S fractions and exclusively located in the low density upper fractions, such as the matrix protein fumarate hydratase (data not shown). TFAM is a mitochondrial protein that is exclusively bound to mtDNA, as the unbound form is immediately degraded. Therefore, the presence of TFAM and mtDNA in the same fractions is a clear indication of the presence of nucleoids.

In nucleoid isolation of Hela cells, TFAM expression detected by Western Blot and the presence of DNA detected by SYBR Green fluorescence are limited to fractions 1-4 of the P samples and constitute the nucleoid fractions (Figure 4.2). No signal was detected for MnSOD in P fractions by Western Blot (data not shown) but MnSOD was found present in S7-10, suggesting that MnSOD is not bound to mtDNA in Hela cells.

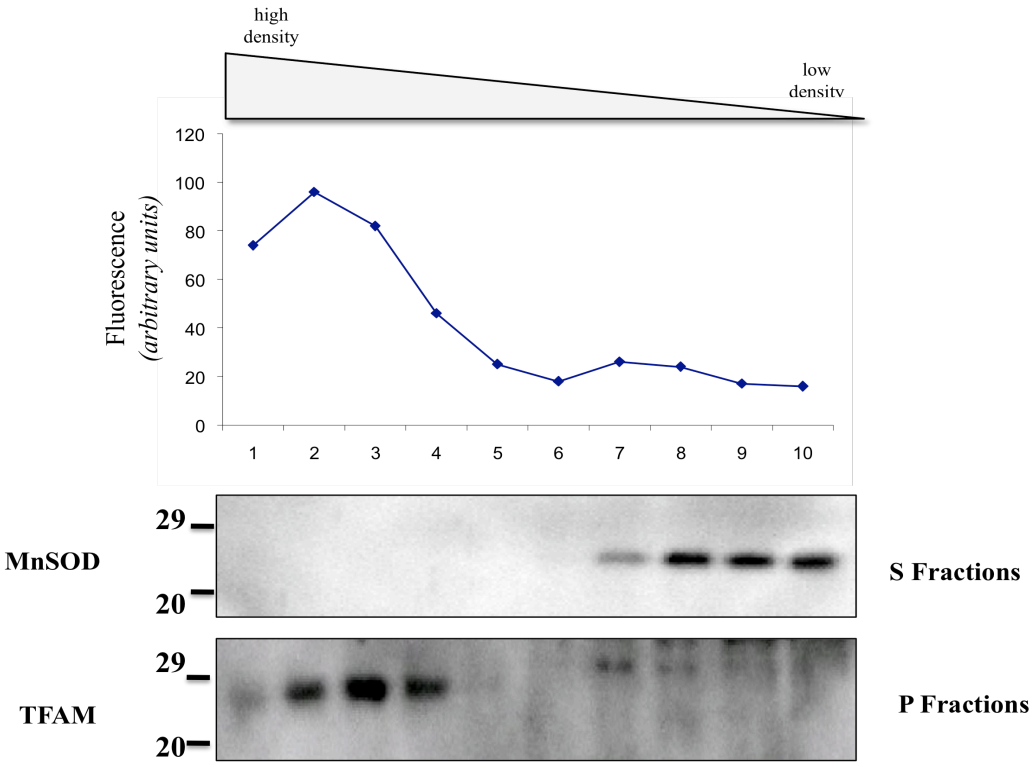

Figure 4.2 : Isolation of nucleoids in Hela cells

Nucleoids were purified from Hela cell mitochondria by step gradient and DNA content was measured in P fractions by SYBR Green fluorescence. All fractions were analyzed for protein expression of MnSOD and TFAM by Western Blot analysis.

LUHMES cells are a human dopaminergic neuronal cell line established by the Leist laboratory (University of Konstanz) that serves as an *in vitro* model for Parkinson's disease [125].

The nucleoid isolation in these cells and the subsequent DNA and TFAM detection allows the identification of the nucleoid containing fractions in P1-4 (Figure 4.3). MnSOD was absent in these fractions and only detected in S6-9 and is therefore only present in its unbound form in this cell line.

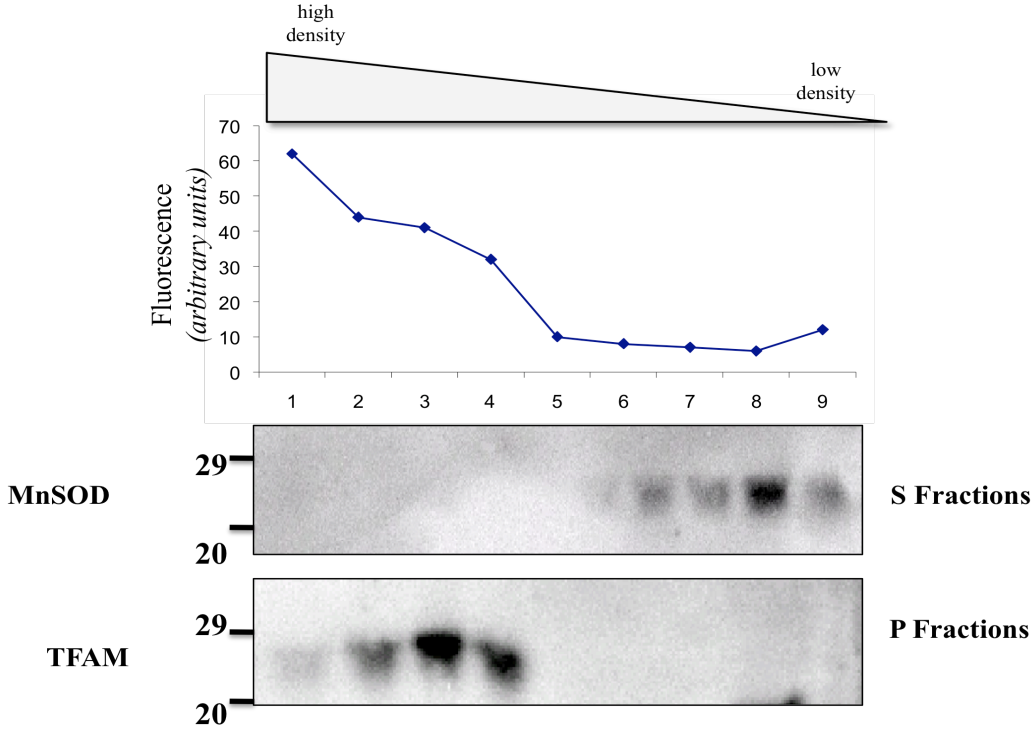

Figure 4.3 : Isolation of nucleoids in LUHMES cells
Nucleoids were purified from stage LUHMES cell mitochondria by step gradient and DNA content was measured in P fractions by SYBR Green fluorescence. All fractions were analyzed for protein expression of MnSOD and TFAM by Western Blot analysis.
In cooperation with S. Schildknecht.

During oogenesis in *Xenopus* laevis, the nucleoid composition is subjected to reorganization, as suggested by the finding that TFAM content increases during this process [48]. This led to the investigation of the binding of MnSOD to mtDNA at different stages of oogenesis. Oocytes were isolated from the ovaries of sexually mature *Xenopus laevis* (surgery conducted by

Oliver Okle) and were sorted one by one into three groups, according to their stage of development: stages 1, 3 and 6 (stage 6 being the final stage).

In stage 1 oocytes, nucleoid fractions were identified as being fractions P1-3, according to TFAM and DNA content (Figure 4.4). MnSOD was detected by Western Blot analysis in high density S fractions but also in all P fractions, including the nucleoid containing fractions. MnSOD is therefore present in the mtDNA-bound form and in the unbound form in stage 1 Xenopus oocytes.

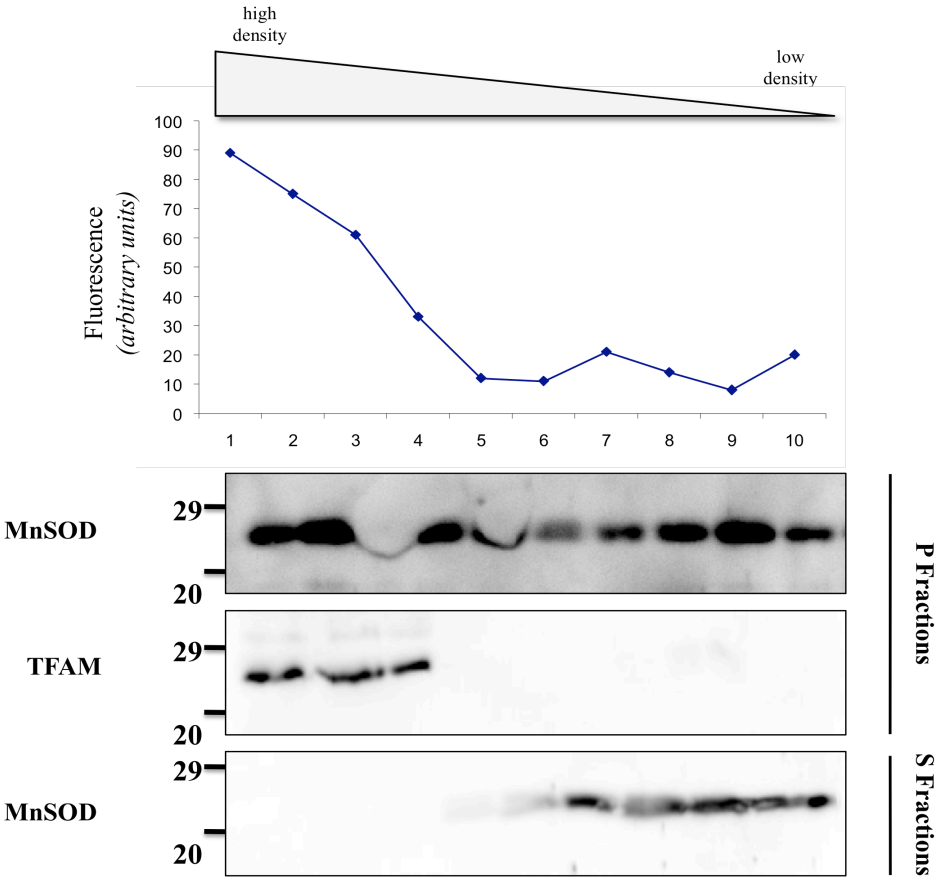

Figure 4.4 : Isolation of nucleoids in Stage 1 *Xenopus laevis* oocytes
Nucleoids were purified from stage 1 *Xenopus laevis* oocyte mitochondria by step gradient and DNA content was measured in P fractions by SYBR Green fluorescence. All fractions were analyzed for protein expression of MnSOD and TFAM by Western Blot analysis.
In cooperation with O. Okle.

Nucleoid isolation of stage 3 oocytes exhibited a different distribution in MnSOD protein expression (Figure 4.5). An unexplained peak in SYBR green fluorescence was measured in fraction 9 but was not measured in reproductions of this experiment and will therefore be ignored. Nucleoids were identified as being contained in fractions P1-4 and MnSOD was only detected in S8-10 fractions, suggesting a lack of association of the enzyme to mtDNA.

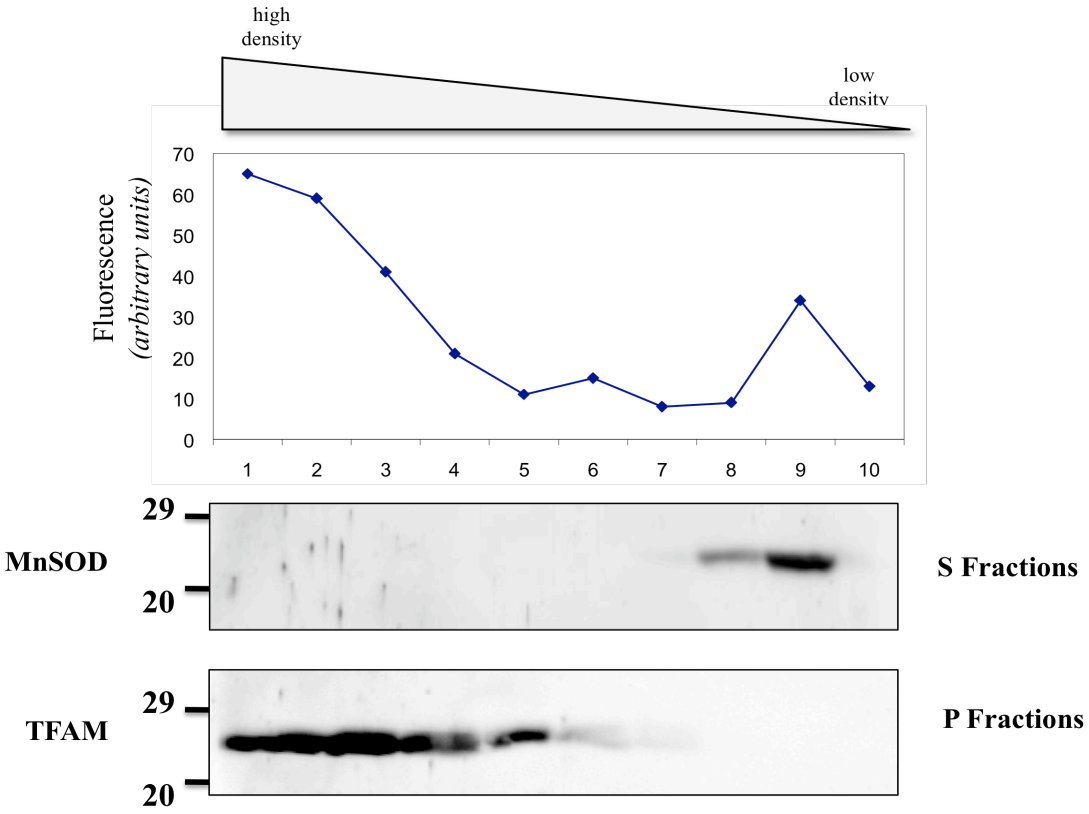

Figure 4.5 : Isolation of nucleoids in Stage 3 *Xenopus laevis* oocytes
Nucleoids were purified from stage 3 *Xenopus laevis* oocyte mitochondria by step gradient and DNA content was measured in P fractions by SYBR Green fluorescence. All fractions were were analyzed for protein expression of MnSOD and TFAM by Western Blot analysis. In cooperation with O. Okle.

In the final stage of oogenesis, nucleoid isolation of the oocytes lead to the detection of nucleoids in fractions P3-6 and MnSOD was present in P3-10 and in S6-10 (Figure 4.6). TFAM was surprisingly also present in low density fractions P7-P10 devoid of mtDNA. The fact that free TFAM is also present in the nucleoid preparations is most likely explained by a detachment from mtDNA during isolation rather than its actual presence in the unbound form in the mitochondrial matrix.

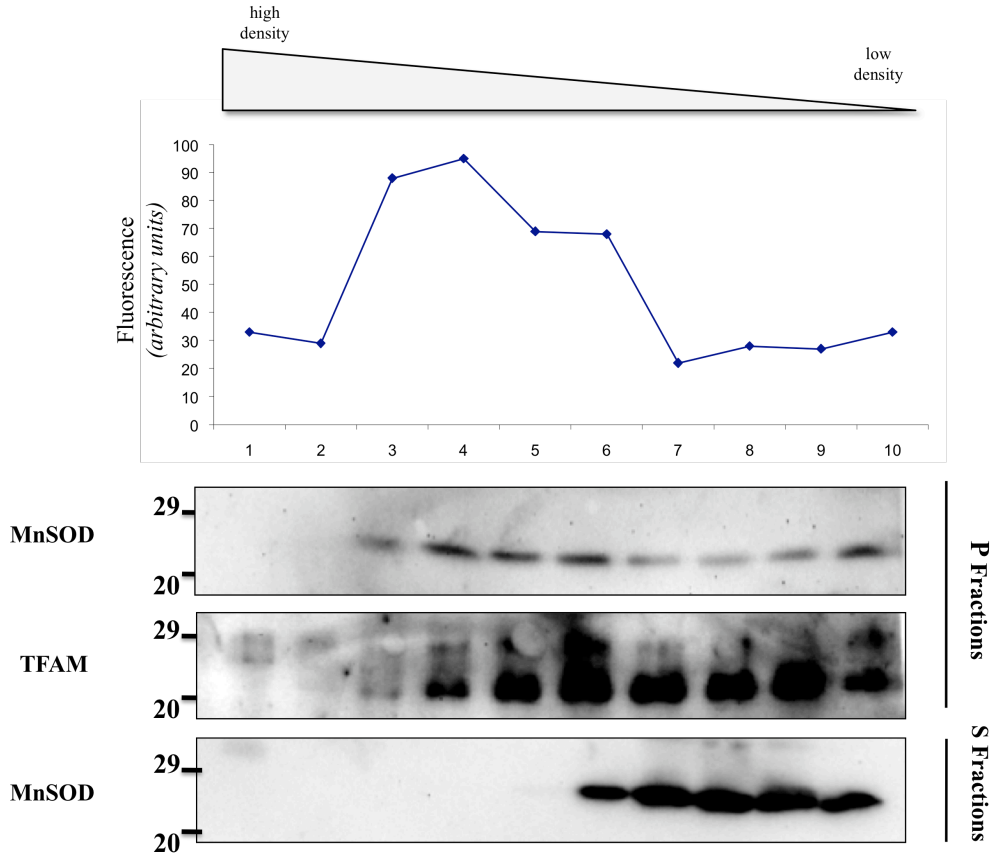

Figure 4.6 : Isolation of nucleoids in Stage 6 *Xenopus laevis* oocytes
Nucleoids were purified from stage 6 *Xenopus laevis* oocyte mitochondria by step gradient and DNA content was measured in P fractions by SYBR Green fluorescence. All fractions were analyzed for protein expression of MnSOD and TFAM by Western Blot analysis.
In cooperation with O. Okle.

To summarize, MnSOD most likely does not associate with mtDNA in Hela and LUHMES cells while it displays differential binding in *Xenopus laevis* oocytes, depending on the stage of development.

4.1.3 Does bound MnSOD confer an enhanced protection compared to unbound MnSOD ?

MnSOD binds to mtDNA in a salt-sensitive manner, suggesting the involvement of ionic forces in the interaction and has been shown to be associated to mtDNA in certain cell models while being dissociated in others. The hypothesis that bound MnSOD is more effective in preventing oxidative damage to mtDNA than the unbound form needs to be validated. For this purpose, we have developed a method for detecting 8-oxodG using a modified protocol of the automated Fluorimetric Detection of Alkaline Unwinding (FADU); the establishment, validation and application of this technique being the focus of chapter 4.2 of the Results

section. The aim was to compare the scavenging efficiency of bound and unbound MnSOD against 3-morpholinosydnonimine (Sin-1) induced 8-oxodG lesions in plasmid DNA.

The assessment of the difference in binding affinity among the MnSOD mutants was unfortunately not possible. Nevertheless, these MnSOD variants were tested for O_2^- scavenging by the modified FADU method. MnSOD mutant concentrations were adjusted to obtain the same enzyme activity and were incubated with plasmid samples prior to Sin-1 treatment. All MnSOD variants displayed a similar protection against Sin-1 induced 8-oxodG and MnSOD QH-KK was the only enzyme to exhibit a slight yet significantly less efficient antioxidant capacity than its wild type counterpart.

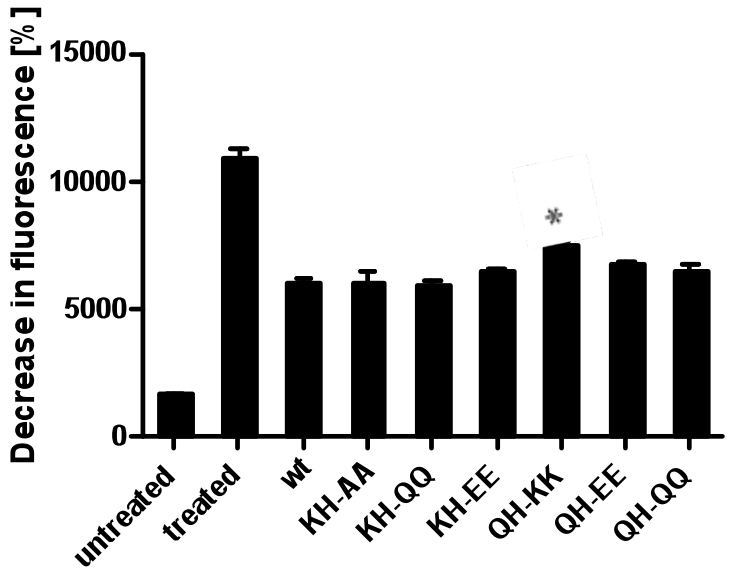

Figure 4.7 : Effect of lysine mutations of MnSOD on the protection against Sin-1 induced 8-oxodG levels in plasmid DNA

Plasmid DNA samples were pre-incubated with MnSOD and 200mM NaCl and treated with 400μM Sin-1. 8-oxodG levels were measured by FADU.

Data are indicated as fractions of fluorescence (FADU) and expressed as the means ± S.D. n=4. Statistical significance of ∗ values is determined by one-way ANOVA and Bonferroni's post-hoc test, $p < 0,05$ vs wt MnSOD.

The mutated MnSOD enzymes did not constitute an appropriate model for comparing activities of the bound and unbound forms as information concerning their binding affinities was still lacking.

Experiments using NaCl to cause MnSOD dissociation from DNA were unfortunately inconclusive with the modified FADU assay, as they showed many discrepancies (data not shown). The fact that the method is not suited for high salt concentrations will be further discussed in chapter 5.2 of the Discussion section.

Preliminary data in which 8-oxodG lesions were measured by HPLC coupled with LC-MS in plasmid DNA treated with Sin-1 in the presence or not of MnSOD and NaCl are presented in Figure 4.8. In the presence of 200mM NaCl, MnSOD protection of DNA against Sin-1 induced 8-oxodG was slightly reduced which is consistent with the hypothesis that unbound MnSOD is less efficient in protecting DNA from oxidative damage. However, these results must be taken with precaution as they have only been performed once and NaCl may also interfere with this method by affecting enzyme activity during the preliminary DNA digestion steps or the retention time during HPLC pre-purification.

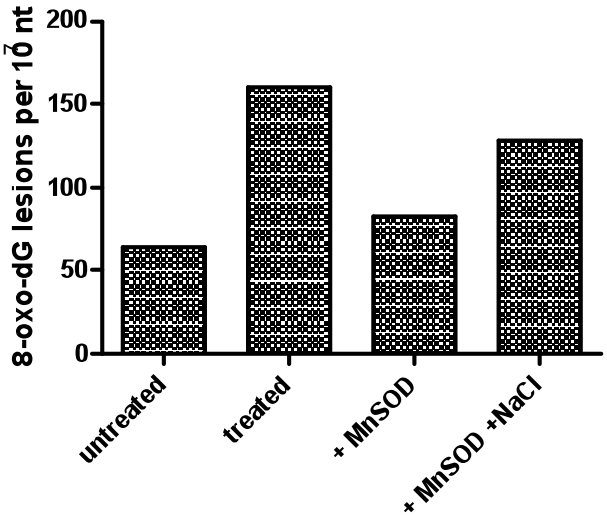

Figure 4. 8 : Effect of NaCl on the protection of MnSOD against in Sin-1 induced 8-oxodG levels in plasmid DNA
Plasmid DNA samples were pre-incubated with MnSOD and 200mM NaCl and treated with 400μM Sin-1. 8-oxodG were measured by HPLC-couples LC/MS.
(experiment was performed one time)

4.2 An automated formamidopyrimidine glycosylase (Fpg)-based FADU method for the detection of 8-oxodG lesions in a plasmid DNA model

4.2.1 Measurement of Sin-1 induced 8-oxodG formation by a Fpg-based FADU method

The measurement of 8-oxodG in nuclear and mitochondrial DNA has received extensive attention and many methods have been developed over the last three decades (further information concerning existing methods available in the Discussion section). Within this wide panel of detection methods, many drawbacks have been reported, including the accumulation of artifactual 8-oxodG formation during sample preparation, the large amounts of DNA required and the many steps involved for each measurement.

Preliminary work from Joachim Kienhöfer allowed an optimization of a new Fpg-based method to detect 8-oxodG, using a modified protocol of the automated Fluorimetric Detection of Alkaline Unwinding (FADU) established by Moreno-Villanueva et al.[121]. The original method offered a quantitative detection of DNA single strand breaks in whole cells as a correlation of the partial denaturation/unwinding of double stranded DNA under controlled alkaline conditions (details of the method in the Material and Methods section). In short, after lysis, cells are subjected to an alkaline buffer, which unwinds the double stranded DNA at the sites of single strand breaks. The addition of the fluorescent probe SYBR Green allows a quantitation of the state of the unwinding; low fluorescence intensities therefore indirectly indicate the presence of a high number of single strand breaks.

A preliminary Fpg incubation step has been added to the original protocol in order to adjust it to the specific detection of 8-oxodG lesions. Indeed, the Fpg enzyme specifically recognizes these lesions and removes them from the DNA double-strand, therefore generating a one base gap with a 5´ and 3´ phosphate, via its AP-lyase activity. This gap is similar to a single-strand break and therefore can be detected by the FADU method.

A 14kbp plasmid was chosen to mimick the mtDNA molecule. Further changes in the automated steps were therefore required for an application to this plasmid DNA model. The dilution of the alkaline buffer, the suppression of the alkaline unwinding step and the maintenance of a constant temperature of -5°C were necessary to prevent a complete unwinding of the DNA and to allow a sensitive detection of the strand breaks.

Plasmid samples were treated with the peroxynitrite generator 3-morpholinosydnonimine (Sin-1). The addition of pure PON in an experimental system leads to an immediate and high

increase in PON concentration. This does not reflect the scenario occurring *in vivo*, where PON exists as a continuous flux. The use of Sin-1 as a source of peroxynitrite is therefore an elegant alternative as it decomposes to give equal fluxes of •NO and O_2^- leading to a continual flux of PON over an extended time, which seems to mimick nicely the physiological situation of PON occurrence in the mitochondrion.

Sin-1 was added to plasmid samples at a concentration of 400μM for 40 mn at 30°C and subsequently incubated with increasing concentrations of Fpg (Figure 4.9). Sin-1 only affected DNA unwinding in the presence of Fpg, thus implying that Sin-1 exclusively generates 8-oxodG lesions and does not generate single strand breaks. This information is of high relevance as other oxidizing agents, such as H_2O_2, have been shown to generate many single strand breaks alongside the 8-oxodG, rendering the specific detection of 8-oxodG in these cases particularly biased (data not shown). Sin-1 is therefore the ideal 8-oxodG inducing molecule for this experimental setup. With increasing concentrations of Fpg, the number of 8-oxodG detected in the presence of Sin-1 increased until a threshhold was attained starting from an Fpg concentration of 0,1 U/μL. This concentration, at which all 8-oxodG sites have been cleaved, was used for all subsequent FADU experiments.

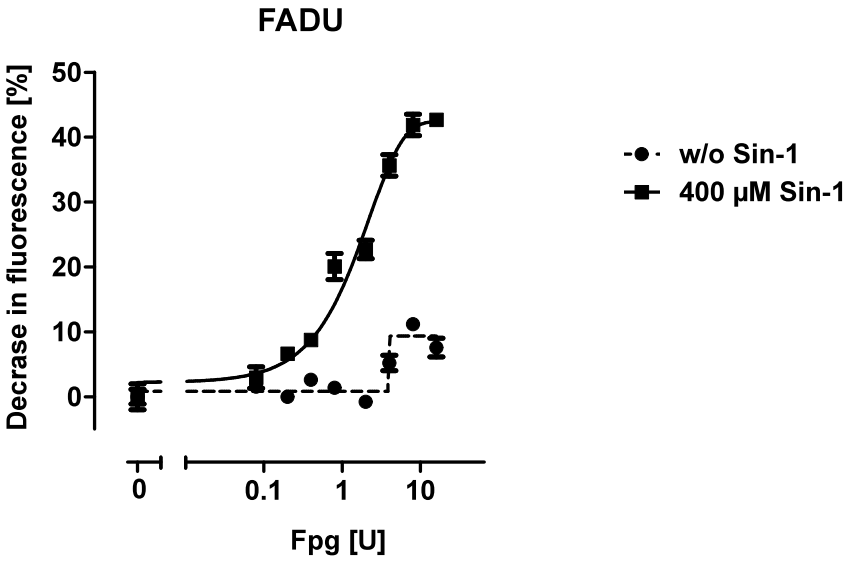

Figure 4.9: Effect of Fpg concentration in 8-oxodG detection in Sin-1 treated plasmid
Plasmid samples were treated with or without 400 μM Sin-1 then incubated with increasing concentrations of Fpg (4-800 mU/μL).
(Experiments were done in quadruplicates and data are expressed as means± S.D)

In order to study the effect of increasing Sin-1 concentrations on 8-oxodG levels, plasmid DNA samples were treated with Sin-1 concentrations ranging from 50 to 400 μM for 40 mn at 30°C . 8-oxodG levels displayed a significant increase with Sin-1 concentrations in a dose-dependent manner (Figure 4.10 panel A).

It was an essential part of this work to validate the FADU assay for the detection of 8-oxodG formation by measuring 8-oxodG levels in the same samples by HPLC coupled with LC/MS The resulting curve confirms the dose-dependent increase of 8-oxodG observed in panel A and the coefficient of determination r^2 of 0,998 calculated by linear regression analysis showed a clear correlation between values measured by both methods (Figure 4.10 panels B-C)

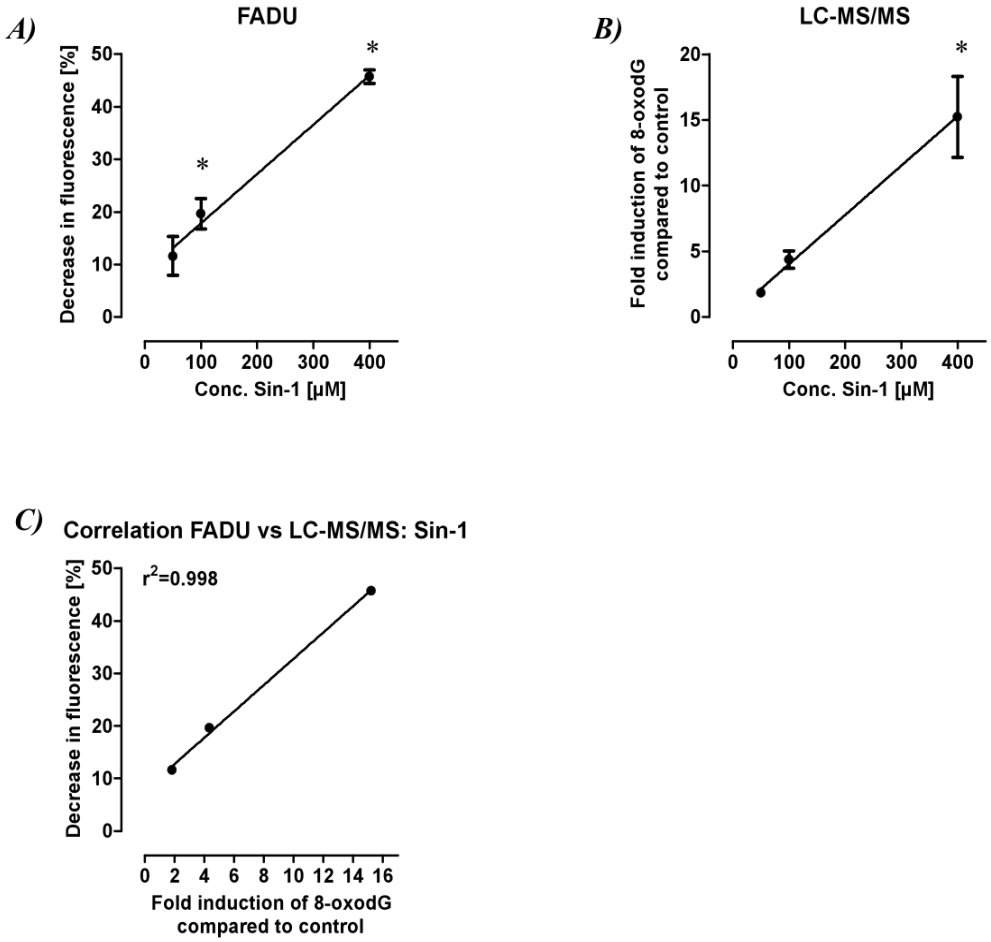

Figure 4.10: Effect of increasing Sin-1 concentration on 8-oxodG levels in plasmid DNA. Plasmid DNA were treated with increasing concentrations of Sin-1 (50-400 μM). 8-oxodG levels were measured ***A)*** by FADU and ***B)*** by HPLC coupled with LC-MS. ***C)*** A linear regression analysis was performed. In cooperation with A. Fischbach and A. Mangerich.
Samples of each experiment were distributed into 2 fractions for FADU and LC-MS measurements. Data are indicated as fractions of fluorescence (FADU) or of 8-oxodG levels of treated samples compared to control and expressed as the means ± S.D. of 3 independent experiments, each n=4. Statistical significance of ∗ values is determined by one-way ANOVA and Bonferroni's post-hoc test, $p < 0,05$ vs 0 μM Sin-1.

4.2.2 Antioxidant scavenging of Sin-1 in a plasmid model

The automated Fpg based FADU method demands little sample preparation, offers a rapid and reliable measurement of 8-oxodG lesions, thus making it a suitable method for screening the protective effects of antioxidant molecules against lesions caused by peroxynitrite.

4.2.2.1 Scavenging of Sin-1-generated O_2^- by MnSOD

In order to study the antioxidant and superoxide scavenging properties of MnSOD, plasmid DNA was supplemented with increasing concentrations of MnSOD (0,94-75ng/μL) prior to Sin-1 incubation (Figure 4.11). FADU (Figure 4.11 panel A) and LC-MS (Figure 4.11 panel B) measurements of 8oxodG highlight the ability of MnSOD to scavenge peroxynitrite by fluxes of NO and O_2^- and concur in demonstrating a dose-dependent protection of the DNA against Sin-1 induced 8-oxodG lesions by MnSOD. Statistical significance was only reached in FADU measured values as LC-MS measured values showed large standard deviations. Nevertheless, the correlation between values from both methods was good, with a r^2 of 0,89 (Figure 4.11 panel C).

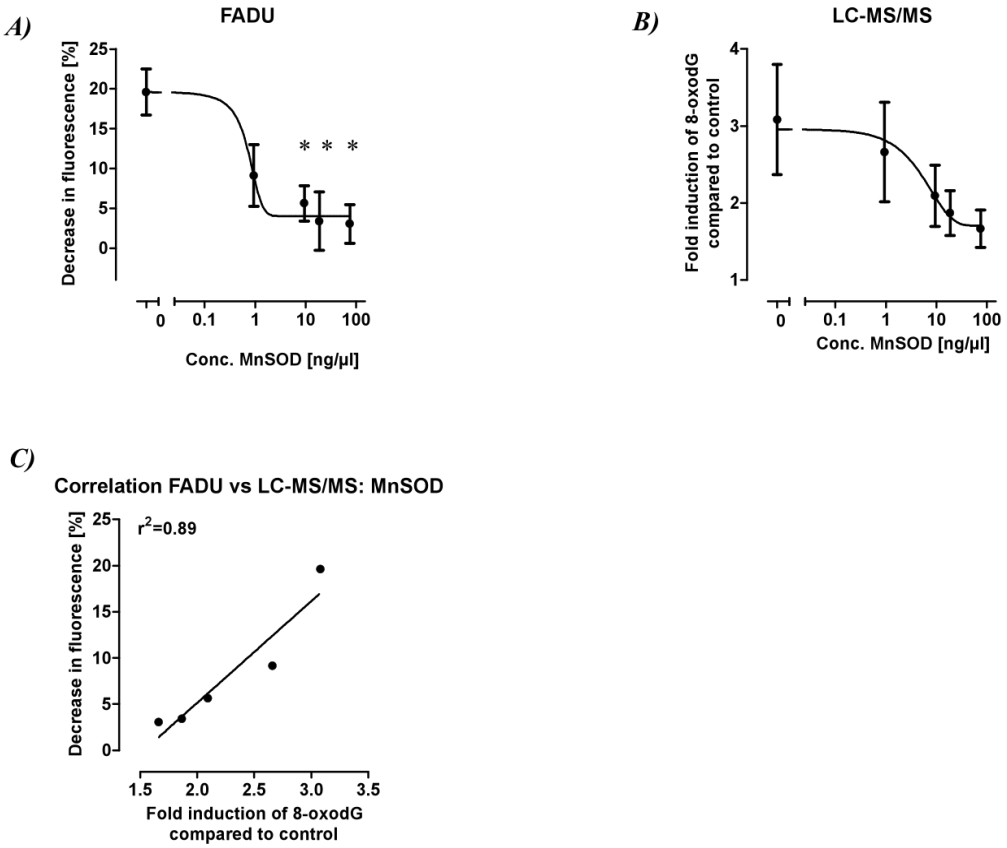

Figure 4.11: Protection of plasmid DNA from Sin-1 induced 8-oxodG lesions by MnSOD. Plasmid samples are supplemented with increasing concentrations of MnSOD, then treated with 100 μM Sin-1. 8-oxodG levels were measured ***A)*** by FADU and ***B)*** by HPLC coupled with LC-MS. ***C)*** A linear regression analysis was performed. In cooperation with A. Fischbach and A. Mangerich.
Samples of each experiment were distributed into 2 fractions for FADU and LC-MS measurements. Data are indicated as fractions of fluorescence (FADU) or of 8-oxodG levels

of treated samples compared to control and expressed as the means ± S.D. of 3 independent experiments, each n=4. Statistical significance of ∗ values is determined by one-way ANOVA and Bonferroni's post-hoc test, $p < 0,05$ vs 0 ng/μL MnSOD.

3.2.2.2 Scavenging of Sin-1 by uric acid

Uric acid is produced from xanthine by the xanthine oxidase enzyme and is known to be the most abundant antioxidant present in human blood and has good selectivity for peroxynitrite. After a pre-incubation with uric acid concentrations ranging from 1 μM to 1 mM, plasmid DNA samples were treated with 100 μM Sin-1 for 40 mn at 30°C (Figure 4.12). FADU and LC-MS measurements reveal a dose-dependent decrease in Sin-1 induced 8-oxodG lesions starting at 1 μM. A complete protection of the DNA seems to appear after an addition of a uric acid concentration higher than 50 μM. Values measured by both methods correlated well with a r^2 of 0,96 (Figure 4.12 panel C)

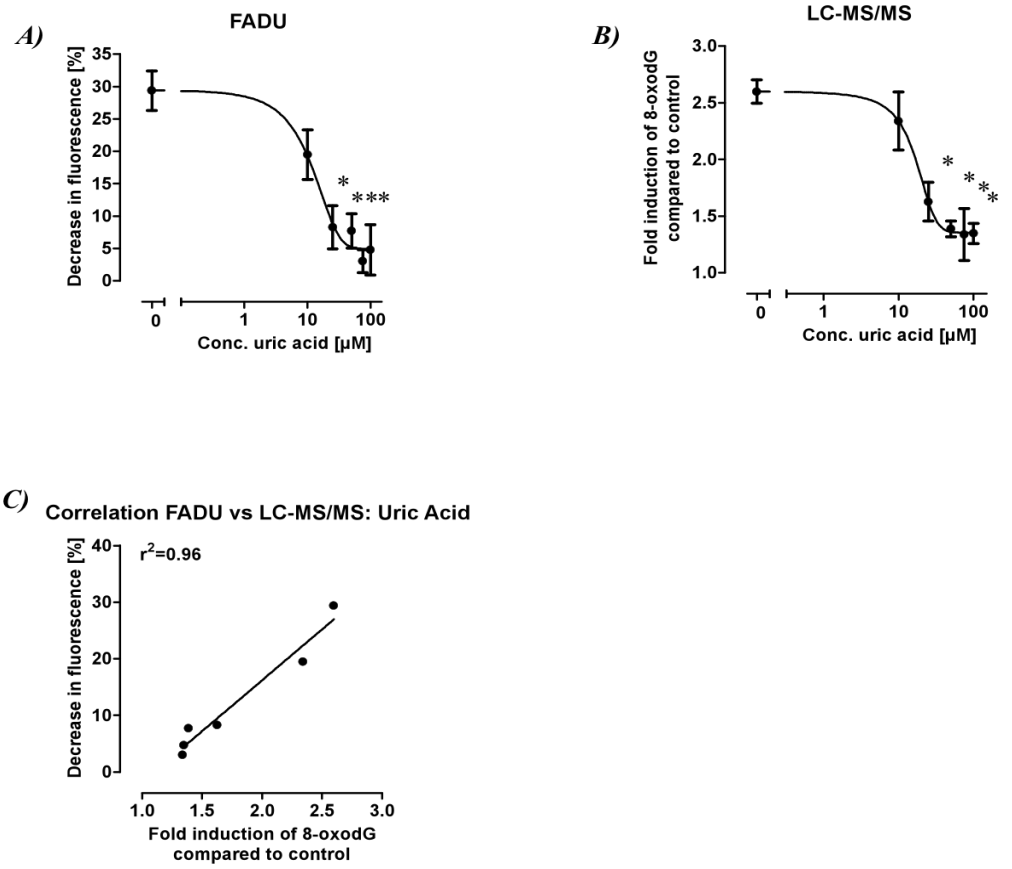

Figure 4.12: Protection of plasmid DNA from Sin-1 induced 8-oxodG lesions by uric acid. Plasmid samples are supplemented with increasing concentrations of uric acid, then treated with 100 μM Sin-1. 8-oxodG levels were measured ***A)*** by FADU and ***B)*** by HPLC

coupled with LC-MS. ***C)*** A linear regression analysis was performed. In cooperation with A. Fischbach and A. Mangerich.
Samples of each experiment were distributed into 2 fractions for FADU and LC-MS measurements. Data are indicated as fractions of fluorescence (FADU) or of 8-oxodG levels of treated samples compared to control and expressed as the means ± S.D. of 3 independent experiments, each n=4. Statistical significance of ∗ values is determined by one-way ANOVA and Bonferroni's post-hoc test, $p < 0{,}05$ vs 0 μM uric acid.

3.2.2.3 Scavenging of Sin-1 by minocycline

Minocycline, a semisynthetic derivative of the tetracycline antibiotic, has drawn particular attention in recent years with the discovery of its neuroprotective and anti-inflammatory effects. So far, little information on the biochemical mechanisms of these effects is known but reports have mentioned a potential antioxidant role against various oxidizing agents [126].

Schildknecht et al. have run a large set of experiments highlighting the role of peroxynitrite as a specific and direct target of minocycline and the following experiment was the result of a collaboration[127].

To study the protective role of minocycline, plasmid DNA was incubated with minocyclin, tetracycline and gentamicin, at concentrations ranging from 0 to 10 μM and treated with 50 μM Sin-1 (Figure 4.13). The detection of 8-oxodG lesions by the FADU method revealed a significant protective effect of tetracycline at a high concentration of 10 μM, whereas gentamicin displayed no such effect at that level. In the case of minocycline, a complete protection of the DNA was already reached at a lower concentration of 5 μM. This concentration is in adequacy with standard concentrations present in the brain after repeated oral intake in clinical studies. The higher PON scavenging capacity of minocycline compared to tetracycline may rely on the presence of an additional dimethylamino substituent in its phenol ring. These results along with the other very conclusive experiments published by Schildlknecht et al. demonstrate a direct protective effect of the minocycline molecule selectively against peroxynitrite at pharmacologically relevant doses.

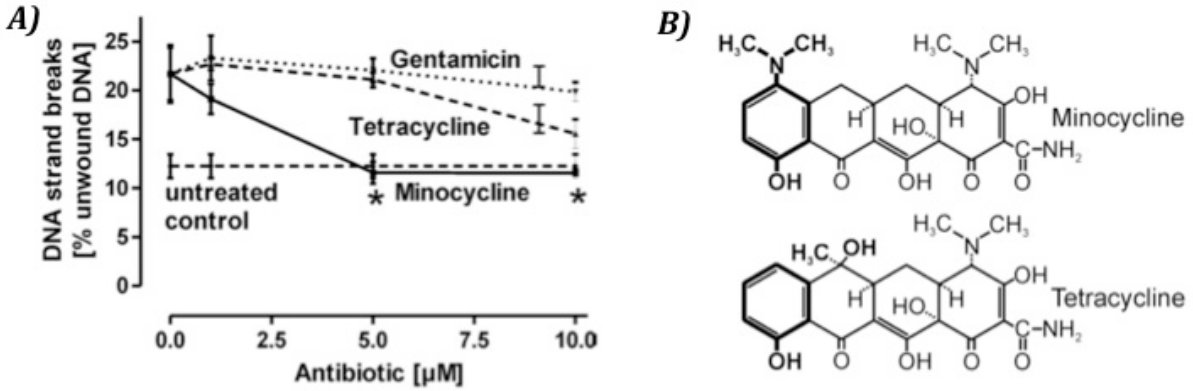

Figure 4.13 (Figure published from Schildknecht et al. 2010 [127]) : Protection of plasmid DNA from Sin-1 induced 8-oxodG lesions by minocycline. ***A)*** Plasmid Samples were supplemented with increasing concentrations of minocycline, gentamicin and tetracycline (0-10 μM), then treated with 50 μM Sin-1. 8-oxodG levels were measured by FADU. ***B)*** Chemical formulas of minocycline and tetracycline. In cooperation with S. Schildknecht.
Data are indicated as fractions of unwound DNA and expressed as the means ± S.D. of quadruplicates. Statistical significance is determined by one-way ANOVA and Bonferroni's post-hoc test, $p < 0{,}05$ vs 0 μM minocycline.

4.3 Peroxynitrite and damage of biomolecules

This studiy was focused on the effects of peroxynitrite, as the understanding of its effects seems crucial, considering the rapidity of its formation, its capacity to diffuse, and the diversity of its targets. The following experiments are aimed at studying the effects of exogenous sources of peroxynitrite on different biomolecules as well as attempting to investigate these effects in LPS-stimulated macrophages, a cell system likely to produce it endogenously.

4.3.1 Peroxynitrite-induced protein nitration: MnSOD nitration and inactivation

Protein nitration is a well-known consequence of peroxynitrite formation and may have considerable effects such as protein inactivation. To study this, mitochondria were isolated from human blood thrombocytes, treated with 500 μM peroxynitrite and nitro-tyrosine (N-Tyr) levels were detected by Western Blot (Figure 4.14, panel A). As expected, N-Tyr levels were considerably increased after treatment.

So far, it has been demonstrated that MnSOD protects DNA from Sin-1 induced 8-oxodG lesions (Figure 4.11). MnSOD acts as a O_2^- scavenger, leaving an excess of •NO. Such conditions still allow small amounts of peroxynitrite to be formed but •NO may itself also display antioxidant properties by reacting with peroxynitrite. The situation may become complex when •NO and O_2^- reach equal concentrations. MnSOD can get tyrosine nitrated and inhibited by excess peroxynitrite[128]. This may have toxic repercussions, as O_2^- mediated damage may take place, eventually leading to mitochondrial dysfunction.

The effect of peroxynitrite on recombinant MnSOD nitration was investigated by incubating MnSOD with 400 μM Sin-1 or 10-1000 μM peroxynitrite and assessing N-Tyr levels by Western Blot using an anti-N-Tyr antibody (Figure 4.14 panel B). At a concentration of 10 μM peroxynitrite, N-Tyr levels did not increase compared to the untreated sample. Above 50 μM, the nitration of MnSOD considerably increased. As anticipated, Sin-1 does not seem to affect the nitration of MnSOD.

The same MnSOD samples were tested for SOD activity using a colorimetric assay based on the coupling of the enzymatic catalysis of the superoxide radical with xanthine oxidase (Figure 4.14 panel C). As peroxynitrite concentrations increased, SOD activity was lowered, inversely correlating with MnSOD nitration.

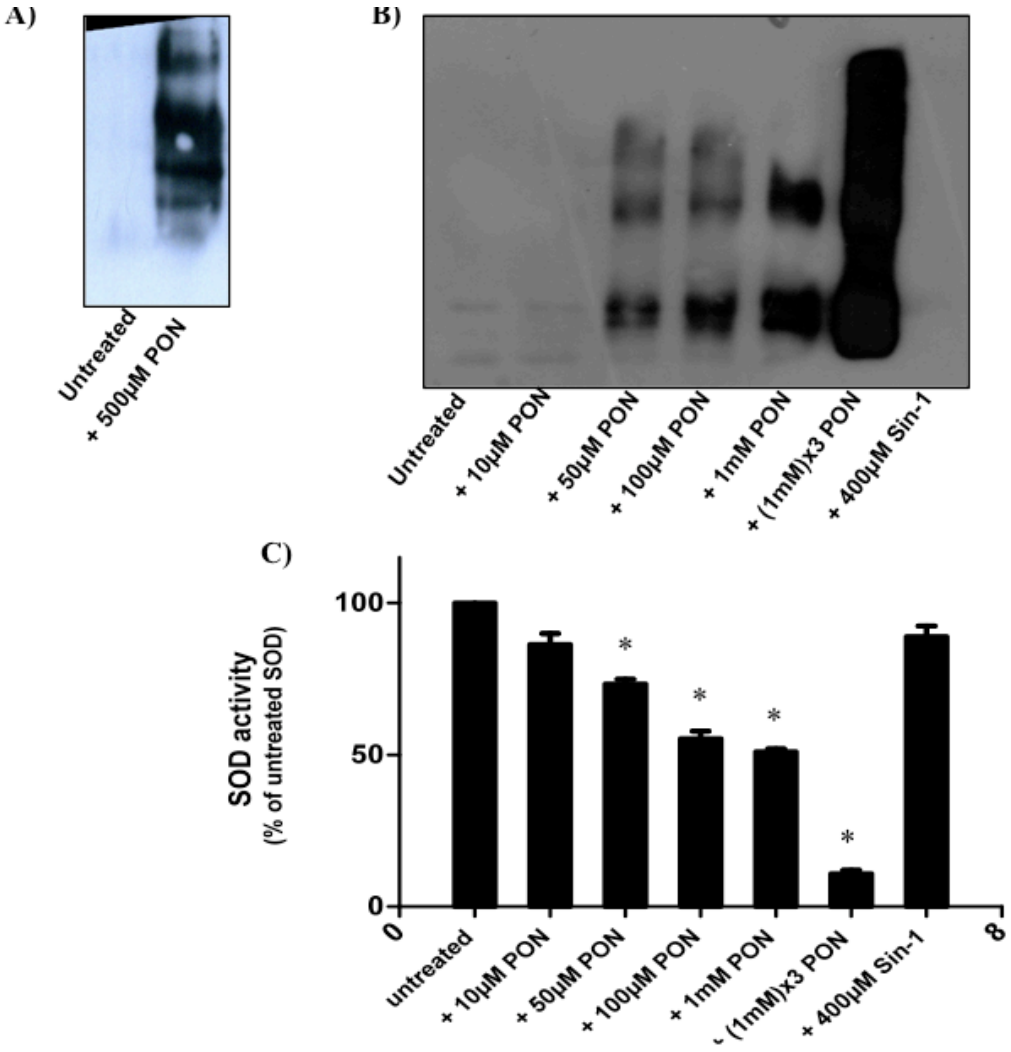

Figure 4.14 : Western Blot analysis of N-Tyr in thrombocyte mitochondria and recombinant MnSOD samples treated with peroxynitrite and SOD activity. ***A)*** Isolated thrombocyte mitochondria were treated with 500 μM peroxynitrite and analyzed by Western Blot for N-Tyr expression. ***B)*** MnSOD samples were treated with 0-1 mM peroxynitrite and analyzed by Western Blot for N-Tyr expression ***C)*** and for SOD activity by a colorimetric SOD activity assay. SOD activity is expressed as a % of the activity of untreated SOD.
Statistical significance of $*$ values is determined by one-way ANOVA and Bonferroni's post-hoc test, $p < 0,05$ vs 0 μM peroxynitrite.

4.3.2 Formation of 8-nitroguanine in Sin-1 treated RAW264.7 cells

As presented in the Introduction section, 8-nitroguanine lesions are a biomarker for oxidative stress and more particularly of the effect of peroxynitrite. The mouse leukaemic monocyte macrophage cell line RAW264.7 was treated with the peroxynitrite donor Sin-1 at a concentration of 1 mM for 10 mn (Figure 4.15). 8-nitroguanine were stained by a rabbit polyclonal anti-8-nitroguanine antibody generously provided by the Kawanishi laboratory and nuclei were counterstained with Hoechst[129]. To our knowledge, this antibody has only been used in immunochemistry and slot blot so far and has not yet been used for immunofluorescence detection. In control cells, an overlay of Hoechst and anti-8-nitroguanine

staining clearly showed an 8-nitroguanine fluorescence exclusively concentrated in the nuclear area. In the literature, untreated RAW264.7 cells also displayed immunoreactivity to an anti-8-nitroguanosine antibody but there is no evidence as to the localisation of the lesions as experiments were conducted by slot blot with total cell lysates [130].

After Sin-1 treatment, the anti-8-nitroguanine staining was stronger in the nucleus but also largely present in the cytoplasm. This cytoplasmic staining can be due to the presence of 8-nitroguanine in mtDNA but may possibly also be a sign of nitration in RNA or in GTP, depending on the specificity of the antibody.

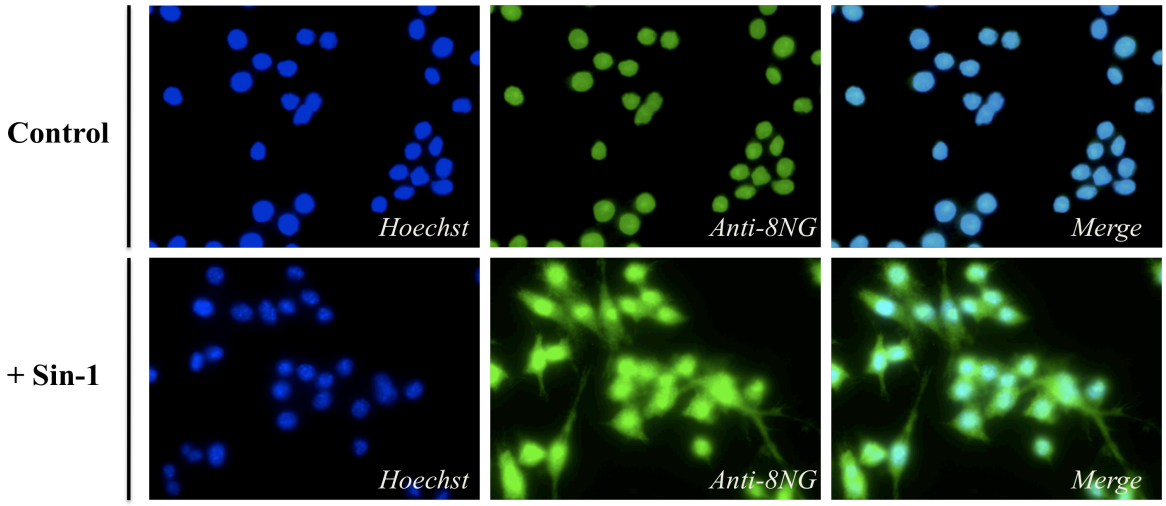

Figure 4.15 Immunofluorescence analysis of 8-nitroguanine formation induced by Sin-1 in cultured RAW264.7 cells. Cells were treated with 1 mM Sin-1 for 10 mn. 8-nitroguanine formation was analyzed using an anti-8-nitroguanine antibody and the fluorophor-labelled secondary antibody Alexa488, nuclei were counterstained by Hoechst staining.

4.3.3 Formation of 8-oxodG in mtDNA of Sin-1 treated RAW264.7 cells

Another important biomarker for oxidative stress induced by peroxynitrite in cells that has been a focus in this work is the 8-oxodG lesion. To accomplish this, RAW264.7 cells were incubated with 1 mM Sin-1 for 10 mn. After careful lysis and mtDNA isolation with addition of appropriate antioxidants to prevent artifactual oxidation, the purity of the mtDNA was validated by amplification of a nuclear and a mitochondrial gene by PCR (Figure 4.16 panel A). The mtDNA fragment mtND5 was amplified in the isolated mtDNA sample (first lane) whereas the nuclear fragment mPARP1 (as a positive control in the third lane) was absent in the same sample (second lane).

LC-MS measurements revealed a slight increase in 8-oxodG levels in Sin-1 treated cells compared to the untreated cells, even though these results must be taken with precaution, taking into account the large error bars (Figure 4.16 panel B).

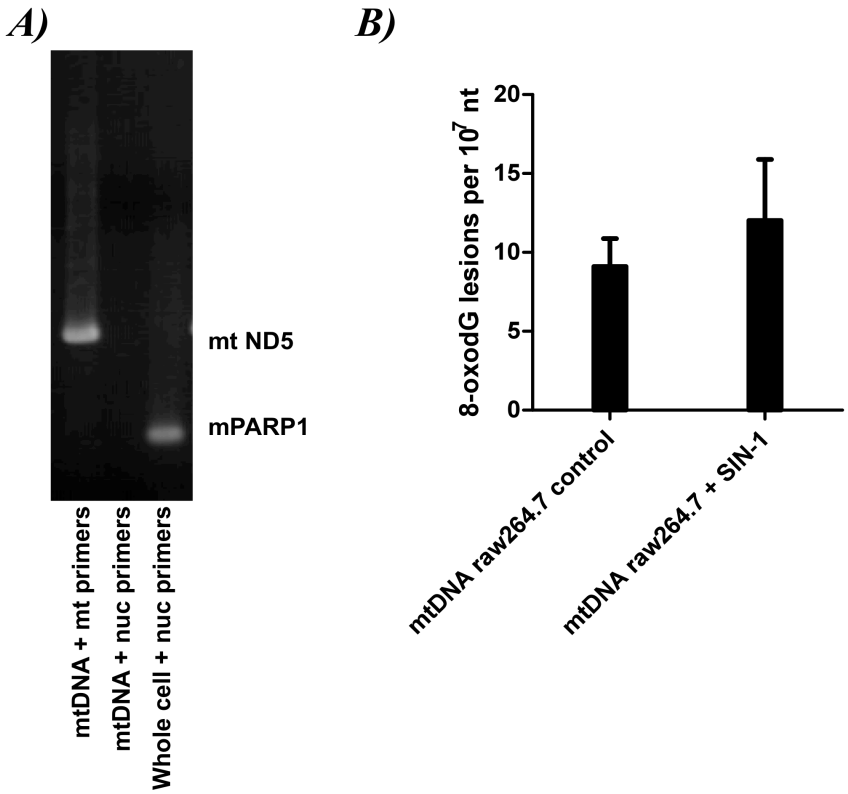

Figure 4.16: 8-oxodG levels in Sin-1 treated RAW264.7cells After RAW264.7 cells were treated with 1 mM Sin-1, mtDNA was isolated. ***A)*** mtDNA purity was verified by PCR. ***B)*** 8-oxodG levels were measured by LC-MS.

4.3.4. Detection of nitrated biomolecules in stimulated RAW264.7 cells

The above-described experiments demonstrate the sensitivity of biomolecules to exogenous peroxynitrite. These effects were further studied in a cellular system able to produce large amounts of peroxynitrite endogenously. The RAW264.7 cell line was therefore chosen as it is known to produce large amounts of •NO upon cytokine or lipopolysaccharide (LPS) activation. The appropriate incubation time with 10 μg/mL LPS was determined by measuring nitrite formation by Griess test as a function of time (Figure 4.17 panel A). Immunofluorescence images did not show a clear increase in cytoplasmic 8-nitroguanine staining between LPS-treated cells after 8 hours and control cells (Figure 4.17 panel B).

Furthermore, 8-oxodG levels measured by LC-MS in isolated mtDNA of treated and untreated cells did not present a significant difference (Figure 4.17 panel C). The experimental conditions as well as the model itself may not be ideal for the production of peroxynitrite, which will be discussed in section 5.3. It is also essential to note that these are preliminary experiments that have not been reproduced for a sufficient significance.

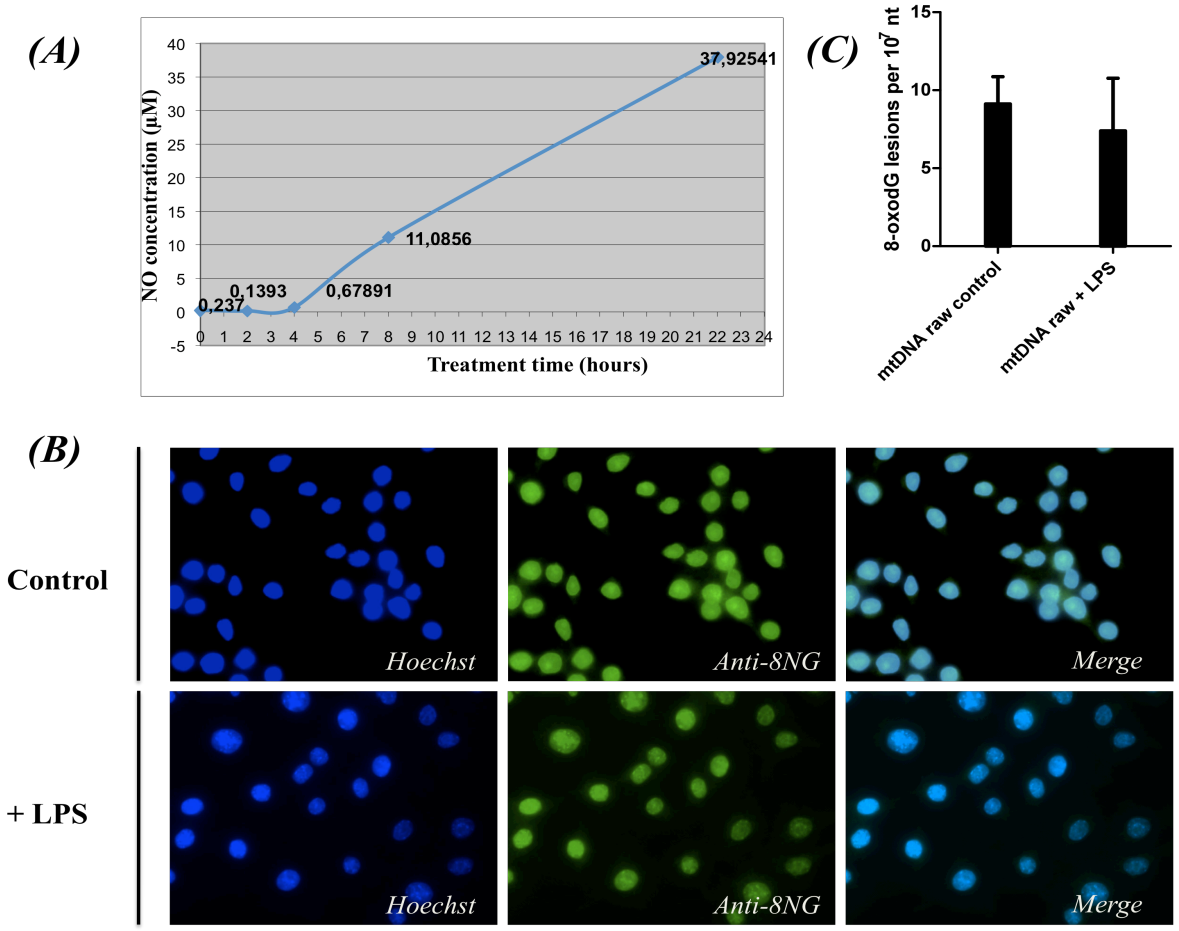

Figure 4.17: Effects of LPS induced •NO production on biomolecules in cultured RAW264.7 cells. ***(A)*** RAW264.7 cells were treated with 10μg/mL LPS for 2, 4, 8 and 22hours and nitrite concentrations (μM) were determined by Griess test. ***(B)*** Cells were treated with 10μg/mL LPS for 8 hours. 8-nitroguanine formation was analyzed using an anti-8-nitroguanine antibody and the fluorophor-labelled secondary antibody Alexa488, nuclei were counterstained by Hoechst staining. ***(C)*** After cells were treated with LPS for 8 hours, mtDNA was isolated and 8-oxodG levels were measured by LC-MS.

5 Discussion

5.1 MnSOD binding to mtDNA

5.1.1 Nature of MnSOD/mtDNA binding

Joachim Kienhöfer was the first to report an association of MnSOD with mtDNA in eukayotic cells and has detected a direct binding of the enzyme to DNA by slot blot filter assay[119]. In the present work, the ability of MnSOD to bind directly to DNA was confirmed and further investigated by an SPR-based experiment using a Biacore chip on which 34-mer oligonucleotides were immobilized. Human recombinant MnSOD was found to bind to the oligonucleotides, a binding that was proven to be salt-sensitive as it could be disrupted by the addition of 50 mM NaCl (Figure 4.1). Joachim Kienhöfer had already reported a salt-sensitive binding with a dissociation of the complex at a NaCl concentration of 200mM by slot blot filter assay; this result was refined with the use of the more sensitive SPR-based technique. It must be noted that *in vivo* mitochondrial salt concentrations do not exceed 5 mM, therefore MnSOD can bind to mtDNA in these conditions[131].

High concentrations of NaCl did not suffice to dissociate TFAM from the DNA; multiple injections of 2M NaCl and 50mM NaOH were necessary to disrupt the binding, suggesting a stronger binding of TFAM than MnSOD to the DNA. This was also implied by the association slopes depicted by the sensorgrams of TFAM and MnSOD. Since MnSOD and TFAM have similar molecular weights (respectively 22,3 kDa and 24,5 kDa), it is possible to directly compare the value of the response units upon equilibrium. While the binding curve of TFAM saturated after an injection time of 100 s injection (Figure 4.1 panel A), the binding curve of wt MnSOD saturated after 1800 s (Figure 4.1 panel D). The fact that TFAM binds more strongly to DNA may be due to the presence of its two HMG boxes and is in agreement with its predominance on the mtDNA molecule as an essential scaffolding protein[132].

MnSOD binding was indeed very weak: when injecting the solution containing MnSOD into the system, we observed a very slow increase in RU difference compared to the reference cell. An equilibrium could not be attained even after an injection time of 2100s (the maximum injection time for the Biacore T100 SPR device) at a maximum protein concentration. The inability to reach equilibrium unfortunately prevented the performance of kinetic experiments that could have allowed the determination of the constant of dissociation Kd.

This weak binding raises the question if it is due to the technical limitation of working with a simplified experimental setup compared to a more complex nucleoid structure. For instance, MnSOD might bind preferentially to specific sequences rather than the random mitochondrial sequence we selected, as had been reported for TFAM[35]. MnSOD binding might also necessitate a more complex folded structure of the DNA compared to the 34-mer oligonucleotide or the presence of neighboring proteins in order to stabilize it. Nevertheless if a weak binding of MnSOD in the mitochondrial setting were to be confirmed, it could be of physiological relevance in the sense that the very high concentration of MnSOD in the mitochondrial matrix already gives it a sterical advantage compared to other molecules for the binding to mtDNA.

Interestingly, according to SPR measurements carried out by Janina Haar, the slope of the ascending part of the binding curve obtained when injecting recombinant *E. coli* MnSOD has a steeper incline than when injecting commercial recombinant human MnSOD at equal concentration. Furthermore, prokaryotic MnSOD exists as a dimer and therefore has half the mass of the tetrameric human MnSOD, meaning that for a given value of response units, twice as many prokaryotic proteins would bind compared to the human version. This would suggest that *E. coli* MnSOD might have a higher binding affinity than its human homologue, possibly due to its dimeric configuration. If this is the case *in vivo*, the loss of binding affinity during evolution might be due to a lesser need of protection of eukaryotic cells which may compensate with other antioxidant sytems. However, these results must be handled with great precaution seeing that that the comparison of binding affinity without calculation of the Kd is very unreliable.

As mentioned above, MnSOD binding is salt-sensitive, implying the involvement of ionic forces in the association. We have postulated that this interaction might be mediated by three different highly conserved lysine residues located at the C- and N-terminus of the protein. After successful site-directed mutagenesis (accomplished by Janina Haar during her Master thesis), the different MnSOD mutants were expressed and purified in *E. coli*. The absence of saturation in the binding curve obtained by Biacore SPR measurements in the case of MnSOD unfortunately prevented us from obtaining quantifiable data and therefore it was not possible to compare binding affinities between mutants. Nevertheless, the observation of a binding of every mutant to DNA, demonstrating that the binding of MnSOD to DNA is not mediated exclusively by these precise lysine residues.

By hypothesizing that bound MnSOD protects DNA more efficiently than its unbound counterpart, the indirect correlation between binding affinities of the mutants andd their

capacity of protecting DNA against Sin-1 induced 8-oxodG lesions by FADU can be made (Figure 4.7). Some of the mutants displayed a weaker protection but it was only statistically significant in the case of MnSOD QH-KK, which would allow the speculation of an involvement of the N-terminal lysine in the binding.

5.1.2 Regulation of MnSOD/mtDNA association

The mechanisms underlying the association/dissociation process of MnSOD are unknown.
It was postulated that MnSOD dissociation from mtDNA may be mediated by acetylation of its lysine residues, in a similar way as with histone dissociation from nuclear DNA. Many parallels have been made between histones and TFAM, particularly in the regulation of gene expression and in DNA compaction, so it is not surprising that acetylation of TFAM has been reported in various rat organs[133]. The presence of certain isoforms of sirtuins (Sirt3 and Sirt5) with a deacetylase activity in mitochondria could allow a regulation of this nature.
As preliminary data suggested that MnSOD mutants truncated at their lysines can bind to DNA, the regulation of its association by acetylation/deacetylation seems unlikely, even though this hypothesis cannot be entirely dismiss as binding *in vitro* and *in vivo* may be different.
Our particular interest for a potential MnSOD acetylation was proven to be justified but not for the purpose of MnSOD binding. Indeed, very recent findings have shown that MnSOD acetylation in mitochondria exists and that it has a role in enzymatic activity regulation[134].
Another explanation for the finding that MnSOD may exist in the associated and dissociated form is that MnSOD binds competitively with TFAM to mtDNA. This hypothesis can be supported by the fact that we did no association of MnSOD to mtDNA was observed in Hela, a cell line in which considerably high levels of TFAM have been reported (Figure 4.2). This hypothesis had led to the postulation that the levels of bound MnSOD would decrease during Xenopus oogenesis, inversely to the increase in TFAM levels which had been reported by Shen et al.[48]. However, the experiments depicted in Figures 4.4-6 did not validate this, as MnSOD was shown to be bound in stage 6 of oogenesis.

5.1.3 Physiological significance of MnSOD/mtDNA binding

We have shown that whether or not MnSOD binds to mtDNA is specific to cell-type, since an association was found in rat and bovine heart, human smooth muscle cells and Jurkat cells

whereas no association was detected in bovine endothelial cells, Hela cells and LUHMES cells (Figures 4.2-6)[124].

The investigation of *Xenopus laevis* oocyte at different stages of development showed that MnSOD was bound or unbound according to the stage of oogenesis. This confirms the dynamism of nucleoid conformation, as was already advanced by the finding that TFAM levels increase during oogenesis in the same model[48]. The pattern of association and dissociation of MnSOD, namely an association in stages 1 and 6 and none in stage 3 must have a physiological significance and may be related to the bottleneck phenomenon.

The lack of MnSOD association with mtDNA in the Parkinson cell model LUHMES is consistent with the hypothesis that bound MnSOD confers a better protection of mtDNA since high levels of mtDNA mutations are reported in neurons from Parkinson patients[125,135].

In all nucleoid isolations displaying MnSOD in the nucleoid containing fractions, MnSOD was also observed in the supernatant fraction, suggesting either that that MnSOD was dissociated from the nucleoid during an isolation step or that MnSOD exists in the bound and unbound form within the same cell. In the latter case, this would mean that MnSOD may be bound in some mitochondria and unbound in others depending on their state, or that within the same mitochondrion, the two forms coexist in order to confer a protection directly at the mtDNA and at the same time within the matrix.

The reasons underlying a dissociation are unknown; it may be due to the structural reorganization of nucleoids in mitochondria undergoing fusion and fission of highly proliferating cells or during the bottleneck segregation of mtDNA molecule, as may be the case with respectively endothelial cells or *Xenopus* oocytes at certain stages. The dissociation may also be driven by metabolical or stress-related processes.

Previous work conducted by our group revealed an association of MnSOD to mtDNA in smooth muscle cells whereas no association was found in endothelial cells[124]. Moreover, smooth muscle cells have been reported to be more resistant to oxidative stress, including peroxynitrite, than endothelial cells[136]. It can be hypothesized that this resistance may partly be conferred by the fact that MnSOD offers a better protection for the mtDNA in the bound form.

This was supposed to be investigated by comparing the scavenging ability of bound and unbound MnSOD of Sin-1 by the Fpg-based Fadu method for detection of 8-oxodG. Unfortunately, as the MnSOD mutants generated all had about equal ability to bind DNA, the results of this experiment were difficult to interpret (Figure 4.7). A preliminary experiment in

which 8-oxodG levels were higher in the presence of dissociating NaCl levels argues in favor of our hypothesis (Figure 4.8).

Nevertheless, it can be argued, simply based on theoretical grounds, that MnSOD binding to the mtDNA is essential to provide a more efficient protection (Figure 5.3 in section 5.3). Nucleoids are associated to the inner membrane, therefore mtDNA is very close to the place of production of $O_2^{\cdot -}$[40]. The fact that MnSOD is bound to mtDNA increases its chances of scavenging $O_2^{\cdot -}$ before it reacts with •NO to form peroxynitrite.

5.2 Methods of 8-oxodG detection

Since the 1980s, various methods to detect 8-oxodG have been established and optimized, including chromatographic methods, immunological assays and assays requiring the use of DNA repair glycosylases. These are listed and discussed below in the purpose of shedding light on the discrepancies in 8-oxodG values seen in the literature. This will allow to situate the Fpg-based FADU method among the pre-existing methods and evaluate its advantages.

The High-Performance Liquid Chromatography coupled with electrochemical detection (HPLC/ECD) has been a pioneer in 8-oxodG measurement[137]. The method is based on the fact that the low oxidation potential of 8-oxodG allows a specific and sensitive detection in the one-electron oxidation mode. However, it presents high levels of artifactual lesions and a lack of internal calibration [138].

The fluorescence post labeling and ^{32}P post labeling coupled with Thin Layer Chromatography (TLC) or HPLC offer a high sensitivity and only require a small amount of DNA [139140]. However, adventitious 8-oxodG from radiolysis of guanine by ^{32}PATP have been detected[141]

Mass spectrometry based methods such as gas chromatography / mass spectrometry (GC/MS) have a tendency to overestimate 8-oxodG levels 10 to 50 fold due in part to the acidic conditions of the DNA hydrolysis as well as the long derivatization step [142,138]. A pre-purification of samples by HPLC, a lowering of the derivatization temperature and the addition of antioxidants have been proven to help avoid this type of artifacts [144].

One of the most specific and sensitive methods for the detection of 8-oxodG remains the reverse phase HPLC coupled with LC/MS [145] and does not require derivatization prior to introduction into the MS. It has been used in this work to validate the Fpg-based FADU method for the detection of 8-oxodG[146,147,148].

All of the methods aforementioned require an extensive processing of the sample prior to measurement.

Conversely, immunological methods have the advantages of demanding little preparation and allowing the analysis of a panel of samples simultaneously. Immunological methods are for instance widely used for detecting 8-oxodG in human fluids such as saliva, urine and plasma, in the form of an ELISA test, as it is a less tedious and cheaper method than HPLC-MS based tests[149]. Antibodies for immunochemistry and immunofluorescence have been developed to detect nuclear and mitochondrial 8-oxodG lesions in cells and tissues[150]. They remain however limited by the weak antigenicity of 8-oxodG as well as the specificity of the

antibody, as significant cross-reactivity of the antibody with the undamaged exceeding nucleobase has been described[151,152]. This explains the great overestimation of 8-oxodG values detected by this method, basal values lying at about 1 per 10^3 bases[153].

Lastly, the comet assay (or single cell electrophoresis assay), alkaline unwinding and alkaline elution techniques can be associated with the use of bacterial base excision repair enzymes in order to detect 8-oxodG [154,139]. Many different variants of these methods have been developed, the most recent being a method combining the comet assay and in situ fluorescent hybridization (FISH) in order to detect oxidized bases at the sequence level[155].

These methods require the use of glycosylase (Fpg) and endonuclease III (EndoIII) specifically convert the oxidized pyrimidine and modified purine bases into DNA strand breaks which in turn can be detected in a very sensitive way by the above listed techniques. With the Fpg based methods, 8-oxodG levels can vary from 0,04 to 0,13 lesions per 10^6 bases depending on cell type[156]. Similar results are achieved by using EndoIII.

However, a major drawback of the comet assay is that it can be relatively tedious as it requires many successive steps.

This limitation was overcome by the establishment of the Fpg-based FADU method for detecting 8-oxodG in our group. Indeed, a wide panel of samples can be pipetted on a 96-well plate and processed simultaneously by the automated liquid handling device. This ensures an equal treatment of samples and considerably saves time and effort. These characteristics of the method are also an advantage over the HPLC-coupled LC/MS method. In the case of the adapted FADU method, after treatment, samples are diluted in a suspension buffer, distributed in the 96-well plate, subjected to the automated addition of successive solutions by the liquid handling device and then submitted to fluorescence readout. The total amount of time required for these steps is approximately 25 mn and the number of samples analyzed concurrently is of about 20 in quadruplicates. Throughput can be further improved by increasing the number of 96-well plates processed at the same time by the robot. In the case of the HPLC-coupled LC/MS method, treated samples must undergo a multitude of steps: digestion, dephosphorylation, filtering, numerous lyophilisations, a pre-purification by HPLC and a separation by LC/MS. Moreover, samples must be purified and analyzed sequentially by the HPLC and the LC/MS, demanding additional time. For the equal number of 20 samples measured in quadruplicates, an estimated period of 10 days is required.

A large number of enzymes are necessary for the processing of samples before HPLC-LC/MS detection and even though the amount of enzymes and buffers were halved compared to the

original protocol from Taghidazeh et al. 2008, it still represents a significant additional cost compared to the FADU assay[123].

Another notable advantage of the modified FADU assay over the HPLC-coupled LC/MS method is the quantity of DNA necessary for a measurement. While only 1 μg of plasmid DNA per measurement was sufficient for the FADU, 25-50 μg were necessary for one measurement by HPLC-LC/MS.

In the literature, Fpg based methods have been reported to render 10-fold lower 8-oxodG values than the more invasive MS based tests [157] as it is hypothesized that less autooxidation reactions due to sample processing occur[156]. However, we have apprehended these potential artifacts arising during HPLC-LC/MS sample preparation by the addition of desferroxamine (0,1 mM) and butylated hydroxylene (0,1 mM).

These low levels of 8-oxodG detected by the Fpg-based method that stated in the literature may also be explained to a lesser extent by an incomplete enzymatic processing of 8-oxodG containing tandem base modifications by Fpg, which undoubtedly is a shortcoming of this method[158]. However this effect may be in part compensated by the fact that Fpg is not entirely specific for 8-oxodG, as it also recognizes FapyGua and FapyAde sites. This may slightly reduce the gap between 8-oxodG values using both methods.

Another significant limitation of the FADU method is the lack of exact quantification due to the absence of an internal standard. Ravanat et al. attempted to introduce [^{18}O]-labeled 8-oxodG containing cellular DNA in samples measured by an Fpg-based comet assay but were unsuccessful[159].

The relatively limited choice of oxidizing agents is an additional constraint of this method. Agents, such as H_2O_2, that induce single strand breaks lead to a complete unwinding of the DNA (even at low concentrations) making it impossible to discriminate between unwinding caused by single strand breaks or by the apurinic sites generated by the Fpg after 8-oxodG recognition. According to our data, Sin-1 does not induce single strand breaks and is therefore the appropriate 8-oxodG inducing molecule for this experimental setup.

Another point that must be addressed is the sensitivity of the FADU setup to certain substances. For example, it would have been practical to test the effect of MnSOD binding to the plasmid DNA on its scavenging ability by dissociating MnSOD and DNA with the addition of NaCl. Unfortunately, NaCl addition led to many discrepancies in the results and might stabilize DNA structure making it resistant to DNA unwinding regardless of the presence of DNA strand breaks.

A major setback of the Fpg-based FADU method is that it seemed to be restricted to the detection of 8-oxodG in a plasmid model as we have not yet been able to apply it to mtDNA in whole mitochondria, despite many attempts. The establishment of such a method in mitochondria would have great benefits, as it would present a simple and rapid means of measuring 8-oxodG without isolation of mtDNA.

To sum up, the Fpg-based FADU method and the HPLC-coupled with LC/MS method each have advantages and a few minor drawbacks for the detection of 8-oxodG lesions (Table 5.1) and the choice of using one over the other should depend on the desired application. The FADU method, by the simplicity of its execution, its high throughput and the small amount of plasmid DNA required, makes it a very good method for screening antioxidant scavenging of Sin-1 induced damage. Such an application was easily illustrated by the experiments carried out with Schildknecht et al. in which we showed the effects of low concentrations of gentamicin, tetracycline and and particularly minocycline on Sin-1 scavenging[127]. The validity of the method was confirmed by measuring 8-oxodG in the same samples by the FADU method and by the universally accepted HPLC LC/MS method. Linear regression analyses revealed a coefficient of determination ranging between 0,89 and 0,998, demonstrating a tight correlation between values from both methods (Figures 4.10-12 panel C).

HPLC-coupled LC/MS would be the preferred method for a quantitative measurement of a small number of samples, regardless of the nature of the DNA (plasmid, mtDNA, nuclear DNA) and the presence of other DNA damage (like endogenous single strand breaks).

	Fpg-based FADU	**HPLC coupled LC/MS**
Amount of DNA / sample	1 μg	25-50 μg
Time for measurement of 20 samples	10 days	25 min
Throughput	high	low
Quantification	quantitative	Semi-quantitative
Sensitiviy	+	++

Table 5.1 : Comparison of the Fpg-based FADU and the HPLC-coupled LC/MS methods for the detection of 8-oxodG

5.3 Peroxynitrite and damage of biomolecules

5.3.1 The effects of peroxynitrite on mtDNA

As evoked in the Introduction section, peroxynitrite is known to cause damage to mtDNA mainly in the form of single strand breaks, 8-oxodG and 8-nitroguanine.

5.3.1.1. 8-oxodG formation by PON and its physiological significance

The detection by the Fpg-based FADU method of 8-oxodG in plasmid DNA treated with Sin-1 showed an increase in a dose-dependent manner (Figure 4.10). By decomposing slowly into equal amounts of •NO and O_2^-, Sin-1 generates a continuous and extended flux of peroxynitrite, more similar to the physiological situation than the addition of peroxynitrite which exposes the DNA to an immediate and very high concentration. Preliminary results (not yet reproduced) showed that Sin-1 incubation of Raw264.7 cells also led to increased levels of 8-oxodG in mtDNA measured by LC/MS (Figure 4.16).

While peroxynitrite generates 8-oxodG in mtDNA, the significance of its consequence on mutagenesis, mitochondrial dysfunction, disease and aging has been an issue of debate.
Out of a variety of mutagenic oxidative lesions, 8-oxodG is the most abundant. It has been thought to be considerably mutagenic : an *in vitro* assay has estimated polγ mispairing of adenine with 8-oxodG at 27%[160]. 8-oxodG can also hinder mtDNA transcription by leading to shortened transcripts and by slightly blocking elongation[161].
Mitochondrial 8-oxodG lesions have been correlated with mitochondrial dysfunction in aging, neurodegeneration and other disorders associated with oxidative stress. Its correlation with aging was described for the first time in 1990 by Ames et al. who reported an increase in 8-oxodG in nuclear DNA and a 2- to 3-fold increase in isolated mtDNA from rat liver with age[162,163]. This tendency of age-related accumulation of 8oxodG in mtDNA and nuclear DNA was confirmed in various tissues of mice and rats[93]. Moreover, a study conducted on six mammalian species showed that 8-oxodG levels in mtDNA of heart and brain was inversely correlated to maximum life span[38].
Interestingly, DNA repair capacity does not seem to be impaired with age; on the contrary, 8-oxodG glycosylase/AP lyase activity measured in rat liver and heart increased with age[164].
It has been reported by a number of different groups that 8-oxodG levels are considerably higher in mtDNA than in nuclear DNA and the vulnerability of the mtDNA to this type of

lesion has been attributed to its proximity to the ETC, its lack of histones and a less efficient repair[165].

However contradictory results concerning 8-oxodG accumulation, their actual mutagenic effects and their involvement in mitochondrial dysfunction and in the aging process have arisen over the years.

Likewise, in tissues displaying high 8-oxodG levels, the number of G to T transversions is low[166].

Moreover, OGG1-null mice show a 20-fold increase in 8-oxodG but no evidence for mitochondrial dysfunction[108,167]. This suggests that the functional impact of this lesion may not be as significant.

Gas chromatography / mass spectrometry measurements conducted on Wistar rat livers revealed no significant age effects on nuclear and mitochondrial 8-oxodG levels[168]. They also did not measure a higher incidence in 8-oxodG lesions in mtDNA compared to nuclear DNA. The predominance of DNA lesions in mtDNA over nuclear DNA is still subject to controversy today and disparities between results are partly explained by the methods of DNA isolation and measurement.

5.3.1.2 8-nitroguanine

The preliminary immunofluorescence data in Figure 4.15 has shown that Sin-1 treatment induced 8-nitroguanine in Raw264.7 macrophages. This contradicts findings of Yermilov et al. in which Sin-1 induced 8-oxodG but not 8-nitroguanine in DNA[83]. The signal detected after Sin-1 treatment in the cytoplasm may be due to the nitration of mtDNA, RNA or GTP. High levels of 8- nitroguanosine 3',5'-cyclic monophosphate (8-nitro-cGMP) have been described as the major nitrated guanine nucleotide product, probably stemming from the nitration of GTP, and are suspected to play a key role in redox regulated signal transduction[169].

In vitro studies demonstrated that the reaction of isolated DNA with exogenous peroxynitrite yield 8-nitroguanine as the main type of nitrated bases[97]. Its spontaneous depurination can lead to the incorporation of an adenine during DNA replication causing a G to T transversion, a common mutation found in a variety of genes from many different types of cancers[170]. High levels of 8-nitroguanine have indeed been associated with inflammation and inflammation-related carcinogenesis[171,172]. Still, the significance is questioned as other forms of DNA damage, such as 8-oxodG and strand breaks prevail quantitively, even during inflammation[111]. The lack of evidence on the relevance of this type of base damage in pathophysiological

conditions can be attributed to the fact that it has not yet been extensively studied in biological systems.

5.3.1.3 DNA damage by peroxynitrite production in macrophages

It has been reported that the majority of the high levels of •NO produced in activated macrophages are converted to peroxynitrite[173]. Macrophages activated by LPS have shown increased levels of oxidation products of DNA bases, possibly due to peroxynitrite formation . This led us to the investigation of the effects of endogenous peroxynitrite formation in LPS-activated macrophages on mitochondrial 8-oxodG levels and on 8-nitroguanine formation (Figure 4.17). Despite a very high •NO production (measured by nitrite concentration of 11 μM), no effect was detected neither on 8-oxodG nor on 8-nitroguanine levels. A reason for this might be that •NO levels are too high for peroxynitrite production. Daiber et al. have demonstrated that a 3-fold excess of •NO compared to O_2^- leads to the generation of nitrosating species, most likely N_2O_3 [174]. Instead of forming 8-nitroguanine, it is possible that under such conditions, these species cause nitrosation to the DNA, which is consistent with the observation that stimulated macrophages accumulate high levels of DNA deamination, a consequence of DNA nitrosation.

5.3.2 The effects of peroxynitrite on protein nitration

5.3.2.1 Protein nitration

Peroxynitrite can induce protein nitration, as shown by Western Blot detection of nitro-tyrosine in mitochondrial extracts of human platelets incubated with exogenous peroxynitrite (Figure 4.14).

Nitration of proteins has been associated with a great number of diseases, including artherosclerosis, ischemic rat lung injury, human acute lung injury and amyotrophic lateral sclerosis[175176].

The nitration of phenolics and tyrosine residues of certain proteins can be catalyzed by CuZnSOD, using peroxynitrite as a substrate[177]. Peroxynitrite reacts with the enzyme by forming a transient cuprous adduct which can donate nitronium ions to phenols or tyrosines. After the release of a hydroxyl radical, CuZnSOD is regenerated[178]. By this mechanism, the metalloenzyme is also able to catalyze its own nitration[177].

5.3.2.2 MnSOD nitration

Peroxynitrite is able to nitrate and subsequently inactivate MnSOD as shown in Figure 4.14 and as reported in the literature. Tyrosine nitration and inactivation of recombinant human MnSOD *in vitro* occurs in a dose-dependent manner from 50 μM to 1 mM peroxynitrite (Figure 4.14). Repeated exposure of the protein to 1 mM peroxynitrite led to increased protein nitration and a loss of almost 90% of the enzyme's activity and while a single treatment of 10 μM had no effect, 3 consecutive treatments at the same concentration were sufficient to detect Tyr-nitration by Western Blot (data not shown). This is explained by the fact that peroxynitrite decomposes rapidly at a physiological pH, with a half-life of 1 s in phosphate buffer; we can therefore imagine that if exposed to continuous fluxes of peroxynitrite, fairly low concentrations should be necessary in order to obtain nitration.

Interestingly, 400 μM Sin-1 did not cause any tyrosine nitration or inactivation of the enzyme. It can be presumed that MnSOD scavenges O_2^- delivered by Sin-1 before it can associate with •NO to form peroxynitrite. Even though one might argue that peroxynitrite formation ($Kd=6{,}7x10^9 M^{-1}s^{-1}$) is much faster than MnSOD scavenging of O_2^- ($Kd=2x10^9 M^{-1}s^{-1}$), it is compensated by the fact that MnSOD (4,5 μM) is in great excess compared to peroxynitrite generated from Sin-1 (0,4 μM). When pre-treating MnSOD with 50 μM PON, the addition of Sin-1 led to further protein nitration, suggesting that when MnSOD is already partially inactivated, it is vulnerable to Sin-1 damaging (data not shown).

The exact mechanism of MnSOD inactivation is unknown but it most likely requires both nitration and oxidation through nitro-tyrosine and dityrosine formation [179]. Three tyrosine residues (Y34, Y45 and Y193) out of a total of 9 tyrosines can be nitrated in the MnSOD molecule[179].The Y34 residue was a plausible candidate for explaining MnSOD inactivation through nitration since crystallographic structure analysis of the enzyme indicated that it is oriented towards the active site and could possibly block O_2^- access by its negative charge. However contradictory results argue on whether or not the nitration of Y34 is the main damage responsible for MnSOD inactivation[128,180].

The reversibility of MnSOD nitration has not shown clear results in the literature but in preliminary experiments in which MnSOD was treated with peroxynitrite and subsequently dithionite, tyrosine nitration was still detected, suggesting that it may not be reversible (data not shown).

Preliminary data has suggested that MnSOD may catalyze its own tyrosine nitration in a similar manner as described for CuZnSOD[177].

MnSOD nitration and inactivation has been associated with a number of diseases (further discussed in section 5.4), which may be explained by a peroxynitrite-mediated amplification cycle (Figure 5.1). Tyrosine nitration and therefore inactivation of MnSOD may lead to increased levels of O_2^- and coincidentally increased peroxynitrite formation which can subsequently lead to the oxidation and nitration of crucial mitochondrial proteins and eventually results in mitochondrial dysfunction and death.

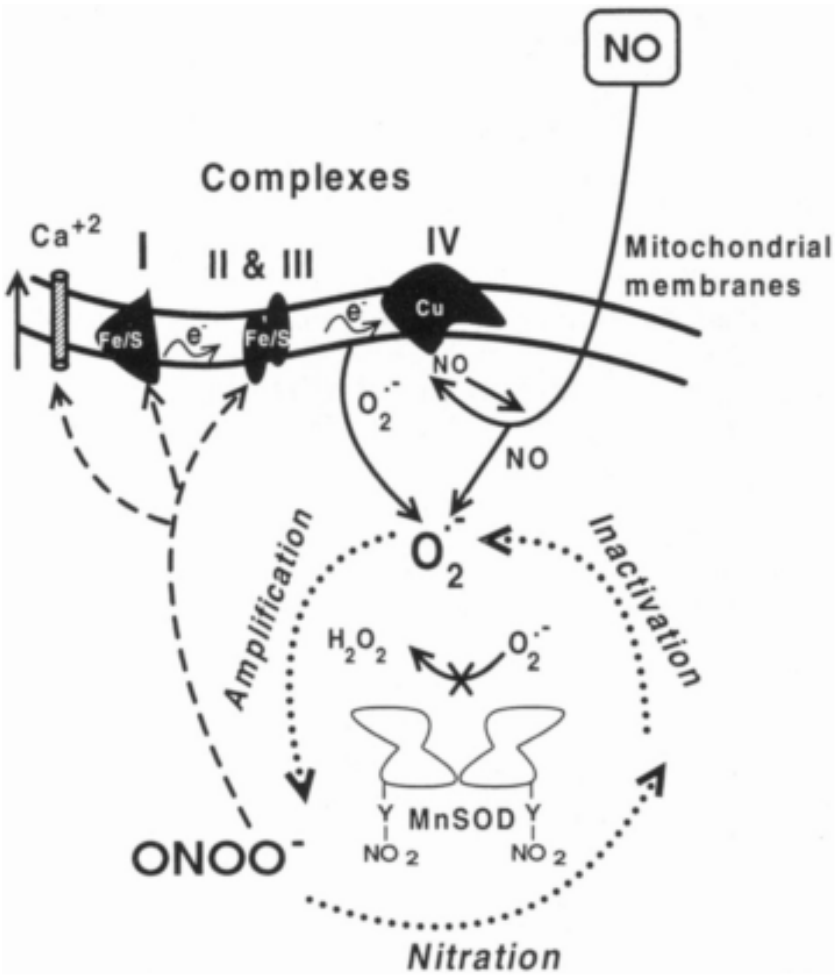

Figure 5.1: Peroxynitrite-mediated amplification cycle
Tyrosine nitration and subsequent inactivation of MnSOD leads to increased levels of O_2^- and PON formation which can lead to the oxidation and nitration of crucial mitochondrial proteins and results in mitochondrial dysfunction and even more peroxynitrite formation.
From[189]

The fact that MnSOD contains 9 tyrosine residues, some of which can be nitrated or oxidized, while CuZnSOD has none and has been shown to be relatively resistant to RONS can seem puzzling from an evolutionary reasoning as it is known that MnSOD is more crucial for cell survival. Thus, it can be speculated that inactivation of MnSOD may be involved in apoptotic pathways or may have a more general role in redox regulation.

5.3.3 Peroxynitrite versus •OH radicals

In the literature, much of the oxidative damage measured *in vivo* has been attributed to the highly reactive •OH radicals. However, we believe that peroxynitrite is the more significant agent in mediating damage to mitochondrial biomolecules than •OH.

Initially, peroxanitrite-induced 8-oxodG were thought to be mediated by •OH radicals but Spencer et al. have proposed a mechanism in which these lesions are directly caused by reaction with peroxynitrite (Figure 5.2)[70]. Data from the Fpg-based FADU assay experiments confirm this hypothesis. Sin-1 does not induce DNA strand breaks as we have seen that its addition to plasmid DNA without the 8-oxodG-specific glycosylase Fpg did not cause DNA unwinding (data not shown). On the other hand, •OH radicals are known to cause a substantial amount of DNA strand breaks which we have also confirmed by FADU experiments using H_2O_2 and a source of iron (data not shown). This clearly implies that 8-oxodG formation is caused by peroxynitrite itself and not its alleged decomposition into •OH.

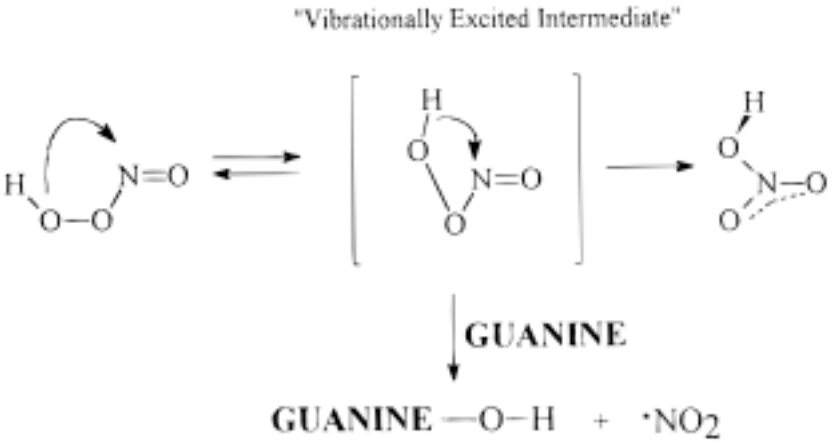

Figure 5.2: Proposed mechanism of 8-oxodG formation by peroxynitrite *(from Spencer et al. 1996)*
The transfer of the hydroxyl group occurs through a vibrationally excited intermediate homolytic cleavage of peroxynitrous acid to leave 8-oxodG and •NO2.
From[70]

This work has shown that MnSOD efficiently prevents the formation of peroxynitrite-induced 8-oxodG in plasmid DNA (Figure 4.11) and we postulate that its major role as a component of mitochondrial nucleoids is the prevention of DNA damage caused by peroxynitrite. It is very plausible that peroxynitrite formation is high in the vicinity of mtDNA since mtDNA is associated with the inner membrane in which •NO accumulates and is produced by mtNOS and where O_2^- is produced by the ETC. A high concentration of MnSOD at the mtDNA is

therefore required and is conferred by its binding. The role of MnSOD in protecting mtDNA from •OH-mediated damage by scavenging O_2^- seems less likely. By dismutating O_2^-, the enzyme releases H_2O_2 which is either further detoxified into H_2O or can yield •OH radicals in the presence of metals. O_2^- itself is not very reactive and by producing H_2O_2, MnSOD enhances the chance of •OH formation. It would be logical that if MnSOD takes such a risk, it is in the interest of creating a lesser evil, in other words in preventing the formation of peroxynitrite (Figure 5.3).

Another argument in favor of the prevalence of peroxynitrite-induced damage in mitochondria is that •OH will react with virtually any organic molecule due to its high reactivity and can therefore only diffuse a short distance. The metal required for the formation of •OH must be located very closely to the target biomolecule in order for a reaction to occur. Conversely, peroxynitrite can diffuse longer distances and can cross lipid barriers which gives it the possibility of reaching a broad spectrum of targets.

It is difficult to assign a particular oxidative lesion to peroxynitrite because all of the reactions it is able to cause are shared by other RONS and therefore the perfect peroxynitrite assay does not exist. However, the presence of nitrated proteins and 8-nitroguanine (Figure 4.14-17) is a clear indication for the action of peroxynitrite, a type of damage that •OH is obviously unable to cause.

The above-listed arguments clearly plead for a higher relevance of peroxynitrite in mediating damage to biomolecules in mitochondria compared to •OH. Hence the role of associated MnSOD in nucleoids may be related more to the prevention of peroxynitrite formation than that of •OH radicals. Nevertheless, much remains to be determined about the precise role of peroxynitrite in different physiological and pathological processes and its involvement in human disease.

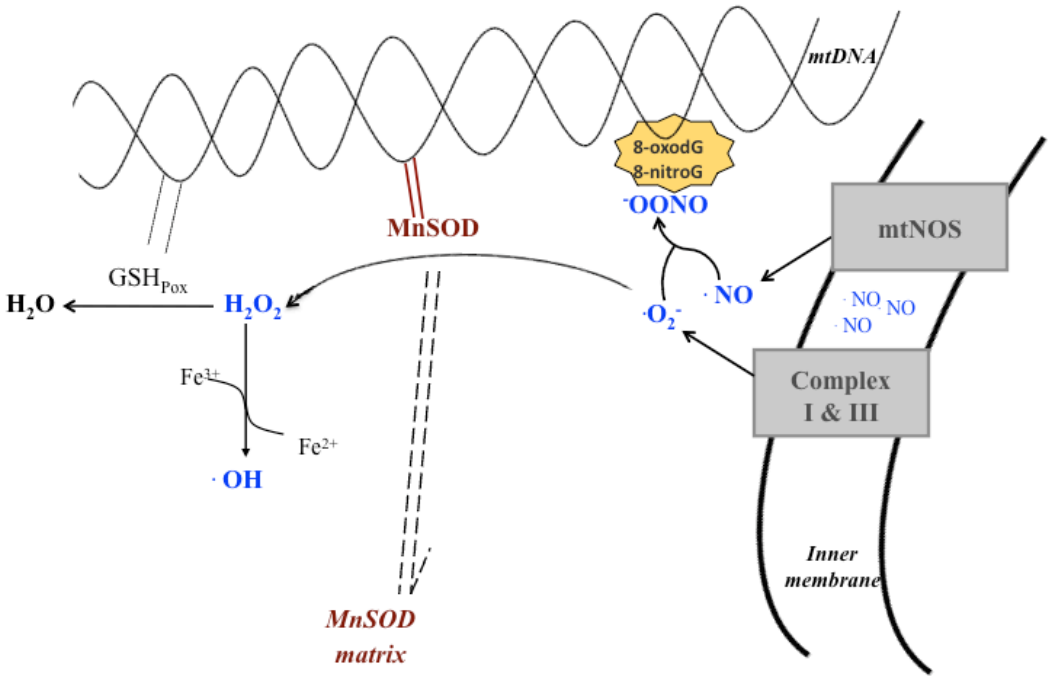

Figure 5.3: Model of peroxynitrite as a major damaging agent of mtDNA
O_2^- and NO are produced by respectively the ETC and mtNOS both located within the inner membrane. These molecules react to form peroxynitrite, an agent that causes 8-oxodG and 8-nitroguanine to mtDNA which is located in close proximity as it is associated with proteins of the inner membrane. DNA bound MnSOD is at ideally situated to prevent this damage by scavenging O_2^-.

5.4 MnSOD in disease and aging

MtDNA damage has been associated with aging and a wide spectrum of diseases, including diabetes, cancer, neurodegenerative and cardiovascular diseases [181,182]. This work has demonstrated that MnSOD is a potent antioxidant that protects DNA from oxidative damage, notably in preventing peroxynitrite-induced 8-oxodG and and it is likely that its binding to mtDNA increases its antioxidant efficiency. But to what extent is MnSOD crucial for the maintenance of mitochondrial integrity and what role does it play in disease and aging ?

5. 4. 1 MnSOD in disease

The presence of MnSOD is absolutely vital for the organism as it has been reported that homozygous mutant mice $Sod2^{-/-}$ die within days or weeks after birth mainly from neurodegeneration or myocardial injury[183,184].
A loss of MnSOD activity has been associated with various diseases such as cancer, progeria, asthma and transplant rejection. It is however uncertain if this decline is caused by a reduced activity of the protein itself or a decreased gene transcription.

MnSOD enzyme activity can be affected by different types of post-translational modifications such as phosphorylation, acetylation and nitration.
Phosphorylation of MnSOD inactivates the enzyme, as reports in heart mitochondria have shown[185]. As previously mentioned, very recent data has shown that MnSOD acetylation and deacetylation on its lysine-122, lysine 53 and lysine-89 play a role on its activation and inactivation[186,186]. The fact that it is mediated by Sirtuin 3 is particularly interesting since its regulation is dependent on changes in mitochondrial nutrient or redox status[134,187,188]. In accordance with the literature, we have shown that MnSOD can be nitrated and subsequently inactivated by PON (Figure 4.14)[128].
During chronic rejection of renal allografts, MnSOD transcription is increased whereas its activity is dramatically decreased, which is in line with the finding that MnSOD is tyrosine nitrated and inactivated[189]. The increase of MnSOD protein expression may be a mechanism of the cell to compensate for MnSOD inactivation by peroxynitrite but as the decrease in activity suggests, the compensation is manifestly insufficient.

A similar phenomenon was observed in alveolar type II epithelial cells in rat lung exposed to hyperoxic conditions[190]. MnSOD nitration has also been reported in rheumatoid arthritis, sepsis and myocarditis[189].

Since tyrosine nitration in proteins has been associated with many pathophysiological conditions, MnSOD nitration may be involved in many more diseases by a peroxynitrite-mediated amplification cycle (Figure 5.2).

Many cancer cells exhibit low levels of MnSOD activity. It has been associated with a polymorphism in the mitochondrial targeting sequence of the enzyme that prevents it from being properly targeted to the mitochondrion[191]. Another mechanism involved in the decrease of MnSOD activity in cancer cells is an impairment of MnSOD gene transcription, as it has been reported in hepatocarcinoma tissues[192]. Inappropriate metal incorporation leading to an inactive MnSOD has also been associated with cancer, notably hepatocarcinoma[193].

Conversely, other reports have argued that MnSOD activity increases in cancer cells compared to their normal counterparts[194,195].

Interestingly, the occurence of various signalling events that drive metastasis in many tumor types have been attributed to the ability of overexpressed MnSOD to modulate the cellular redox-environment through increased production of H_2O_2[196].

5.4.2. MnSOD in aging

Although no experiments in this work have been directly related to the aging process, it is nevertheless of interest to situate the role of MnSOD as an antioxidant in the present context of aging theories.

Over 50 years ago, Harman et al. proposed a model in which free radicals were involved in the aging process[71]. It stipulates that progressive and irreversible accumulation of oxidative damage leads to a loss of physiological function and to an aging phenotype. Ever since, the free radical theory of aging, also known as the „oxidative stress theory of aging“, has gained popularity. The theory has been challenged numerously, has evolved over the years and given rise to many different models even though the concept itself still remains central in understanding the aging process. After the discovery of the mitochondrial genome, Harman extended the concept to the mitochondrial theory of aging in which cumulative damage to the mtDNA plays a central part in the aging process[197]. The theory was further refined by Miquel et al. in the sense that he proposed that primarily fixed post-mitotic cells were subject to mtDNA damage with aging[198].

Another model derived from the oxidative stress theory is the „Survival Of the Slowest“ model (SOS). It is based on the belief that mitochondria with reduced respiratory function due to mutations in the mtDNA suffer less frequent lysosomal degradation, because they dispense oxidative damage more slowly on their own membranes. This slower turnover of mitochondria leads to an accumulation of defective mitochondria carrying damage mtDNA and therefore to an aging of the cell[199]. However this model has not received much enthusiasm and has been widely criticized.

So far, the most popular model based on the oxidative stress theory of aging involves the so-called „vicious cycle“. Since mtDNA encodes essentially for proteins of the ETC, oxidative damage to the mtDNA would lead to defective complexes which in turn would produce more RONS, and through a vicious cycle even more mtDNA damage[200].

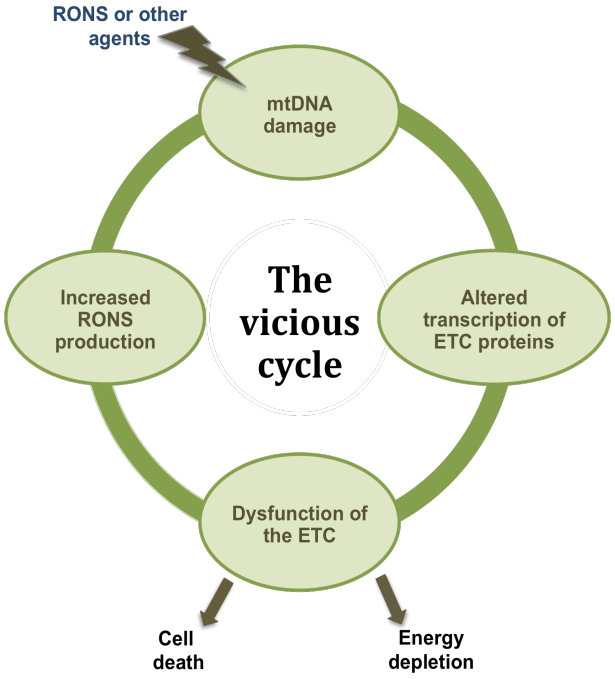

Figure 5.4: **The „vicious cycle theory“ of mitochondrial ROS production**
MtDNA damage caused by RONS or other damaging agents may lead to mutations which can either reduce transcription or lead to the transcription and translation of altered proteins of the ETC. This may cause dysfunction of the ETC and result in energy depletion, cell death or can increase RONS production which will in turn damage mtDNA and so forth, a process known as the vicious cycle.

Over the years, a substantial body of evidence has supported the oxidative stress theory of aging. Accumulation of damage to lipids, proteins and DNA has been observed in a wide panel of tissues and animal models. Also, long-living animals have been shown to accumulate less oxidative damage such as mitochondrial 8-oxodG than the more rapidly aging animals.

The observation that MnSOD activity decreases with age in human skin fibroblasts and in the skeletal muscle is an indicator that MnSOD may be involved in the aging process[201,202].
The recent finding in our group that the MnSOD is bound to mtDNA is consistent with the oxidative theory of aging. The presence of MnSOD and glutathione peroxidase as an antioxidant system within the nucleoid structure confers a better protection of the DNA against $O_2^{\cdot-}$-mediated damage. It was also shown that MnSOD protects DNA against peroxynitrite-induced 8-oxodG, a specific DNA lesion that accumulates with aging. The fact that peroxynitrite causes MnSOD nitration and coincidentally its inactivation may lead to an increase in oeroxynitrite formation and a subsequent increase in mitochondrial 8-oxodG.
A deletion of MnSOD in Saccharomyces cerevisiae has been shown to accelerate chronological aging whereas an overexpression increased lifespan[203]. Similarly, overexpression of MnSOD in Drosophila melanogaster extended lifespan by an average of 16%[204]. These results suggesting an involvement of the antioxidant enzyme in lifespan are however contradicted by studies conducted in mammalian transgenic knockout models.
It is important to note that the vast amount of data consistent with the oxidative theory of aging is correlative and does no present a direct link between oxidative damage and aging.

The validity of this theory has been questioned in recent years, with the emergence of contradictory results.
The role of MnSOD in aging has been a topic of great controversy and has been the subject of many studies notably in transgenic animal models. Although Sod2 $^{-/-}$ mice exhibited severe mitochondrial oxidative damage, they did not serve as an appropriate model for the study of lifespan and aging since they died shortly after birth from neurological and cardiac defects[183184]. Van Remmen et al. therefore opted for the more viable Sod2$^{+/-}$ mice heterozygous for MnSOD and displaying 50% less MnSOD activity in all tissues throughout life[205206207]. The mutant mice showed a considerable increase in mitochondrial and nuclear 8-oxodG levels compared to wt animals as well as with age, and a decreased GSH/GSSG ratio, indicating an increased oxidative stress. Mitochondrial function was also altered in these mice: with a reduction in ATP production and a decrease in ETC complexes I and V activity in skeletal muscle. However, mutant mice did not show any significant difference in lifespan compared to wild-type mice. Old Sod2$^{+/-}$ mice exhibited in the same way as wild type mice biomarkers of aging such as cataract formation, defective immune response and formation of glycoxidation products in skin collagen but did show a higher incidence of cancer.

The Van Remmen group has conducted research on 18 different genetic manipulations in antioxidant systems, using mouse models and with the exception of $Sod1^{-/-}$ mice, no effect on lifespan was detected. For instance, Gpx1-/-, Gpx4+/-, and Trx2+/- mice exhibited higher oxidative damage levels but no reduction in lifespan.

The reduced CuZnSOD activity in $Sod1^{-/-}$ mice was associated with increased oxidative damage, a very high incidence of age-related diseases and a shortened lifespan[208]. However, Van Remmen et al. argue that the reduced lifespan in these animals might not necessarily be due to premature aging but rather to a novel pathology from the genetic mutation. This is why a better indication of how an enzyme affects lifespan would be an increase in lifespan (for example in an overexpression) than a decrease that could be due to other factors, such as disease. A 2-fold overexpression of MnSOD in mice led to a decrease in lipid peroxidation, a reinforced resistance against oxidative stress and a decrease in age-related mitochondrial dysfunction but failed to show any alteration in lifespan or age-related disorders mice. However, a study conducted in a different group showed an increase in lifespan in MnSOD overexpressing mice. Overexpression of CuZnSOD, catalase and glutathione peroxidase 4 in mice resulted in increased resistance to oxidative stress but had no effect on lifespan.

Another transgenic mouse experiment brought doubt to the oxidative theory of aging. In homozygous knockin mice expressing a proof-reading-deficient form of polymerase Polgγ, an accumulation of 3-5-fold levels of point mutations and an increase in deletions were reported[209]. This was associated with a reduced lifespan and a premature age-related phenotype, hence showing a causative link between mtDNA mutation accumulation and aging phenotypes. Surprisingly, no increase in oxidative stress markers was observed[210]. It should be considered, however that under physiological conditions, the potential markers for oxidative stress are degraded. According to Zheng et al., inherent error frequency mediated by DNA polγ is the primary source of mitochondrial point mutations in human tissues rather than oxidative stress[211].

Lastly, the comparison of two species of rodents with different maximum lifespans further challenged the oxidative stress theory of aging: the naked mole rat at 28,3 years and *Mus musculus* at 3,5 years showed that the long-lived naked mole rat surprisingly exhibited higher levels of DNA damage, lipid peroxidation and protein carbonylation at a young age[212].

Oxidative damage to mtDNA is central in explaining the aging process, according to the oxidative stress theory of aging. The demonstration by our group that MnSOD binds to mtDNA ensuring its protection and the ability of the enzyme to prevent peroxynitrite-induced

8-oxodG suggests that it is likely to be involved in the aging process. However, as previously discussed, MnSOD $^{+/-}$ mice did not exhibit premature aging despite higher levels of oxidative stress[207]. Moreover, the minor impact of 8-oxodG levels on mutation rate and on mitochondrial dysfunction casts doubt on the actual relevance of this particular oxidative lesion in the aging process (as mentioned in section 5.3 of the discussion).

In light of this conflicing data, it is likely that the aging process undergoes a more complex regulation that might be finely orchestrated by a network of redox reactions. This redox regulation consists of a balance between oxidation-based reactions and all of the counteracting defense, repair and adaptative mechanisms. As previously described, a wide range of enzymes can be activated or inactivated –some reversibly- by various types of RONS-induced modifications (such as tyrosine nitration, S-nitrosation, methionine sulfoxidation) which can affect various signalling events, taking part in the so-called redox regulation. An imbalance between RONS generation and clearance gives rise to oxidative stress resulting in an accumulation of damage to proteins (nitration, carboxylation), lipids (peroxidation) and DNA (8-oxodG, strand breaks). This damage of biomolecules can occur at a young age but is largely repaired or rapidly degraded, making it difficult to detect while it tends to accumulate in older individuals due to repair and degradation deficiencies and participates in the aging process.

The study on Polγ-deficient mice suggests that a deficiency in repair of mtDNA affects aging rather than elevated oxidative DNA damage due to an age-related increase in oxidative stress. Oxidative damage in mtDNA may accumulate even in young individuals without any incidence on mitochondrial dysfunction. This can be explained by the fact that mtDNA is present in multiple copies in mitochondria and can be redistributed during mitochondrial fusion and fission in the aim of preserving a minimal level of intact mtDNA copies per mitochondrion. This correlates well with the existence of a threshhold of 80% of mutation rate that must be reached in mtDNA before a heteroplasmic cell exhibits mitochondrial dysfunction[213].

It must nevertheless be noted that DNA repair capacity is not necessarily impaired with age as 8-oxodG glycosylase/AP lyase activity measured in rat liver and heart was reported to increase with age[164]. This case however is referring to the repair of 8-oxodG, a lesion that has shown little actual functional relevance.

As for oxidized proteins, it was stated in the Introduction section that their accumulation is regulated by their degradation rate, meaning that protein damage may also be largely present in young individuals but escapes detection due to rapid turnover. The study comparing naked

mole rat to the common mouse *mus musculus* corroborates this theory [212]. The long living naked mole rat already accumulates oxidative damage at a young age, which could be argued to be explained to a certain extent by its sudden exposure to high oxygen concentrations in the laboratory environment compared its hypoxic lifestyle. Nevertheless, protein structure and integrity are better maintained than in mice. They display low levels of protein ubiquitination and higher proteosome activity which explains their higher turnover.

These two studies suggest that age-related mitochondrial dysfunction may be explained by a deficiency in repair mechanisms and degradation of oxidative damage leading to an accumulation of mtDNA mutations and oxidized proteins rather than an increase in oxidative stress itself and a deficiency in antioxidant activity.

Mutations in mtDNA and a lack of protein degradation may lead to deficient enzymes in the ETC which will generate less ATP. This decrease in energy may lead to a loss of mitochondrial and cell function leading to its death by apoptosis or necrosis.

To summarize, the presence of MnSOD is without a doubt critical for cell survival by limiting oxidative stress notably to mtDNA and its binding is likely to confer an enhanced protection. While a loss in its activity has been associated with numerous diseases, its impact on aging has not been demonstrated.

5.5 Conclusion

Although the exact mechanism of the association of MnSOD to mtDNA has not yet been elucidated, the results in this study have brought to light some new evidence on the binding properties of the enzyme. Binding of the enzyme does not depend on the three accessible N- and C-terminal lysines, or at least not solely as mutants of these residues all displayed the ability to bind to double stranded DNA detected by a SPR-based assay. The weakness of the binding observed by the very slow association phase might be due to the simplicity of the experimental setup and may not be representative of the scenario occurring *in vivo*. MnSOD might have preferred sites of binding on the mitochondrial genome, require a more complex DNA conformation than that of the short 34-mer nucleotide or necessitate a particular surrounding of nucleoid proteins for a stable binding. The sterical advantage of MnSOD in the mitochondrial matrix may also explain the weakness of the interaction which would not need to be of high affinity to take place.

This interaction seems to be dynamic as it was shown that whether it takes place or not is dependent on cell type and can also vary within a same cell model such as the Xenopus oocyte during its different stages of oogenesis. It can be been hypothesized that the binding is dependent on cell division, metabolic state, redox state or stress-related processes.

MnSOD binding most likely confers a reinforced protection of mtDNA since its concentration at that site is therefore automatically increased. Superoxide concentrations surrounding mtDNA are believably high as it is associated with the inner membrane via some of its nucleoid components. Moreover, NO is produced by mtNOS in the inner membrane and NO is known to diffuse very easily and to have a high affinity for the lipid bilayer meaning that the chances of forming peroxynitrite with neighboring superoxide, one of the fastest occurring cellular reaction are high. MnSOD, as shown by the results of this study, is capable of preventing peroxynitrite-induced damage by scavenging O_2^- before it reacts with NO, which is only possible if the enzyme is in excess.

These experiments were conducted with the Fpg-based FADU method fo the detection of 8-oxodG and its optimization and validation has been a major part of this work. It can serve as a novel assay for screening antioxidants due to its simplicity, reproducibility and high throughput. Its application to the detection of 8-oxodG in mtDNA still remains a challenge but would open exciting new perspectives as it would offer a simple and reliable method for detecting oxidative damage in whole isolated mitochondria.

It is clear that mtDNA is highly prone to oxidative damage due to its close proximity to the ETC and is involved in a variety of diseases and in the aging process. MnSOD is able to protect it from oxidative damage caused by peroxynitrite, a highly reactive molecule which is assumed to be responsible for a large part of oxidative cell damage and also plays a role in redox regulation mechanisms due to its high reactivity and diffusion capacity. The association or dissociation of MnSOD to mtDNA is crucial for the prevention of peroxynitrite-mediated damage and is in this respect relevant in pathological processes.

6 References

1. Gray, M. W. Mitochondrial Evolution. *Science* **283**, 1476–1481 (1999).
2. Nass, S. & Nass, . Intramitochondrial fibers with DNA characteristics II. Enzymatic and other hydrolytic treatments *The Journal of cell biology* **19**, 613–29 (1963).
3. Nosek, J., Tomáska, L., Fukuhara, H., Suyama, Y. & Kovác, L. Linear mitochondrial genomes: 30 years down the line. *Trends in genetics : TIG* **14**, 184–8 (1998).
4. Langkjaer, R. B. Sequence analysis of three mitochondrial DNA molecules reveals interesting differences among Saccharomyces yeasts. *Nucleic Acids Research* **31**, 3081–3091 (2003).
5. Galtier, N. The intriguing evolutionary dynamics of plant mitochondrial DNA. *BMC biology* **9**, 61 (2011).
6. Nass, M. M. Mitochondrial DNA. I. Intramitochondrial distribution and structural relations of single- and double-length circular DNA. *Journal of molecular biology* **42**, 521–8 (1969).
7. Anderson, S. *et al*. Sequence and organization of the human mitochondrial genome. *Nature* **290**, 457–65 (1981).
8. Bibb, M. J., Van Etten, R. A., Wright, C. T., Walberg, M. W. & Clayton, D. A. Sequence and gene organization of mouse mitochondrial DNA. *Cell* **26**, 167–80 (1981).
9. Claros, M. G. *et al*. Limitations to in vivo import of hydrophobic proteins into yeast mitochondria. The case of a cytoplasmically synthesized apocytochrome b. *European journal of biochemistry / FEBS* **228**, 762–71 (1995).
10. Allen, J. F. Control of gene expression by redox potential and the requirement for chloroplast and mitochondrial genomes. *Journal of theoretical biology* **165**, 609–31 (1993).
11. Henriquez, F. L., Richards, T. a, Roberts, F., McLeod, R. & Roberts, C. W. The unusual mitochondrial compartment of Cryptosporidium parvum. *Trends in parasitology* **21**, 68–74 (2005).
12. Morais, R., Desjardins, P., Turmel, C. & Zinkewich-Péotti, K. Development and characterization of continuous avian cell lines depleted of mitochondrial DNA. *In vitro cellular & developmental biology : journal of the Tissue Culture Association* **24**, 649–58 (1988).
13. King, M. P. & Attardi, G. Human cells lacking mtDNA: repopulation with exogenous mitochondria by complementation. *Science (New York, N.Y.)* **246**, 500–3 (1989).
14. Bellance, N., Lestienne, P. & Rossignol, R. Mitochondria: from bioenergetics to the metabolic regulation of carcinogenesis. *Frontiers in bioscience : a journal and virtual library* **14**, 4015–34 (2009).
15. Shadel, G. S. & Clayton, D. a Mitochondrial DNA maintenance in vertebrates. *Annual review of biochemistry* **66**, 409–35 (1997).
16. Larizza, A., Pesole, G., Reyes, A., Sbisà, E. & Saccone, C. Lineage specificity of the evolutionary dynamics of the mtDNA D-loop region in rodents. *Journal of molecular evolution* **54**, 145–55 (2002).
17. Clayton, D. A. Replication of animal mitochondrial DNA. *Cell* **28**, 693–705 (1982).

18. Fish, J., Raule, N. & Attardi, G. Discovery of a major D-loop replication origin reveals two modes of human mtDNA synthesis. *Science (New York, N.Y.)* **306**, 2098–101 (2004).

19. Brown, T. a, Cecconi, C., Tkachuk, A. N., Bustamante, C. & Clayton, D. a Replication of mitochondrial DNA occurs by strand displacement with alternative light-strand origins, not via a strand-coupled mechanism. *Genes & development* **19**, 2466–76 (2005).

20. Brown, W. M., George, M. & Wilson, a C. Rapid evolution of animal mitochondrial DNA. *Proceedings of the National Academy of Sciences of the United States of America* **76**, 1967–71 (1979).

21. Nunnari, J. *et al*. Mitochondrial transmission during mating in Saccharomyces cerevisiae is determined by mitochondrial fusion and fission and the intramitochondrial segregation of mitochondrial DNA. *Molecular biology of the cell* **8**, 1233–42 (1997).

22. De Giorgi, F., Lartigue, L. & Ichas, F. Electrical coupling and plasticity of the mitochondrial network. *Cell calcium* **28**, 365–70

23. Thompson, W. E., Ramalho-Santos, J. & Sutovsky, P. Ubiquitination of prohibitin in mammalian sperm mitochondria: possible roles in the regulation of mitochondrial inheritance and sperm quality control. *Biology of reproduction* **69**, 254–60 (2003).

24. Ashley, M. V., Laipis, P. J. & Hauswirth, W. W. Rapid segregation of heteroplasmic bovine mitochondria. *Nucleic acids research* **17**, 7325–31 (1989).

25. © 1996 Nature Publishing Group http://www.nature.com/naturegenetics. *Group* (1996).

26. Jenuth, J. P., Peterson, A. C., Fu, K. & Shoubridge, E. A. Random genetic drift in the female germline explains the rapid segregation of mammalian mitochondrial DNA. *Nature genetics* **14**, 146–51 (1996).

27. Cao, L. *et al*. The mitochondrial bottleneck occurs without reduction of mtDNA content in female mouse germ cells. *Nature genetics* **39**, 386–90 (2007).

28. Cao, L. *et al*. New evidence confirms that the mitochondrial bottleneck is generated without reduction of mitochondrial DNA content in early primordial germ cells of mice. *PLoS genetics* **5**, e1000756 (2009).

29. Brown, D. T., Samuels, D. C., Michael, E. M., Turnbull, D. M. & Chinnery, P. F. Random genetic drift determines the level of mutant mtDNA in human primary oocytes. *American journal of human genetics* **68**, 533–6 (2001).

30. Ruiz-pesini, E. & Ã, D. C. W. Evidence for Adaptive Selection Acting on the tRNA and rRNA Genes of Human Mitochondrial DNA. **27**, 1072–1081 (2006).

31. Kukat, C., Wurm, C. A., Spåhr, H., Falkenberg, M. & Larsson, N. Super-resolution microscopy reveals that mammalian mitochondrial nucleoids have a uniform size and frequently contain a single copy of mtDNA. *PNAS* (2011).

32. Bogenhagen, D. F., Rousseau, D. & Burke, S. The Layered Structure of Human Mitochondrial. *Journal of Biological Chemistry* **283**, 3665–3675 (2008).

33. Cotney, J., Wang, Z. & Shadel, G. S. Relative abundance of the human mitochondrial transcription system and distinct roles for h-mtTFB1 and h-mtTFB2 in mitochondrial biogenesis and gene expression. *Nucleic acids research* **35**, 4042–54 (2007).

34. Takamatsu, C. *et al*. Regulation of mitochondrial D-loops by transcription factor A and single-stranded DNA-binding protein. *EMBO reports* **3**, 451–6 (2002).

35. Fisher, R. P., Lisowsky, T., Parisi, M. A. & Clayton, D. A. DNA wrapping and bending by a mitochondrial high mobility group-like transcriptional activator protein. *The Journal of biological chemistry* **267**, 3358–67 (1992).

36. Grosschedl, R., Giese, K. & Pagel, J. HMG domain proteins: architectural elements in the assembly of nucleoprotein structures. *Trends in genetics : TIG* **10**, 94–100 (1994).

37. Ekstrand, M. I. *et al*. Mitochondrial transcription factor A regulates mtDNA copy number in mammals. *Human molecular genetics* **13**, 935–44 (2004).

38. Barja, G. & Herrero, a Oxidative damage to mitochondrial DNA is inversely related to maximum life span in the heart and brain of mammals. *FASEB* **14**, 312–8 (2000).

39. Hamilton, M. L. *et al*. Does oxidative damage to DNA increase with age? **98**, 10469–10474 (2001).

40. Wang, Y. & Bogenhagen, D. F. Human Mitochondrial DNA Nucleoids Are Linked to Protein Folding Machinery and Metabolic Enzymes at the Mitochondrial Inner Membrane *Journal of Biological Chemistry* **281**, 25791–25802 (2006).

41. Reyes, a *et al*. Actin and myosin contribute to mammalian mitochondrial DNA maintenance. *Nucleic acids research* **39**, 5098–108 (2011).

42. He, J. *et al*. The AAA+ protein ATAD3 has displacement loop binding properties and is involved in mitochondrial nucleoid organization. *The Journal of cell biology* **176**, 141–6 (2007).

43. Wang, Y. & Bogenhagen, D. F. Human Mitochondrial DNA Nucleoids Are Linked to Protein Folding Machinery and Metabolic Enzymes at the Mitochondrial Inner Membrane *Journal of Biological Chemistry* **281**, 25791–25802 (2006).

44. Jacobs, H. T., Lehtinen, S. K. & Spelbrink, J. N. No sex please , we're mitochondria : a hypothesis on the somatic unit of inheritance of mammalian mtDNA. *BioEssays* 564–572 (2000).

45. D'Aurelio, M. *et al*. Heterologous mitochondrial DNA recombination in human cells. *Human molecular genetics* **13**, 3171–9 (2004).

46. Gilkerson, R. W., Schon, E. A., Hernandez, E. & Davidson, M. M. *Cell* 1117–1128 (2008).doi:10.1083/jcb.200712101

47. Garrido, N. *et al*. Composition and Dynamics of Human Mitochondrial Nucleoids. *Molecular Biology of the Cell* **14**, 1583–1596 (2003).

48. Shen, E. L. & Bogenhagen, D. F. Developmentally-regulated packaging of mitochondrial DNA by the HMG-box protein mtTFA during Xenopus oogenesis. *Spring* **29**, 2822–2828 (2001).

49. Lesnefsky, E. J., Moghaddas, S., Tandler, B., Kerner, J. & Hoppel, C. L. Mitochondrial dysfunction in cardiac disease: ischemia--reperfusion, aging, and heart failure. *Journal of molecular and cellular cardiology* **33**, 1065–89 (2001).

50. Sugioka, K. *et al*. Mechanism of O2- generation in reduction and oxidation cycle of ubiquinones in a model of mitochondrial electron transport systems. *Biochimica et biophysica acta* **936**, 377–85 (1988).

51. Zhang, L., Yu, L. & Yu, C. A. Generation of superoxide anion by succinate-cytochrome c reductase from bovine heart mitochondria. *The Journal of biological chemistry* **273**, 33972–6 (1998).

52. Kwong, L. K. & Sohal, R. S. Substrate and site specificity of hydrogen peroxide generation in mouse mitochondria. *Archives of biochemistry and biophysics* **350**, 118–26 (1998).

53. Barja, G. Mitochondrial oxygen radical generation and leak: sites of production in states 4 and 3, organ specificity, and relation to aging and longevity. *Journal of bioenergetics and biomembranes* **31**, 347–66 (1999).

54. Fridovich, I. Mitochondria : are they the seat of senescence ? *Aging Cell* 13–16 (2004).doi:10.1111/j.1474-9728.2003.00075.x

55. Coon, M. J., Ding, X. X., Pernecky, S. J. & Vaz, A. D. Cytochrome P450: progress and predictions. *FASEB journal : official publication of the Federation of American Societies for Experimental Biology* **6**, 669–73 (1992).

56. Babior, B. M. The NADPH oxidase of endothelial cells. *IUBMB life* **50**, 267–9

57. Yokoyama, Y. *et al*. Circulating xanthine oxidase: potential mediator of ischemic injury. *The American journal of physiology* **258**, G564–70 (1990).

58. Nathan, C. Specificity of a third kind : reactive oxygen and nitrogen intermediates in cell signaling. *Microbiology and Immunology* (2003)

59. Alvarez, S., Valdez, L. B., Zaobornyj, T. & Boveris, A. Oxygen dependence of mitochondrial nitric oxide synthase activity. *Biochemical and biophysical research communications* **305**, 771–5 (2003).

60. Ghafourifar, P. & Richter, C. Nitric oxide synthase activity in mitochondria. *FEBS Letters* **418**, 291–296 (1997).

61. Wagner, D. A., Young, V. R. & Tannenbaum, S. R. Mammalian nitrate biosynthesis: incorporation of 15NH3 into nitrate is enhanced by endotoxin treatment. *Proceedings of the National Academy of Sciences of the United States of America* **80**, 4518–21 (1983).

62. Bolaños, J. P., Moro, M. A., Lizasoain, I. & Almeida, A. Mitochondria and reactive oxygen and nitrogen species in neurological disorders and stroke: Therapeutic implications. *Advanced drug delivery reviews* **61**, 1299–315 (2009).

63. Ursini, F. *et al*. Diversity of glutathione peroxidases. *Methods in enzymology* **252**, 38–53 (1995).

64. Radi, R. *et al*. Detection of catalase in rat heart mitochondria. *The Journal of biological chemistry* **266**, 22028–34 (1991).

65. Davies, K. J. A., Delsignores, M. E. & Lin, S. W. Protein Damage and Degradation by Oxygen Radicals 11. *Society* **1858**, 9902–9907 (1987).

66. Grune, T., Reinheckel, T. & Davies, K. J. Degradation of oxidized proteins in K562 human hematopoietic cells by proteasome. *The Journal of biological chemistry* **271**, 15504–9 (1996).

67. Richman, P. G. & Meister, A. Regulation of gamma-glutamyl-cysteine synthetase by nonallosteric feedback inhibition by glutathione. *The Journal of biological chemistry* **250**, 1422–6 (1975).

68. Iñarrea, P. *et al*. Mitochondrial respiratory chain and thioredoxin reductase regulate intermembrane Cu,Zn-superoxide dismutase activity: implications for mitochondrial energy metabolism and apoptosis. *The Biochemical journal* **405**, 173–9 (2007).

69. Matés, J. M. & Sánchez-Jiménez, F. M. Role of reactive oxygen species in apoptosis: implications for cancer therapy. *The international journal of biochemistry & cell biology* **32**, 157–70 (2000).

70. Spencer, J. P. *et al*. Base modification and strand breakage in isolated calf thymus DNA and in DNA from human skin epidermal keratinocytes exposed to peroxynitrite or 3-morpholinosydnonimine. *Chemical research in toxicology* **9**, 1152–8 (1996).

71. HARMAN, D. Aging: a theory based on free radical and radiation chemistry. *Journal of gerontology* **11**, 298–300 (1956).

72. Bae, Y. S. *et al*. Epidermal growth factor (EGF)-induced generation of hydrogen peroxide. Role in EGF receptor-mediated tyrosine phosphorylation. *The Journal of biological chemistry* **272**, 217–21 (1997).

73. Sundaresan, M., Yu, Z. X., Ferrans, V. J., Irani, K. & Finkel, T. Requirement for generation of H2O2 for platelet-derived growth factor signal transduction. *Science (New York, N.Y.)* **270**, 296–9 (1995).

74. Guyton, K. Z., Liu, Y., Gorospe, M., Xu, Q. & Holbrook, N. J. Activation of Mitogen-activated Protein Kinase by H 2 O 2. **271**, 4138–4142 (1996).

75. Hecht, D. & Zick, Y. Selective inhibition of protein tyrosine phosphatase activities by H2O2 and vanadate in vitro. *Biochemical and biophysical research communications* **188**, 773–9 (1992).

76. Kretz-Remy, C., Bates, E. E. & Arrigo, A. P. Amino acid analogs activate NF-kappaB through redox-dependent IkappaB-alpha degradation by the proteasome without apparent IkappaB-alpha phosphorylation. Consequence on HIV-1 long terminal repeat activation. *The Journal of biological chemistry* **273**, 3180–91 (1998).

77. Demple, B. Study of redox-regulated transcription factors in prokaryotes. *Methods (San Diego, Calif.)* **11**, 267–78 (1997).

78. Branch, C. Oxygen radicals and signaling Toren Finkel. *Current Opinion in Cell Biology* 248–253 (1998).

79. Poderoso, J. J. *et al*. Nitric oxide inhibits electron transfer and increases superoxide radical production in rat heart mitochondria and submitochondrial particles. *Archives of biochemistry and biophysics* **328**, 85–92 (1996).

80. Ushmorov, A. *et al*. Nitric-oxide-induced apoptosis in human leukemic lines requires mitochondrial lipid degradation and cytochrome C release. *Blood* **93**, 2342–52 (1999).

81. Saavedra, J. E. *et al*. Targeting nitric oxide (NO) delivery in vivo. Design of a liver-selective NO donor prodrug that blocks tumor necrosis factor-alpha-induced apoptosis and toxicity in the liver. *Journal of medicinal chemistry* **40**, 1947–54 (1997).

82. Pinzar, E. *et al*. Angiotensin II induces tyrosine nitration and activation of ERK1/2 in vascular smooth muscle cells. *FEBS letters* **579**, 5100–4 (2005).

83. Yermilov, V., Rubio, J. & Ohshima, H. Formation of 8-nitroguanine in DNA treated with peroxynitrite in vitro and its rapid removal from DNA by depurination. *Reactions* **376**, 207–210 (1995).

84. Kasai, H. & Nishimura, S. Hydroxylation of the C-8 position of deoxyguanosine by reducing agents in the presence of oxygen. *Nucleic acids symposium series* 165–7 (1983)

85. Neeley, W. L. & Essigmann, J. M. Mechanisms of formation, genotoxicity, and mutation of guanine oxidation products. *Chemical research in toxicology* **19**, 491–505 (2006).

86. Yu, H., Venkatarangan, L., Wishnok, J. S. & Tannenbaum, S. R. Quantitation of four guanine oxidation products from reaction of DNA with varying doses of peroxynitrite. *Chemical research in toxicology* **18**, 1849–57 (2005).

87. Wood, M. L., Dizdaroglu, M., Gajewski, E. & Essigmann, J. M. Mechanistic studies of ionizing radiation and oxidative mutagenesis: genetic effects of a single 8-hydroxyguanine (7-hydro-8-oxoguanine) residue inserted at a unique site in a viral genome. *Biochemistry* **29**, 7024–32 (1990).

88. Chen, Q. I. N., Fischer, A. N. N., Reagan, J. D., Yan, L. & Ames, B. N. diploid. **92**, 4337–4341 (1995).

89. Kasai, H. *et al*. Formation of 8-hydroxyguanine moiety in cellular DNA by agents producing oxygen radicals and evidence for its repair. *Carcinogenesis* **7**, 1849–51 (1986).

90. Chengs, K. C., Cahills, D. S., Kasais, H., Nishimuras, S. & Loebs, L. A. 8-Hydroxyguanine, an Abundant Form of Oxidative DNA Damage, Causes G .--) T and A + C Substitutions*. *Cancer Research* 166–172 (1991).

91. Shibutani, S., Takeshita, M. & Grollman, A. P. Insertion of specific bases during DNA synthesis past the oxidation-damaged base 8-oxodG. *Nature* **349**, 431–4 (1991).

92. Kuchino, Y. *et al*. Misreading of DNA templates containing 8-hydroxydeoxyguanosine at the modified base and at adjacent residues. *Nature* **327**, 77–9

93. Hudson, E. K. *et al*. Age-associated change in mitochondrial DNA damage. *Free radical research* **29**, 573–9 (1998).

94. Biology, C. Age-associated Change in Mitochondrial DNA Damage. **29**, 573–579 (1998).

95. Wallace, D. C., Brown, M. D. & Lott, M. T. Mitochondrial DNA variation in human evolution and disease. *Gene* **238**, 211–30 (1999).

96. Anson, R. M., Hudson, E. & Bohr, V. A. Mitochondrial endogenous oxidative damage has been overestimated. *The FASEB Journal* 355–360

97. Yermilov, V. *et al*. Formation of 8-nitroguanine by the reaction of guanine with peroxynitrite in vitro. *Carcinogenesis* **16**, 2045–50 (1995).

98. Shafirovich, V., Mock, S., Kolbanovskiy, A. & Geacintov, N. E. Photochemically catalyzed generation of site-specific 8-nitroguanine adducts in DNA by the reaction of long-lived neutral guanine radicals with nitrogen dioxide. *Chemical research in toxicology* **15**, 591–7 (2002).

99. Chen, H. J. C., Chang, C. M. & Chen, Y. M. Hemoprotein-mediated reduction of nitrated DNA bases in the presence of reducing agents. *Free radical biology & medicine* **34**, 254–68 (2003).

100. Clayton, D. a, Doda, J. N. & Friedberg, E. C. The absence of a pyrimidine dimer repair mechanism in mammalian mitochondria. *Proceedings of the National Academy of Sciences of the United States of America* **71**, 2777–81 (1974).

101. Miyaki, M., Yatagai, K. & Ono, T. Strand breaks of mammalian mitochondrial DNA induced by carcinogens. *Chemico-biological interactions* **17**, 321–9 (1977).

102. Anderson, C. T. M. & Friedberg, E. C. Nucleic Acids Research. *Nucleic Acids Research* 875–888 (1980).

103. Myers, K. A., Saffhill, R. & O'Connor, P. J. Repair of alkylated purines in the hepatic DNA of mitochondria and nuclei in the rat. *Carcinogenesis* **9**, 285–92 (1988).

104. Liu, P. *et al*. Removal of oxidative DNA damage via FEN1-dependent long-patch base excision repair in human cell mitochondria. *Molecular and cellular biology* **28**, 4975–87 (2008).

105. Souza-pinto, N. C. D. *et al*. NIH Public Access. *DNA Repair* **8**, 704–719 (2010).

106. Thyagarajan, B., Padua, R. A. & Campbell, C. Mammalian mitochondria possess homologous DNA recombination activity. *The Journal of biological chemistry* **271**, 27536–43 (1996).

107. Nishioka, K. *et al*. Expression and differential intracellular localization of two major forms of human 8-oxoguanine DNA glycosylase encoded by alternatively spliced OGG1 mRNAs. *Molecular biology of the cell* **10**, 1637–52 (1999).

108. Souza-pinto, N. C. D. *et al*. Repair of 8-Oxodeoxyguanosine Lesions in Mitochondrial DNA Depends on the Oxoguanine DNA Glycosylase (OGG1) Gene and 8-Oxoguanine Accumulates in the Mitochondrial DNA of OGG1-defective Mice Advances in Brief Repair of 8-Oxodeoxyguanosine Lesions in Mito. *Cancer* (2001).

109. Maynard, S., Schurman, S. H., Harboe, C., Souza-pinto, N. C. D. & Ã, V. A. B. Base excision repair of oxidative DNA damage and association with cancer and aging. *October* **30**, 2–10 (2009).

110. Hudson, E. K. *et al*. Age-associated change in mitochondrial DNA damage. *Free radical research* **29**, 573–9 (1998).

111. Tuo J., Luo L. Importance of guanine nitration and hydroxylation in **29**, 147–155 (2000).

112. Kanki, T. *et al*. Mitochondrial Nucleoid and Transcription Factor A. *Annals of the New York Academy of Sciences* **1011**, 61–68 (2004).

113. Guliaeva, N. A., Kuznetsova, E. A. & Gaziev, A. I. [Proteins associated with mitochondrial DNA protect it against the action of X-rays and hydrogen peroxide]. *Biofizika* **51**, 692–7

114. Yoshida, Y. *et al*. Human mitochondrial transcription factor A binds preferentially to oxidatively damaged DNA. *Biochemical and biophysical research communications* **295**, 945–51 (2002).

115. Wang, J., Silva, J. P., Gustafsson, C. M., Rustin, P. & Larsson, N. G. Increased in vivo apoptosis in cells lacking mitochondrial DNA gene expression. *Proceedings of the National Academy of Sciences of the United States of America* **98**, 4038–43 (2001).

116. Yoshida, Y. *et al*. p53 Physically Interacts with Mitochondrial Transcription Factor A and Differentially Regulates Binding to Damaged DNA p53 Physically Interacts with Mitochondrial Transcription Factor A and Differentially Regulates Binding to Damaged DNA 1. *Cancer Research* 3729–3734 (2003).

117. Rourke, T. W. O., Doudican, N. A., Mackereth, M. D., Doetsch, P. W. & Shadel, G. S. Mitochondrial Dysfunction Due to Oxidative Mitochondrial DNA Damage Is Reduced through Cooperative Actions of Diverse Proteins. *Society* **22**, 4086–4093 (2002).

118. Weinstein, L. & Brenowitz, M. of Escherichia coZi K-12. *Biochemistry* (1994).

119. Kienhöfer, J. Association of mitochondrial antioxidant enzymes with mitochondrial DNA as integral nucleoid constituents Dissertation. *Naturwissenschaften* (2009).

120. Cooper, M. a Label-free screening of bio-molecular interactions. *Analytical and bioanalytical chemistry* **377**, 834–42 (2003).

121. Cadet, J. *et al*. Facts and artifacts in the measurement of oxidative base damage to DNA. *Free radical research* **29**, 541–50 (1998).

122. Moreno-villanueva, M. *et al*. A modified and automated version of the ' Fluorimetric Detection of Alkaline DNA Unwinding ' method to quantify formation and repair of DNA strand breaks. *Cancer Research* **9**, 1–9 (2009).

123. Taghizadeh, K. *et al*. Quantification of DNA damage products resulting from deamination , oxidation and reaction with products of lipid peroxidation by liquid chromatography isotope dilution tandem mass spectrometry. *Nature* **3**, 2005–2008 (2008).

124. Kienhöfer *et al*. Association of mitochondrial antioxidant enzymes with mitochondrial DNA as integral nucleoid constituents. *The FASEB Journal*

125. Schildknecht, S. The human dopaminergic neuronal cell line LUHMES as in vitro model for Parkinson ´ s disease. **25**, 38894–38894 (2008).

126. Kraus, R. L. *et al*. Antioxidant properties of minocycline: neuroprotection in an oxidative stress assay and direct radical-scavenging activity. *Journal of neurochemistry* **94**, 819–27 (2005).

127. Schildknecht, S. *et al*. Neuroprotection by Minocycline Caused by Direct and Specific Scavenging of Peroxynitrite . *Journal of Biological Chemistry* **286**, 4991–5002 (2011).

128. MacMillan-Crow, L. A. & Thompson, J. A. Tyrosine modifications and inactivation of active site manganese superoxide dismutase mutant (Y34F) by peroxynitrite. *Archives of biochemistry and biophysics* **366**, 82–8 (1999).

129. Pinlaor, S. *et al*. 8-Nitroguanine formation in the liver of hamsters infected with Opisthorchis viverrini. *Biochemical and Biophysical Research Communications* **309**, 567–571 (2003).

130. Akaike, T. *et al*. 8-Nitroguanosine Formation in Viral Pneumonia and Its Implication for Pathogenesis. *Proceedings of the National Academy of Sciences of the United States of America* **100**, 685–90 (2003).

131. Babsky, A., Doliba, N., Savchenko, A., Wehrli, S. & Osbakken, M. Na+ effects on mitochondrial respiration and oxidative phosphorylation in diabetic hearts. *Experimental biology and medicine (Maywood, N.J.)* **226**, 543–51 (2001).

132. Parisi, M. A. & Clayton, D. A. Similarity of human mitochondrial transcription factor 1 to high mobility group proteins. *Science (New York, N.Y.)* **252**, 965–9 (1991).

133. Dinardo, M. M. *et al*. Acetylation and level of mitochondrial transcription factor A in several organs of young and old rats. *Biochemical and biophysical research communications* **301**, 187–91 (2003).

134. Ozden, O. *et al*. Acetylation of MnSOD directs enzymatic activity responding to cellular nutrient status or oxidative stress. *Aging* **3**, 102–7 (2011).

135. Friedlich, A. L. *et al*. Oxidative Stress in Parkinson ' s Disease. 38–42 (2009).

136. Ballinger, S. W. *et al*. Hydrogen peroxide- and peroxynitrite-induced mitochondrial DNA damage and dysfunction in vascular endothelial and smooth muscle cells. *Circulation research* **86**, 960–6 (2000).

137. Floyd, R. A., Watson, J. J., Wong, P. K., Altmiller, D. H. & Rickard, R. C. Hydroxyl free radical adduct of deoxyguanosine: sensitive detection and mechanisms of formation. *Free radical research communications* **1**, 163–72 (1986).

138. Ravanat, J. L., Turesky, R. J., Gremaud, E., Trudel, L. J. & Stadler, R. H. Determination of 8-oxoguanine in DNA by gas chromatography--mass spectrometry and HPLC--electrochemical detection: overestimation of the background level of the oxidized base by the gas chromatography--mass spectrometry assay. *Chemical research in toxicology* **8**, 1039–45 (1995).

139. Gedik, C. M. & Collins, A. Establishing the background level of base oxidation in human lymphocyte DNA: results of an interlaboratory validation study. *The FASEB journal : official publication of the Federation of American Societies for Experimental Biology* **19**, 82–4 (2005).

140. Gupta, R. C. & Arif, J. M. An improved (32)P-postlabeling assay for the sensitive detection of 8-oxodeoxyguanosine in tissue DNA. *Chemical research in toxicology* **14**, 951–7 (2001).

141. Lutgerink, J. T. *et al*. Detection of 8-hydroxyguanine in small amounts of DNA by 32P postlabeling. *Analytical biochemistry* **201**, 127–33 (1992).

142. Möller, L. & Hofer, T. [32P]ATP mediates formation of 8-hydroxy-2'-deoxyguanosine from 2'-deoxyguanosine, a possible problem in the 32P-postlabeling assay. *Carcinogenesis* **18**, 2415–9 (1997).

143. Dizdaroglu, M. Facts About the Artifacts in the Measurement of Oxidative DNA Base Damage by Gas Chromatography-Mass Spectrometry I. **29**, 551–563 (1998).

144. Halliwell, B. & Dizdaroglu, M. The measurement of oxidative damage to DNA by HPLC and GC/MS techniques. *Free radical research communications* **16**, 75–87 (1992).

145. Jenner, A., England, T. G., Aruoma, O. I. & Halliwell, B. Measurement of oxidative DNA damage by gas chromatography-mass spectrometry: ethanethiol prevents artifactual generation of oxidized DNA bases. *The Biochemical journal* **331 (Pt 2**, 365–9 (1998).

146. Cadet, J. *et al*. Assessment of oxidative base damage to isolated and cellular DNA by HPLC-MS/MS measurement. *Free radical biology & medicine* **33**, 441–9 (2002).

147. Frelon, S. *et al*. High-performance liquid chromatography--tandem mass spectrometry measurement of radiation-induced base damage to isolated and cellular DNA. *Chemical research in toxicology* **13**, 1002–10 (2000).

148. Podmore, I. D., Cooper, D., Evans, M. D., Wood, M. & Lunec, J. Simultaneous measurement of 8-oxo-2'-deoxyguanosine and 8-oxo-2'-deoxyadenosine by HPLC-MS/MS. *Biochemical and biophysical research communications* **277**, 764–70 (2000).

149. Cooke, M. S. *et al*. Evaluation of enzyme-linked immunosorbent assay and liquid chromatography-tandem mass spectrometry methodology for the analysis of 8-oxo-7,8-dihydro-2'-deoxyguanosine in saliva and urine. *Free radical biology & medicine* **41**, 1829–36 (2006).

150. Oka, S. *et al*. Two distinct pathways of cell death triggered by oxidative damage to nuclear and mitochondrial DNAs. *The EMBO journal* **27**, 421–32 (2008).

151. Mitchell, D. L. *et al*. Development and application of a novel immunoassay for measuring oxidative DNA damage in the environment. *Photochemistry and photobiology* **75**, 257–65 (2002).

152. Serrano, J., Palmeira, C. M., Wallace, K. B. & Kuehl, D. W. Determination of 8-hydroxydeoxyguanosine in biological tissue by liquid chromatography/electrospray

ionization-mass spectrometry/mass spectrometry. *Rapid communications in mass spectrometry : RCM* **10**, 1789–91 (1996).

153. Musarrat, J., Arezina-Wilson, J. & Wani, A. A. Prognostic and aetiological relevance of 8-hydroxyguanosine in human breast carcinogenesis. *European journal of cancer (Oxford, England : 1990)* **32A**, 1209–14 (1996).

154. Musarrat, J. & Wani, A. A. Quantitative immunoanaiysis of promutagenic 8-hydroxy-2 ' - deoxyguanosine in oxidized DNA. *Program* **15**, 2037–2043 (1994).

155. Shaposhnikov, S., Thomsen, P. D. & Collins, A. R. Combining fluorescent in situ hybridization with the comet assay for targeted examination of DNA damage and repair. *Methods in molecular biology (Clifton, N.J.)* **682**, 115–32 (2011).

156. Pflaum, M., Will, O. & Epe, B. Determination of steady-state levels of oxidative DNA base modifications in mammalian cells by means of repair endonucleases. *Carcinogenesis* **18**, 2225–31 (1997).

157. Epe, B., Ballmaier, D., Roussyn, I., Briviba, K. & Sies, H. DNA damage by peroxynitrite characterized with DNA repair enzymes. *Nucleic acids research* **24**, 4105–10 (1996).

158. Bergeron, F., Auvré, F., Radicella, J. P. & Ravanat, J.-L. HO* radicals induce an unexpected high proportion of tandem base lesions refractory to repair by DNA glycosylases. *Proceedings of the National Academy of Sciences of the United States of America* **107**, 5528–33 (2010).

159. Ravanat, J.-L. *et al*. Singlet oxygen-mediated damage to cellular DNA determined by the comet assay associated with DNA repair enzymes. *Biological chemistry* **385**, 17–20 (2004).

160. Pinz, K. G., Shibutani, S. & Bogenhagen, D. F. Action of mitochondrial DNA polymerase gamma at sites of base loss or oxidative damage. *The Journal of biological chemistry* **270**, 9202–6 (1995).

161. Kuraoka, I. *et al*. Effects of endogenous DNA base lesions on transcription elongation by mammalian RNA polymerase II. Implications for transcription-coupled DNA repair and transcriptional mutagenesis. *The Journal of biological chemistry* **278**, 7294–9 (2003).

162. Fraga, C. G., Shigenaga, M. K., Park, J. W., Degan, P. & Ames, B. N. Oxidative damage to DNA during aging: 8-hydroxy-2'-deoxyguanosine in rat organ DNA and urine. *Proceedings of the National Academy of Sciences of the United States of America* **87**, 4533–7 (1990).

163. Ames, B. N., Shigenaga, M. K. & Hagen, T. M. Oxidants, antioxidants, and the degenerative diseases of aging. *Proceedings of the National Academy of Sciences of the United States of America* **90**, 7915–22 (1993).

164. Souza-Pinto, N. C., Croteau, D. L., Hudson, E. K., Hansford, R. G. & Bohr, V. A. Age-associated increase in 8-oxo-deoxyguanosine glycosylase/AP lyase activity in rat mitochondria. *Nucleic acids research* **27**, 1935–42 (1999).

165. Of, C., Base, O., In, D. & Dna, N. Comparison of oxidative base damage . **24**, 722–725 (1998).

166. Bogenhagen, D. F. Does mtDNA nucleoid organization impact aging? *Experimental gerontology* **45**, 473–7 (2010).

167. Stuart, J. a, Bourque, B. M., de Souza-Pinto, N. C. & Bohr, V. a No evidence of mitochondrial respiratory dysfunction in OGG1-null mice deficient in removal of 8-

oxodeoxyguanine from mitochondrial DNA. *Free radical biology & medicine* **38**, 737–45 (2005).

168. Anson, R. M., Sentürker, S., Dizdaroglu, M. & Bohr, V. A. Measurement of oxidatively induced base lesions in liver from Wistar rats of different ages. *Free radical biology & medicine* **27**, 456–62 (1999).
169. Ihara, H., Sawa, T., Nakabeppu, Y. & Akaike, T. Nucleotides function as endogenous chemical sensors for oxidative stress signaling. **48**, 33–39 (2011).
170. Greenblatt, M. S., Bennett, W. P., Hollstein, M. & Harris, C. C. Mutations in the p53 tumor suppressor gene: clues to cancer etiology and molecular pathogenesis. *Cancer research* **54**, 4855–78 (1994).
171. Sawa, T. & Ohshima, H. Nitrative DNA damage in inflammation and its possible role in carcinogenesis. *Nitric oxide : biology and chemistry / official journal of the Nitric Oxide Society* **14**, 91–100 (2006).
172. Murata, M., Thanan, R., Ma, N. & Kawanishi, S. Role of nitrative and oxidative DNA damage in inflammation-related carcinogenesis. *Journal of biomedicine & biotechnology* **2012**, 623019 (2012).
173. Ischiropoulos, H., Zhu, L. & Beckman, J. S. Peroxynitrite formation from macrophage-derived nitric oxide. *Archives of biochemistry and biophysics* **298**, 446–51 (1992).
174. Daiber, A., Frein, D., Namgaladze, D. & Ullrich, V. Oxidation and Nitrosation in the Nitrogen Monoxide / Superoxide System *. **277**, 11882–11888 (2002).
175. Beckmann, J. S. *et al*. Extensive nitration of protein tyrosines in human atherosclerosis detected by immunohistochemistry. *Biological chemistry Hoppe-Seyler* **375**, 81–8 (1994).
176. Ischiropoulos, H., al-Mehdi, A. B. & Fisher, A. B. Reactive species in ischemic rat lung injury: contribution of peroxynitrite. *The American journal of physiology* **269**, L158–64 (1995).
177. Ischiropoulos, H. *et al*. Peroxynitrite-mediated tyrosine nitration catalyzed by superoxide dismutase. *Archives of biochemistry and biophysics* **298**, 431–7 (1992).
178. Beckman, J. S. & Crow, J. P. Pathological implications of nitric oxide, superoxide and peroxynitrite formation. *Biochemical Society transactions* **21**, 330–4 (1993).
179. MacMillan-Crow, L. A., Crow, J. P. & Thompson, J. A. Peroxynitrite-mediated inactivation of manganese superoxide dismutase involves nitration and oxidation of critical tyrosine residues. *Biochemistry* **37**, 1613–22 (1998).
180. Quijano, C. *et al*. Reaction of peroxynitrite with Mn-superoxide dismutase. Role of the metal center in decomposition kinetics and nitration. *The Journal of biological chemistry* **276**, 11631–8 (2001).
181. Malik, Q. & Herbert, K. E. Oxidative and non-oxidative DNA damage and cardiovascular disease. *Free radical research* **46**, 554–64 (2012).
182. Wallace, D. C. Mitochondrial defects in neurodegenerative diseases. *Mental Retardation and Developmental Disabilities Research Reviews* **166**, 158–166 (2001).
183. © 1995 Nature Publishing Group http://www.nature.com/naturegenetics. (1995).
184. Lu, N., Huang, S. & Matzuk, M. M. Neurodegeneration, myocardial. **93**, 9782–9787 (1996).
185. Hopper, R. K. *et al*. Mitochondrial matrix phosphoproteome: effect of extra mitochondrial calcium. *Biochemistry* **45**, 2524–36 (2006).

186. Tao, R. *et al*. Sirt3-mediated deacetylation of evolutionarily conserved lysine 122 regulates MnSOD activity in response to stress. *Molecular cell* **40**, 893–904 (2010).

187. Scher, M. B., Vaquero, A. & Reinberg, D. SirT3 is a nuclear NAD+-dependent histone deacetylase that translocates to the mitochondria upon cellular stress. *Genes & development* **21**, 920–8 (2007).

188. Schlicker, C. *et al*. Substrates and regulation mechanisms for the human mitochondrial sirtuins Sirt3 and Sirt5. *Journal of molecular biology* **382**, 790–801 (2008).

189. MacMillan-Crow, L. A., Crow, J. P., Kerby, J. D., Beckman, J. S. & Thompson, J. A. Nitration and inactivation of manganese superoxide dismutase in chronic rejection of human renal allografts. *Proceedings of the National Academy of Sciences of the United States of America* **93**, 11853–8 (1996).

190. Chang, L. Y., Kang, B. H., Slot, J. W., Vincent, R. & Crapo, J. D. Immunocytochemical localization of the sites of superoxide dismutase induction by hyperoxia in rat lungs. *Laboratory investigation; a journal of technical methods and pathology* **73**, 29–39 (1995).

191. Gregroy, E. M., Yost, F. J. & Fridovich, I. Superoxide dismutases of Escherichia coli: intracellular localization and functions. *Journal of bacteriology* **115**, 987–91 (1973).

192. Ling, G. N., Kolebic, T. & Damadian, R. Low paramagnetic-ion content in cancer cells: its significance in cancer detection by magnetic resonance imaging. *Physiological chemistry and physics and medical NMR* **22**, 1–14 (1990).

193. Finley, J. W. & Davis, C. D. Manganese deficiency and toxicity: are high or low dietary amounts of manganese cause for concern? *BioFactors (Oxford, England)* **10**, 15–24 (1999).

194. Izutani, R. *et al*. Expression of manganese superoxide dismutase in esophageal and gastric cancers. *Journal of gastroenterology* **33**, 816–22 (1998).

195. Kahlos, K. *et al*. Manganese superoxide dismutase in healthy human pleural mesothelium and in malignant pleural mesothelioma. *American journal of respiratory cell and molecular biology* **18**, 570–80 (1998).

196. Hempel, N., Carrico, P. M. & Melendez, J. A. Manganese superoxide dismutase (Sod2) and redox-control of signaling events that drive metastasis. *Anti-cancer agents in medicinal chemistry* **11**, 191–201 (2011).

197. Harman, D. The biologic clock: the mitochondria? *Journal of the American Geriatrics Society* **20**, 145–7 (1972).

198. Miquel, J., Economos, A. C., Fleming, J. & Johnson, J. E. Mitochondrial role in cell aging. *Experimental gerontology* **15**, 575–91 (1980).

199. de Grey, A. D. A proposed refinement of the mitochondrial free radical theory of aging. *BioEssays : news and reviews in molecular, cellular and developmental biology* **19**, 161–6 (1997).

200. Bandy, B. & Davison, A. J. Mitochondrial mutations may increase oxidative stress: implications for carcinogenesis and aging? *Free radical biology & medicine* **8**, 523–39 (1990).

201. Pansarasa, O., Bertorelli, L., Vecchiet, J., Felzani, G. & Marzatico, F. Age-dependent changes of antioxidant activities and markers of free radical damage in human skeletal muscle. *Free radical biology & medicine* **27**, 617–22 (1999).

202. Lu, C. Y., Lee, H. C., Fahn, H. J. & Wei, Y. H. Oxidative damage elicited by imbalance of free radical scavenging enzymes is associated with large-scale mtDNA deletions in aging human skin. *Mutation research* **423**, 11–21 (1999).

203. Longo, V. D., Gralla, E. B. & Valentine, J. S. Superoxide Dismutase Activity Is Essential for Stationary Phase Survival in Saccharomyces cerevisiae. **271**, 12275–12280 (1996).

204. Sun, J., Folk, D., Bradley, T. J. & Tower, J. Induced overexpression of mitochondrial Mn-superoxide dismutase extends the life span of adult Drosophila melanogaster. *Genetics* **161**, 661–72 (2002).

205. Van Remmen, H. *et al*. Characterization of the antioxidant status of the heterozygous manganese superoxide dismutase knockout mouse. *Archives of biochemistry and biophysics* **363**, 91–7 (1999).

206. Van Remmen, H. *et al*. Life-long reduction in MnSOD activity results in increased DNA damage and higher incidence of cancer but does not accelerate aging. *Physiological genomics* **16**, 29–37 (2003).

207. Mansouri, A. *et al*. Alterations in mitochondrial function, hydrogen peroxide release and oxidative damage in mouse hind-limb skeletal muscle during aging. *Mechanisms of ageing and development* **127**, 298–306 (2006).

208. Muller, F. L. *et al*. Absence of CuZn superoxide dismutase leads to elevated oxidative stress and acceleration of age-dependent skeletal muscle atrophy. *Free radical biology & medicine* **40**, 1993–2004 (2006).

209. Trifunovic, A. *et al*. Premature ageing in mice expressing defective mitochondrial DNA polymerase. *Nature* **429**, 417–23 (2004).

210. Kujoth, G. C. *et al*. Mitochondrial DNA mutations, oxidative stress, and apoptosis in mammalian aging. *Science (New York, N.Y.)* **309**, 481–4 (2005).

211. Zheng, W., Khrapko, K., Coller, H. A., Thilly, W. G. & Copeland, W. C. Origins of human mitochondrial point mutations as DNA polymerase ⁄ -mediated errors. *Scanning* **599**, 11–20 (2006).

212. Pe, V. I. *et al*. Protein stability and resistance to oxidative stress are determinants of longevity in the longest-living rodent , the naked mole-rat. *PNAS* **106**, 1–6 (2009).

213. Taylor, R. W. & Turnbull, D. M. Mitochondrial DNA mutations in human disease. *Nature reviews. Genetics* **6**, 389–402 (2005).

7 Appendix

7.1 Abbreviations

8-oxodG	8-oxo-7,8-dihydroguanine
ADP	Adenosine diphosphate
ATP	Adenosine-5'-triphosphate
ALS	Amyotrophic Lateral Sclerosis
Amp	Ampicillin
AP site	Apurinic and apyrimidinic site
APS	Ammonium persulfate
BER	Base excision repair
Bp	Base pairs
BSA	Bovine serum albumine
ddH2O	Double distilled water
D-loop	Displacement-loop
DMSO	Dimethyl sulfoxide
dN	Deoxyribonucleotide
DNA	Deoxyribonucleic acid
E. coli	Escherichia coli
ECL	Enhanced chemiluminescence
EDTA	Ethylenediamine-tetraacetic acid
ETC	Electron transport chain
FADU	Fluorimetric analysis of DNA unwinding
FBS	Fetal bovine serum
Fpg	Formamidopyrimidine DNA glycosylase
G	Gravitational acceleration
GB	Gradient buffer
GSH	Glutathione
GPx1	Glutathione peroxidase 1
H	Hour
Hepes	N-(2-hydroxyethyl)-piperazine-N'-2-ethanesulfonic acid
HMG	High Mobility Group
HRP	Horseradish polymerase
H-strand	Heavy strand
iNOS	Inducible NO synthase
IPTG	Isopropyl β-D-1-thiogalactopyranoside
kBp	Kilo base pairs
kDa	Kilo Dalton
LB	Luria-Bertani broth
LSP	Light strand promoter
L-strand	Light strand
Min	Minute
mtDNA	Mitochondrial DNA
mtNOS	Mitochondrial NO synthase
mtSSB	Mitochondrial single-strand binding protein
NE2	Nucleoid isolation buffer
NER	Nucleotide excision repair
nNOS	Neuronal NO synthase
OGG1	8-oxoguanine glycosylase
p0	Mitochondrial DNA deficient cells

PARP	Poly(ADP-ribose) polymerase
PBS	Phosphate buffered saline
PCR	Polymerase chain reaction
PMSF	Phenylmethylsulphonylfluoride
Pol γ	Polymerase gamma
PON	Peroxynitrite
Prx	Peroxiredoxin
RNA	Ribonucleic acid
RNS	Reactive nitrogen species
ROS	Reactive oxygen species
Rpm	Rotations per minute
SDS-PAGE	Sodium dodecyl sulfate polyacrylamide gel electrophoresis
SOD1 (CuZnSOD)	Copper, zinc superoxide dismutase
SOD2 (MnSOD)	Manganese containing superoxide dismutase
SOD3 (EC-SOD)	Extracellular superoxide dismutase
SPR	Surface Plasmon Resonance
TFAM	Mitochondrial transcription factor A
Trx	Thioredoxin
U	Unit
Wt	Wild type
XO	Xanthine oxidase

7.2 List of figures

7.3 List of tables